# FY 2011
# Engineering
## *Innovations, Research, and Technology*
# Report

Lawrence Livermore
National Laboratory

## About the Cover

Additive manufacturing techniques deliver three-dimensional microstructures with previously unobtainable material properties.

Livermore engineers Chris Spadaccini (left) and Eric Duoss experiment with the direct ink-writing process.

## Acknowledgements

**LLNL-TR-554711/April 2012**                                       **ENG-11-0070**

# FY2011
# Engineering
*Innovations, Research, and Technology*
# Report

# Introduction

*A Message From*

## Monya A. Lane
**Associate Director for Engineering**

*T*HIS report summarizes key research, development, and technology advancements in Lawrence Livermore National Laboratory's Engineering Directorate for FY2011. These efforts exemplify Engineering's nearly 60-year history of developing and applying the technology innovations needed for the Laboratory's national security missions, and embody Engineering's mission to "Enable program success today and ensure the Laboratory's vitality tomorrow."

Leading off the report is a section featuring compelling engineering innovations. These innovations range from advanced adaptive optics technologies enabling the direct imaging of extrasolar planets; to an automated, modular, microfluidic platform for preparing biosamples for pathogen detection; to techniques to enhance the performance of next-generation explosives detection systems installed at airports. All are examples of the forward-looking application of innovative engineering to pressing national problems and challenging customer requirements.

Engineering's capability development strategy includes both fundamental research and technology development. Engineering research creates the competencies of the future where discovery-class groundwork is required. Our technology development (or reduction to practice) efforts enable many of the research breakthroughs across the Laboratory to translate from the world of basic research to the national security missions of the Laboratory. This portfolio approach produces new and advanced technological capabilities, and is a unique component of the value proposition of the Lawrence Livermore Laboratory. The balance of the report highlights this work in research and technology, organized into thematic technical areas: Advanced Manufacturing; Computational Engineering; Engineering Information Systems; Micro/Nano-Devices and Structures; and Measurement Technologies. Our investments in these areas serve not only known programmatic requirements of today and tomorrow, but also anticipate the breakthrough engineering innovations that will be needed in the future.

## Advanced Manufacturing

Advanced Manufacturing is a new and rapidly developing area for Engineering, and includes developmental efforts in "designer" materials that can be custom-made at the micro- and nanostructural level and that include complex geometries with micrometer-scale precision. Development of such materials, along with the appropriate fabrication and manufacturing technologies, can have a profound effect on a host of LLNL programmatic applications, from production of laser fusion targets to advanced sensor components.

FY2011 efforts included commencing a Disruptive Fabrication Technologies initiative aimed at fundamentally understanding and developing new additive micromanufacturing techniques that enable both designer materials and 3-D mesoscale structures; and development work on fabricating a massively parallel, multiaxis microreflector array for high-speed projection of a directed light field.

## Computational Engineering

Computational Engineering efforts focus on the research, development, and deployment of computational engineering technologies that provide the foundational capabilities to address most facets of Engineering's mission, ranging from fundamental advances to enable accurate modeling of full-scale DOE and DoD systems performing at their limits, to advances for treating photonic and microfluidic systems.

FY2011 projects encompassed in-situ observations of twinning and phase transformations at the crystal scale and the first direct experimental evidence of a predicted phase transformation mechanism in iron; high-fidelity computation to study how traumas create localized mechanical loads in the brain and the correlation of these loads to observed injuries; additional work on developing a new Lagrange embedded mesh technique for multiphysics simulations; and adding improvements to our existing lattice-Boltzmann polymer code to enable fully turbulent, multiscale simulations of drag reduction.

## Engineering Information Systems

Knowledge discovery encompasses a wide variety of technologies with the goal of broadly generating new understanding or knowledge of relevant situations, thereby allowing anticipation or prediction of possible outcomes. With this understanding, a more comprehensive solution may be possible for problems as complex as the prediction of disease outbreaks or advance warning of terrorist threats.

Our FY2011 efforts were centered on creating data models as a first step toward establishing a foundation in energy systems informatics as a resource for LLNL projects, as well as for the greater energy utility user base; and creating innovative computational learning algorithms that will enable the use of sophisticated predictive modeling techniques on modern streaming data sources.

## Micro/Nano-Devices and Structures

Micro/nano-scale manufacturing encompasses technology efforts that fuel the commercial growth of microelectronics and sensors, while simultaneously customizing these technologies for unique, noncommercial applications that are mission-specific to the Laboratory and DOE. The Laboratory's R&D talent and unique fabrication facilities have enabled highly innovative and custom solutions to technology needs in Stockpile Stewardship, Homeland Security, and Intelligence.

FY2011 projects included work on developing microfluidic devices with integrated microchannels and membrane filters for separating and concentrating viruses; new, complimentary embedded sensing capabilities for monitoring the stockpile: optic-fiber-based surface-enhanced Raman scattering and photo-acoustic spectroscopy; enabling transparent ceramic optics with unique properties based on tailored nanostructures; improving the performance of cadmium–zinc–telluride gamma radiation detectors; and characterizing phenomena of DNA microarray hybridization, regeneration, and selective release.

## Measurement Technologies

Measurement Technologies comprise activities in nondestructive characterization, metrology, sensor systems, and ultrafast technologies for advanced diagnostics. The advances in this area are essential for the future experimental needs in Inertial Confinement Fusion, High-Energy-Density Physics, Weapons, and Department of Homeland Security programs.

Our FY2011 projects consisted of initial work to demonstrate a noninvasive, real-time voice-authentication capability using nonacoustic electromagnetic voice sensing; a study of the use of x-ray array sources for improved imaging in nondestructive evaluation (NDE) applications; gaining a fundamental understanding of the acceleration gradients in Dense Plasma Focus (DPF) Z-pinch plasmas in order to examine how these plasmas can be systematically exploited for accelerator applications; and developing ultrafast, sensitive optical radiation gamma, neutron, and proton detectors.

# Contents

# Engineering
## Innovations

# BLU-129/B: Rapid Design, Development, and Fielding of a Very Low-Collateral-Damage Weapon

**Kip Hamilton**
925-422-5879
hamilton6@llnl.gov

IN many modern combat zones, America's adversaries strategically locate their forces within urban environments, providing them with possible asymmetric ground advantages. Urban environments negate many traditional U.S. military advantages, such as massive firepower, by exploiting the U.S.'s unwillingness to risk injury to nearby friendly forces, cultural sites, or noncombatants.

An innovative class of conventional weapon was needed to give commanders the desired effect on targets while avoiding excessive collateral damage. Such a weapon would remove limits on missions and allow our forces to engage adversaries in close proximity to damage-sensitive areas. The BLU-129/B guided bomb is such a weapon, allowing combatant commanders to target areas previously considered off limits. Its innovative composite casing was designed to minimize fragmentation and thereby decrease damage and injury to nearby structures and personnel.

## Quick Response to an Immediate Need

In response to a Department of Defense (DoD) urgent request for a very-low-collateral-damage weapon, a program was formed between Lawrence Livermore National Laboratory (LLNL) and the Air Force Research Laboratory (AFRL). The program goal was to rapidly design, develop, test, produce, and field a new, very-low-collateral-damage warhead, later designated BLU-129/B



Figure 1. BLU-129/B warhead with laser JDAM guidance kit.



Figure 2. The curing oven (left), large turning lathe (center), and five-axis machining center (right) were acquired to support the BLU-129/B project.

by the Air Force. The BLU-129/B is a 500-pound guided bomb designed to match the physical features of a standard Mk-82 general-purpose bomb, but with a carbon-fiber casing that disintegrates into harmless particles upon detonation, limiting the bomb's damage range (see Figure 1).

Munitions specialists from LLNL and AFRL embarked on an extremely aggressive five-month project to design and test an advanced warhead, and accelerate the weapon's technical maturity for immediate transition to an equally aggressive Quick Reaction Capability (QRC) acquisition program at the Air Armament Center (AAC), Eglin Air Force Base, FL. The initial phase of the program was referred to as the Precision Lethality Mk-82 Risk Reduction Effort prior to the weapon being given the identifier of BLU-129/B.

During the QRC phase of the program, LLNL worked closely with the AAC Program Office to prioritize requirements, build warhead prototypes to test performance and integration with inventoried guidance kits, and transition the LLNL-developed manufacturing technology to an industrial partner, Aerojet Corporation. This program was a model of close cooperation between the munitions research, development, and production communities to rapidly provide a valuable new capability to the warfighter.

## Using Systems Integration to Set the Stage

In order to meet the needs of this time-critical mission, LLNL senior management ranked the project as "high-priority" and supported the team throughout the design and development process by tapping systems engineering expertise to rapidly assemble key personnel across multiple engineering divisions and implementing needed facility capabilities.

Additionally, to address warhead production rates and the lack of specialized capabilities required for this project, the Engineering Directorate acted to add three major pieces of equipment to aid in manufacturing large carbon-fiber components: a large curing oven, a large turning lathe, and a five-axis machining center (see Figure 2).

Finally, to facilitate a smooth transition to the QRC, LLNL created an industrial partnership with Aerojet that included a contract to provide winding mandrels for case manufacturing. This partnership proved very valuable for both institutions and contributed to the program's success.

## Aggressive Response to Engineering Challenges

DoD QRC programs are challenging, requiring aggressive, success-oriented schedules. Consequently, once the BLU-129/B project was set in motion, only a well-orchestrated team

committed to the mission could meet the established milestones. The time-critical nature of the project produced a number of engineering challenges, each of which were overcome.

**Design Modeling and Refinement**

LLNL scientists were given only a few months to design a composite-cased warhead that would maintain the outer mold line and mass properties of the standard Mk-82 while easily integrating with applicable precision guidance kits and aircraft. The most technically challenging aspect of the design process was making sure the case had sufficient strength and stiffness to attain the required penetration goals.

Advanced engineering analysis was employed to design the warhead, and multiple iterations were performed to balance the goals of a minimum number of metal components (for low collateral damage), maximum high explosive fill volume (for near-field lethality), and sufficient case strength (for penetration). The bulk of the design efforts were focused on attaining the penetration capability using ALE3D code while other quasi-static analyses of local components were performed using the implicit structural analysis code NIKE3D (see Figure 3).

Model validation was performed by analyzing legacy LLNL composite munitions, comparing LLNL simulation results with AFRL simulation results,
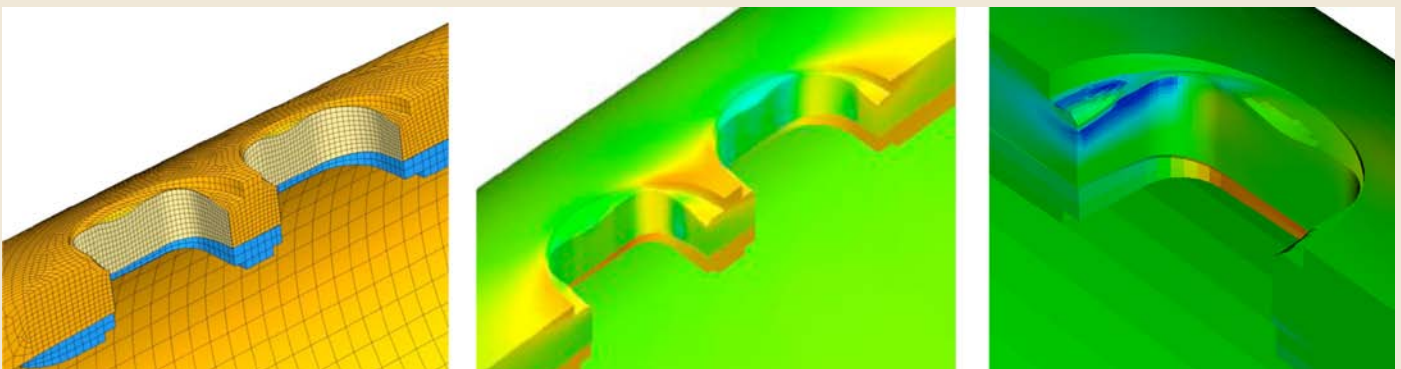


**Figure 3. Samples of the modeling simulation and results of the composite case features.**

and comparing metal cased Mk-82 simulations with known behavior. This validation showed conservatism in the analysis methodology and yielded increased confidence in the baseline results.

**Interface Design**

The physical properties of the BLU-129/B warhead were intentionally customized to closely match the standard Mk-82, with the case having the same outer shape and identical interfaces to maintain compatibility with existing fuses and precision guidance kits, and to provide ready application to a broad range of military aircraft. One of the main challenges of a composite-cased warhead was joining the nonsteel body with metal components to facilitate using the standard metal weapon interfaces.

Applying lessons learned on similar LLNL composite munitions projects, engineers crafted innovative approaches in each component design by using facets and ridges to trap metal couplers with the carbon fiber winding process, thus assuring a robust interface.

**Manufacturing**

While the design was being iterated, engineers worked to create drawings and manufacture the needed hardware to support the accelerated program schedule (see Figure 4). The hardware included both warhead components and the tooling required to build and assemble the final product. A large part of the challenge was to prioritize the design and manufacture of components so that they arrived just in time to support warhead fabrication. By utilizing LLNL in-house machine shop capabilities operating at their maximum capacity, and through close cooperation with project engineers, the machinists were able to deliver product to meet demand.

Working within the Engineering Directorate to obtain qualified personnel allowed winding teams to become established early and become trained to be proficient in working with the filament-winding machine. The most senior operators were selected to lead wind teams in order to work multiple shifts. Meticulous records were kept to maintain consistency in case fabrication (see Figure 5), and these records were passed along to our industrial partner. Forensic evaluations of cured case samples were used to trend important case production parameters such as density, glass transition temperature, porosity, and fiber volume fraction.
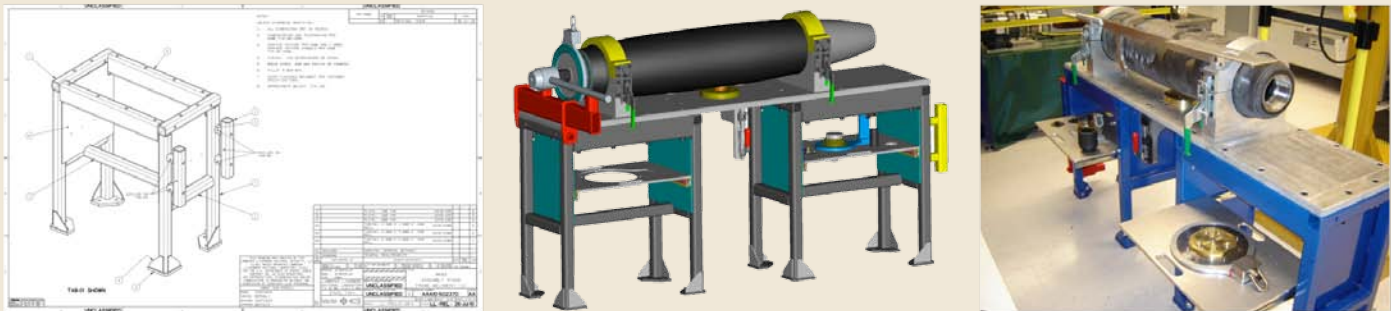


Figure 4. Manufacturing of custom assembly tooling was vital to meet warhead delivery schedule.



Figure 5. Case winds were carefully monitored and measured to provide consistency.

### Structural Testing

A wide variety of structural tests were performed on the BLU-129/B warhead to verify that it could withstand the structural loads induced from the full flight envelope of Air Force, Navy, and Marine Corps aircraft (see Figure 6). The tests were to prove that the carbon-fiber case would show no signs of structural failure or permanent deformation following static and fatigue loadings. Once requirements were established, LLNL test engineers developed test plans and test fixtures.

As with the warhead design process, the testing effort also required design, analysis, and tooling fabrications be performed under tight deadlines.

Project test engineers performed multiple tests that included lug loads, aft joint loads, forward joint loads, ejection loads, swaybrace loads, case fatigue, case bending, case compression, and modal frequency. Detailed reports were provided to the QRC Program Office to support flight safety.

### Transition to Industry

Throughout the entire program, LLNL engaged its industrial partner Aerojet in all aspects of the warhead manufacturing and assembly processes in order to ease the transition from LLNL warhead prototypes to Aerojet warhead production; this represented a unique scenario. LLNL provided Aerojet with detailed design drawings, complete winding profiles, step-by-step assembly procedures, and a duplicate set of assembly tooling.

During Aerojet production, LLNL acted as an independent assessment board for the QRC Project Office to respond to any deviations in product or process. LLNL also provided structural testing support to prove-out the deviations prior to committing resources.

### Innovation, Agility, and Collaboration

The BLU-129/B warhead met or exceeded all established requirements, and the manufacturing capability has been successfully transitioned to Aerojet. Near the end of 2011, the BLU-129/B was authorized for operational fielding on multiple aircraft. It is currently available for use by U.S. commanders.

This program showcased how close cooperation between the munitions research, development, and production communities enabled rapid deployment of a new capability to the U.S. warfighter, a capability that is providing greater overall mission flexibility.
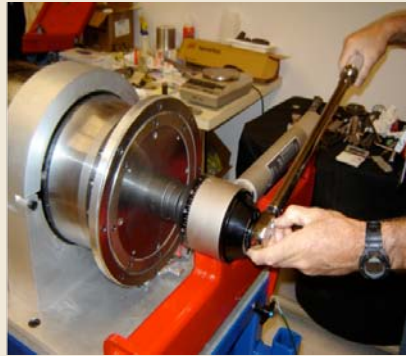


**Figure 6. Warhead test configurations were varied to validate the robustness of the case.**

# Advancing Aviation Security

**Harry E. Martz, Jr.**
925-423-4269
martz2@llnl.gov

*A*IR travel is a popular mode of transportation. Each year, more than 600 million people board U.S. flights for business or pleasure. As demonstrated on 9/11, a coordinated terrorist strike on commercial airlines has devastating consequences where many lives could be lost and the nation's economy could be crippled. The Transportation Security Administration (TSA) has worked diligently to enhance security at airports and on flights so that people and cargo can continue to move freely. Today, all passengers and every piece of checked or carry-on luggage are screened before they are permitted on an aircraft. X-ray systems and walk-through metal detectors allow security personnel to identify dangerous metal objects, such as guns and knives. A more complex problem is the detection of explosives, where detection technologies such as multiple-energy X-ray radiography, computed tomography (CT), full-body scanners using millimeter wave and X-ray backscatter, and other techniques are used to screen for explosives hidden in luggage, in cargo, and on the people boarding the aircraft.

Scientists and engineers at the Lawrence Livermore National Laboratory (LLNL) are working with the Department of Homeland Security (DHS), Science and Technology Directorate (S&T), Explosives Division (EXD) to help improve aviation security by evaluating and enhancing the performance of next-generation explosives detection technologies. LLNL is providing subject matter expertise to TSA for their multibillion-dollar procurements of explosive detection systems (EDS) for the nation's airports, and is also providing recommendations

for process and system improvements. To further improve aviation security, EXD is funding research at LLNL to develop advanced explosives detection technologies that can more accurately discriminate between a wide range of explosives and nonthreat materials. One challenge with scanning for explosives is that some nonthreatening materials share similar characteristics with actual threats, leading to false positives or false alarms. When an alarm is generated, security personnel must review the scan images to clear the alarm or manually open and verify the contents of a bag, which can increase labor costs and lead to passenger delays.

The Livermore efforts currently focus on CT-based applications. First developed for the medical field as a method for diagnosing disease, x-ray CT has become instrumental in various industrial nondestructive evaluation (NDE) applications. Explosives detection equipment that incorporates CT uses a broad-spectrum x-ray beam to capture projections of an object, in particular the objects inside a piece of luggage. The CT system then applies complex reconstruction algorithms to the projections to produce a three-dimensional representation of the luggage and its contents. Automated threat-detection algorithms (also referred to as threat-recognition algorithms) further process the images to separate each item and flag potential threats for further review (see Figure 1). Transportation security officers can then examine these images and the relevant data to determine whether further interrogation is needed. LLNL has also performed research on advanced x-ray

systems to inspect carry-on bags and is helping to better understand the performance of x-ray backscatter and millimeter-wave passenger screening systems.

## Engineering Solutions

The Livermore effort includes the development of a DHS image database that holds a vast catalog of x-ray and other properties of explosive threats and nonthreat materials. LLNL, in collaboration with the National Explosives Engineering Sciences Security Center (NEXESS), is responsible for defining how explosive test objects are formulated and prepared for use in evaluating the EDS being procured by TSA for U.S. airports. Livermore provides DHS with assistance in establishing quality assurance metrics for collecting data using real explosive specimens designed to evaluate the performance of the vendor systems. LLNL is performing research and development on advanced CT algorithms to ensure that they produce precise reconstruction and segmentation results. Livermore is also investigating new source and detector hardware to enhance the performance of existing or next-generation technologies. LLNL is exploring methods to further improve the performance of automated threat-detection algorithms as the number of passengers in the U.S. continues to increase and the luggage they pack gets more complex. LLNL is also working with DHS's Center for Excellence (COE) for Explosives Awareness and Localization of Explosives-Related Threats (ALERT) at Northeastern University to help get third parties to look at solutions to explosives

detection, including image reconstruction, segmentation, and automatic threat-detection algorithms.

Livermore is responsible for developing, operating, and maintaining the DHS image database that provides for storage and distribution of DHS program data and documents. It is a critical national resource for protecting documents and data so they are available for further research. Data and documents are generated at LLNL and other facilities that support the DHS explosive detection efforts. Examples of documents stored or generated in this database system include program-wide raw data from CT and other explosive detection systems, reconstructed and segmented data generated from the raw data, technical data reports, quality

assurance documents, specification documents, and many other documents. Livermore has accumulated approximately 90 terabytes of program data and documents that are stored in this database.

Livermore is responsible for establishing how explosive formulations are produced and specimens are prepared that are used in evaluating the performance of the various vendor explosive detection systems. Formulation preparation data sheets and handling procedures are generated for other labs to use in preparing the specimens. Livermore has two CT systems located in the High Explosives Applications Facility (HEAF) that are used to scan real explosives in a safe manner and to validate the formulation process and

provide a baseline for quality assurance. Some of the explosives used in this process are sensitive and can only be produced and handled remotely. Consequently, Livermore scientists and engineers developed a system for remotely producing and scanning sensitive liquid explosives (see Figure 2). The system is designed so that no pumps or valves are used in the transfer of the liquid explosive for safety reasons. This is accomplished using gravity, low pressure gas and low friction materials for tubing and containers. This system has been successfully used to produce and scan sensitive liquids for DHS. Engineers are currently evaluating other robotic methods for handling sensitive materials that are not liquids.
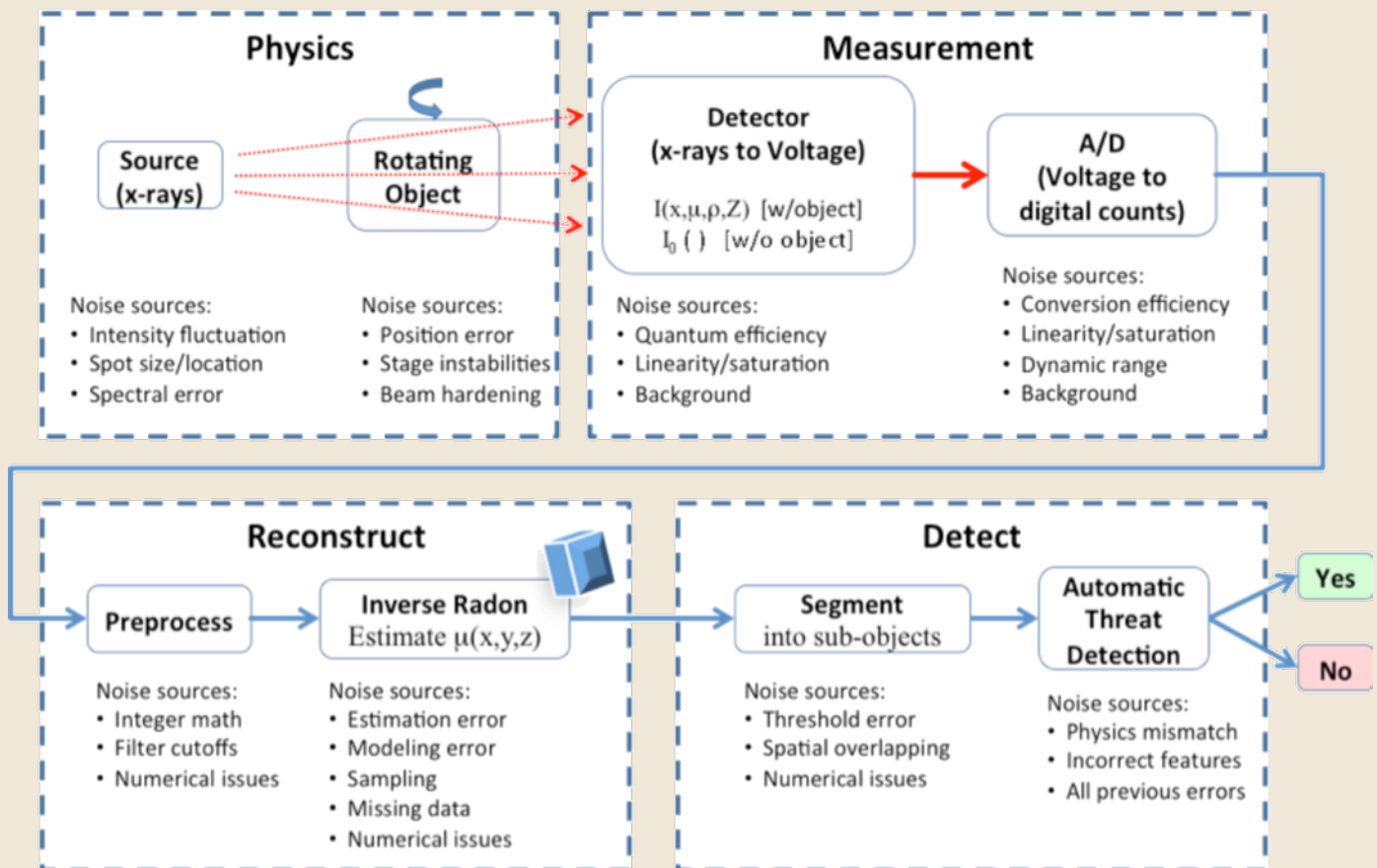


**Figure 1. CT method.** Images obtained from current CT-based explosives detection systems provide estimates of the linear attenuation coefficients and other features of the items inside luggage. These attenuation coefficients depend strongly on a material's density and elemental composition and on the x-ray source and detector used to measure them.

Livermore engineers are evaluating reconstruction, segmentation, and automated threat-detection algorithms to determine how to improve EDS (see Figure 3) and methods for use in advanced x-ray dual-energy techniques. In this detection scheme, the detector measures the linear attenuation coefficients of materials at two x-ray energies, one low in the spectrum and the other high. The two measurements provide a stronger basis for interpreting an object's elemental composition and density, thus improving the system's detection capabilities with fewer false alarms.



Figure 2. (top) Remote handling system used for the production of sensitive liquid explosives and Pelican case that holds the specimen that is scanned in the CT system. (right) The open Pelican case shows the specimen bottle inside that is filled with the sensitive liquid explosive prior to a CT scan.



At the energies used to scan luggage, x-ray attenuation is determined by three kinds of interaction processes occurring between the x rays and the object: coherent scattering, photoelectric absorption, and Compton scattering. In coherent scattering, incident x rays are deflected by atoms in an object, whereas in the photoelectric effect, they are completely absorbed. With Compton scattering, the x-ray energy is partially transferred to an electron that is then excited or ejected from an atom. Current detection techniques combine the first two processes into a single parameter. However, it may be possible to obtain a more precise signature of the types of atoms within objects and thus more effectively identify specific explosive materials by measuring all three interactions. Livermore scientists and engineers are using the Laboratory's high-performance computers to model the three interaction processes. These models can artificially adjust the physics parameters, such as x-ray spectra, to improve the understanding of materials and object characterization. With that knowledge, the researchers can evaluate the algorithms used in existing explosives detection systems and reconfigure the codes for enhanced performance.

Reconstruction algorithms process the projections from CT systems and correct for imperfections in the image quality. In some cases, artifacts, or errors introduced as part of the processing and reconstruction, compromise the image quality. Artifacts such as beam hardening, rings, and streaks can compound the problem. Improved reconstruction algorithms would reduce artifacts in CT images and enhance segmentation to more clearly define objects and their boundaries, increasing threat detection while decreasing the false-alarm rate and thus reducing the intervention required by security personnel.

Segmentation is the process of separating and digitally extracting the objects that make up a bag. Once a bag has been segmented, each object can be examined to determine its features.
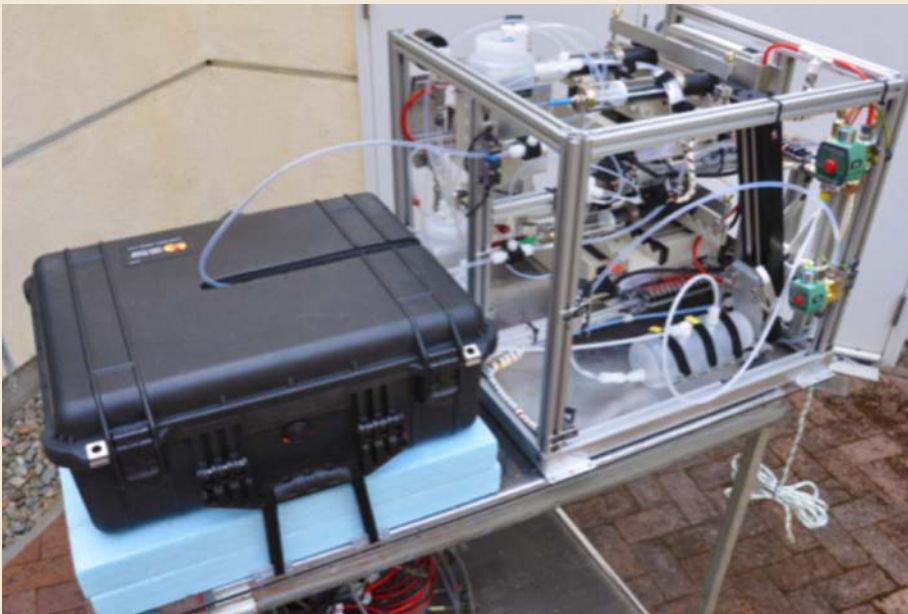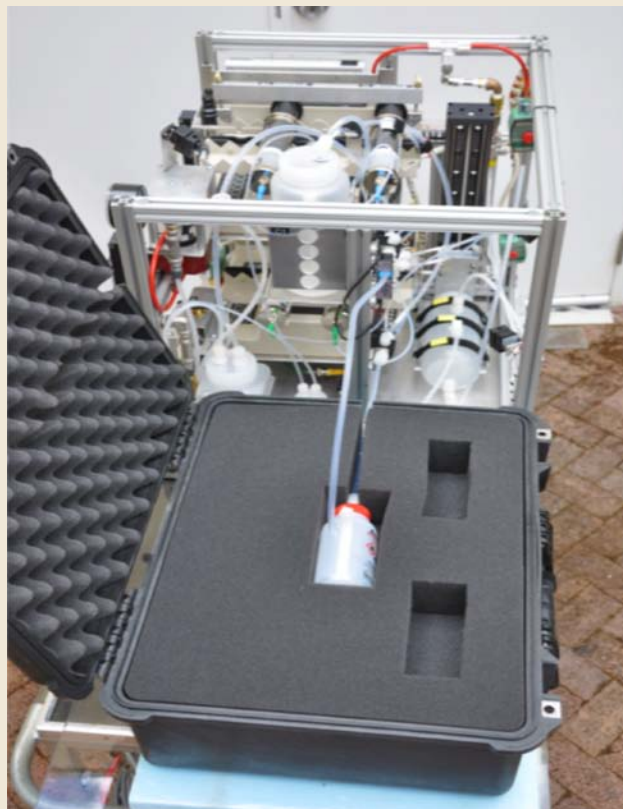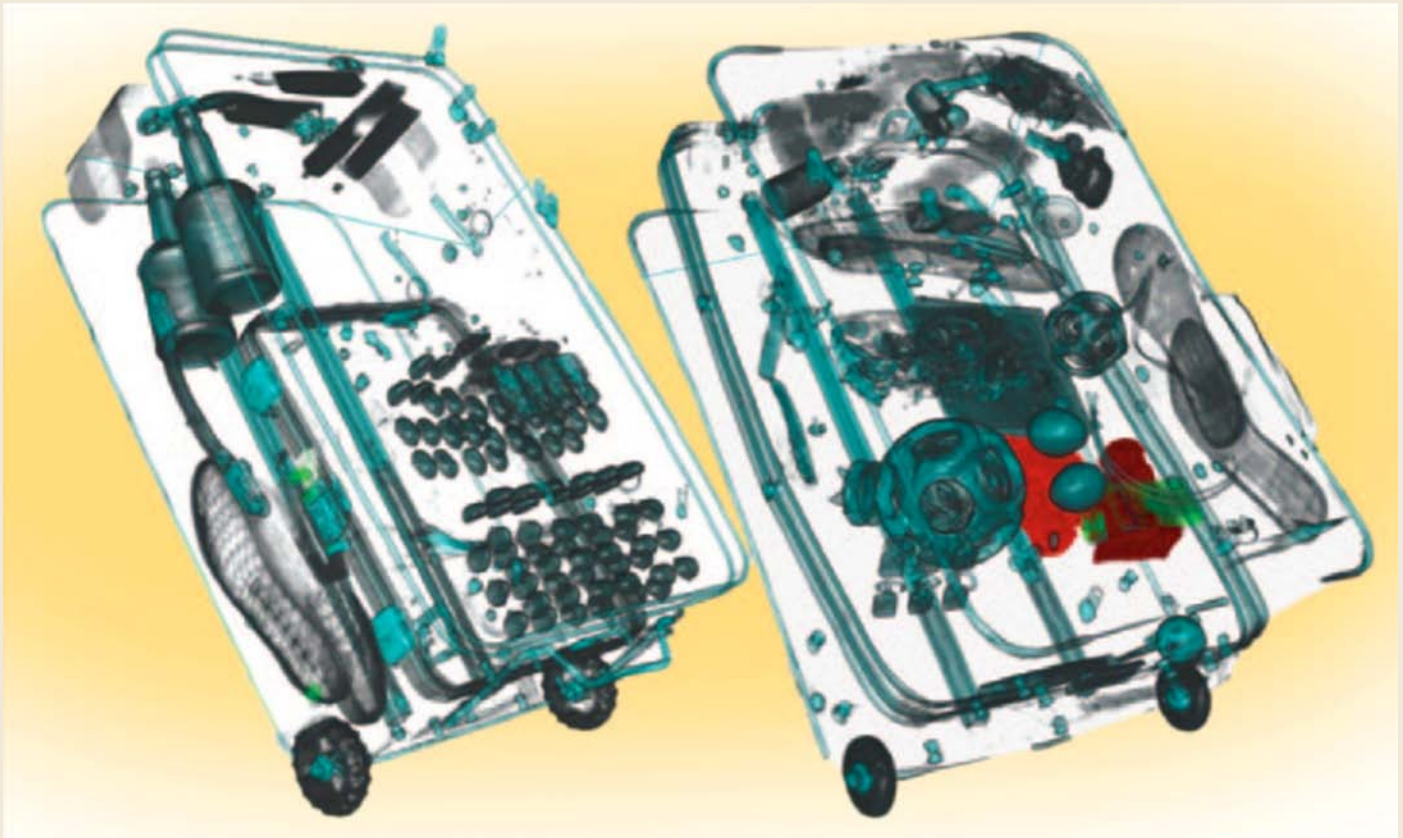
**Figure 3. Computed tomography systems produce two- and three-dimensional digital images showing the contents of a bag. Transportation security personnel can review such an image to determine if a threat is present or to clear a false alarm. Areas highlighted in red indicate potential threats. (Courtesy of Safran Morpho Detection.)**

Examples of features include mass, volume, mean attenuation, and texture metrics. These features are used by automated threat-detection algorithms. A poor segmentation might break an object into pieces or merge multiple objects, thereby making the work of the automated threat-detection more difficult. Livermore scientists and engineers are working on methods of measuring how well an algorithm performs in the segmentation task. These metrics are having a major impact on the development of segmentation algorithms being considered for incorporation into EDSs.

Automated threat-detection algorithms analyze the CT images and extract relevant characteristics such as x-ray attenuation, density, effective atomic number, and mass of different materials in a scanned bag. The system then compares data generated by the algorithms with values of known explosives to classify each material as either a threat or a nonthreat. To improve the results produced in such comparisons, LLNL scientists and engineers are redesigning the algorithms to better interpret the complex data, including multiple-energy measurements. The researchers are also developing an expanded database of explosives properties to serve as a reference for the algorithms that process the CT data. The database will also be useful for other researchers working in this field, whether they are at other laboratories, government agencies, or academic institutions or with current or potential industrial partners. These improvements should allow explosives detection technologies to more accurately differentiate threats from nonthreats and thus enhance detection capabilities, reduce false-alarm rates, and increase the system's operational efficiency.

Ultimately, the research performed at Livermore and the resulting modifications to existing technologies will allow the DHS S&T's EXD, through the Transportation Security Administration, to deploy more efficient detection systems. LLNL scientists and engineers are advancing the technologies used at airports to screen for dangerous materials. Thanks to Livermore's expertise in NDE, high explosives formulation, and high-performance computing, airport security personnel are becoming better equipped to stay one step ahead of the nation's adversaries, keeping airline passengers safer in an increasingly hostile world.

# Advanced Adaptive Optics for the Direct Imaging of Exoplanets

**Lisa A. Poyneer**
925-423-3360
poyneer1@llnl.gov

*I*N the last 20 years, researchers have learned that planets exist around other stars and that these exoplanets are relatively common and come in an astonishing range of sizes and orbits. If scientists could directly image and spectroscopically analyze an exoplanet's light, they would be able to determine what the planet is made of, its surface temperature, the strength of its gravity and, potentially, whether it harbors life.

Of the 700 exoplanets detected so far, almost all have been found by indirect means. (Only very recently have astronomers been able to directly image exoplanets.) Indirect methods prevail because direct imaging is extremely difficult: the planet is usually at least one million to more than one billion times fainter than its host star. This ratio of intensity is referred to as the contrast. High-contrast imaging requires a coronagraph to suppress diffraction; otherwise, the star's light overwhelms the planet. A further complication for ground-based observation is turbulence in the Earth's atmosphere that muddles the star's light and hides the exoplanet in the glare. Adaptive optics (AO) reduces the deleterious effects of the atmosphere (see Figure 1), enabling direct exoplanet imaging. LLNL has a groundbreaking history in AO, including the development of the first major astronomical laser-guide star AO system at Lick Observatory, Mt. Hamilton, CA.

The Gemini Planet Imager (GPI), developed by LLNL with collaborating institutions, is a new instrument for the Gemini South Observatory in Cerro Pachón, Chile. GPI is designed to image planets that are one to ten million times fainter than their host stars and closer than one arc second to them. In order to achieve this unprecedented level of contrast, we have developed several advanced AO technologies and algorithms (see Figure 1). These techniques all represent a new way of addressing fundamental—and in some cases, long-standing—challenges in the field, and provide a technological path forward for AO performance and high-contrast imaging well beyond what is presently achievable with general-purpose AO systems.

## Reducing the Computational Cost of AO

The first essential step in building an AO system for planet detection is having a mirror with thousands of control points (actuators), which are updated every millisecond. Higher rates allow the AO system to better keep up with the dynamic atmosphere; more actuators allow the deformable mirror (DM) to approximate more accurately the phase aberration's spatial structure. The primary barrier to faster and larger systems is the computational cost of the wavefront reconstruction, which is the step where the measurements of the wavefront gradient are converted into phase commands that could be placed on the DM. The traditional implementation of matrix-based wavefront reconstruction is too expensive. An alternate and much more computationally efficient approach is to view the reconstruction process as an inverse filtering problem. Our technique, termed Fourier Transform Reconstruction (FTR), contains a detailed model for the response of the AO wavefront sensor and then uses the Discrete Fourier Transform to apply the inverse Wiener filter. FTR reduces the computational burden for GPI by a factor of 50, allowing the control system to be built with commercially available hardware rather than expensive custom components. Though fast iterative solvers for the matrix approach have been developed, the most efficient still require five times more computation than FTR for GPI.
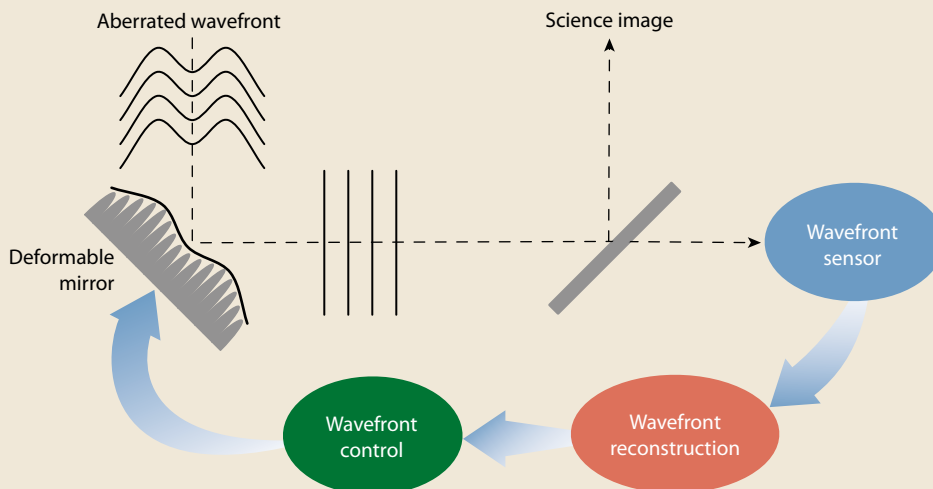


**Figure 1. Adaptive Optics improves image quality by correcting the aberrated incoming wavefront. Correction is performed by phase conjugation with the adjustable surface of a deformable mirror. GPI's advanced wavefront sensing, reconstruction, and control methods enable high-contrast direct imaging.**

## Filtering and Optimizing for Higher Fidelity

A high-frame-rate, high-order AO system is capable of producing an image of a star that is nearly diffraction-limited, though low-contrast (see Figure 2a). In this regime, AO performance is fundamentally limited by the internal aliasing in the wavefront sensor. High spatial frequency phase errors are incorrectly measured as low spatial frequency ones, leading to significant performance degradation in closed loop. Just as an audio signal is low-pass filtered before sampling and A-to-D conversion, the wavefront phase can be low-pass filtered before being measured and sampled by the wavefront sensor. We have developed an anti-aliasing filter that is implemented optically as a field stop in the focal plane in the Shack-Hartmann wavefront sensor. For typical GPI operating conditions, this spatially-filtered wavefront sensor attenuates high spatial frequency phase power by a factor of 1000, essentially removing the aliasing error term. This simple but highly effective solution was immediately adopted internationally by competing and planned future high-contrast AO instruments.

Once the spatially filtered wavefront sensor is in use, the underlying system errors due to sensor noise and temporal lags in the control system are revealed (see Figure 2b). These system errors produce a structured halo of scattered light. This halo of light, which obscures faint planets, can be further reduced by optimizing the AO control system. An existing approach is termed modal gain optimization, in which the control loop gain for each independent mode of the system is estimated from system telemetry using a power-spectral density (PSD) method. We have adapted and improved this approach into a method termed Optimized-gain Fourier Control (OFC). When using FTR, each Fourier mode of the wavefront is uncorrelated and can be controlled independently. Each Fourier coefficient of the residual wavefront is directly available during operation, vastly reducing the computational cost of estimating the signal and noise temporal PSDs. The optimized gains are applied as a separate filter in Fourier space, again achieving substantial computational savings. The final advantage of OFC is that the Fourier modes directly control spatial locations in the high-contrast image: optimizing the control loops directly minimizes the scattered light everywhere that we would look for a planet (see Figure 2c).

Without this adaptive optimization to current operating conditions, GPI's AO system would have suboptimal contrast at nearly all locations inside its control region in the image.

## Predictively Adapting to Atmospheric Changes

The OFC framework allows the controller to adapt to current operating conditions. Nevertheless, the actual integral controller that is used is quite simple. In astronomical AO, layers of wind in the earth's atmosphere can appear to blow turbulence across the aperture in a process termed frozen flow. This creates structure that a predictive controller could exploit. Developing such a predictive controller has been a long-standing challenge in astronomical AO, and has been actively pursued in recent years. We have developed a method, called Predictive Fourier Control (PFC), that is well-founded (based on linear–quadratic Gaussian control), computationally efficient, and uses data-driven adaptation.

Because the Fourier modes are spatially and temporally uncorrelated under frozen flow, each Fourier mode can be predicted independently. This results in a drastic reduction of the model complexity and computational



1e-6        1e-3
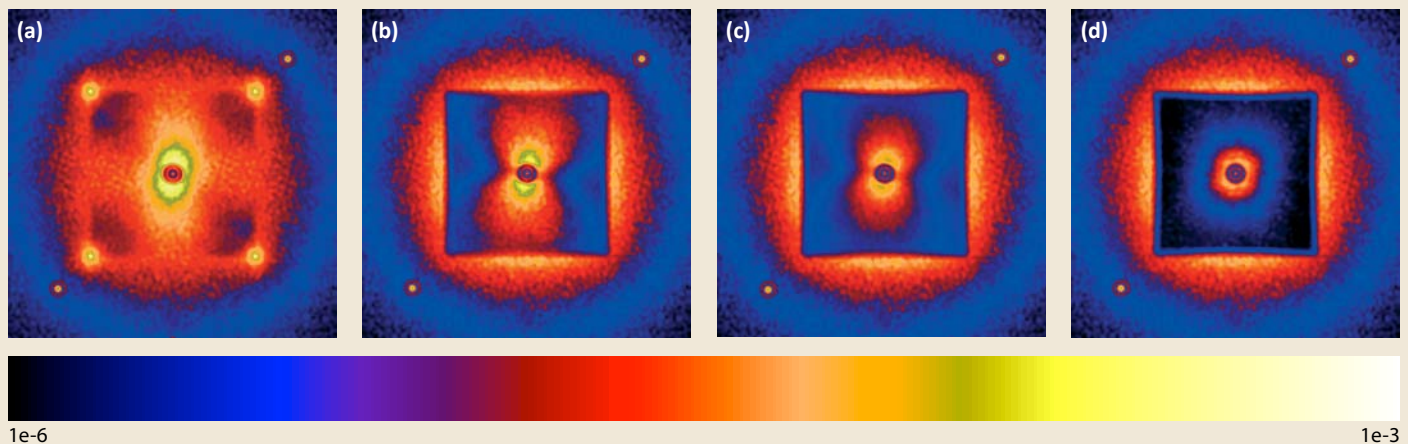
**Figure 2. Simulated GPI AO coronagraphic images demonstrating the performance improvement with new advanced algorithms. Log-scale scattered light levels are from $10^6$ to $10^3$ less than the planet's brightness. (a) FTR enables a system with thousands of actuators. The resulting image is nearly diffraction-limited but has low contrast due to a structured halo of scattered light. (b) The spatially filtered wavefront sensor prevents aliasing and creates a "dark hole" of improved contrast. The remaining scattered light in the dark hole in this simulation is from residual atmospheric and noise errors. (c) OFC determines the optimal controller gain for each Fourier mode during closed-loop operation, resulting in improved performance throughout the dark hole. The hourglass shape of scattered light is due to frozen-flow atmospheric turbulence. (d) PFC detects multiple layers and uses a Kalman filter to predict the turbulence and to further improve contrast.**

cost compared to matrix-based control. Furthermore, the temporal power spectrum of a Fourier mode has a compact and easily identifiable shape under frozen flow: each layer contributes to a narrow peak of power in temporal frequency (see Figure 3a). Hence, specific atmospheric layers can be identified easily using the same closed-loop telemetry and PSDs that we calculate for OFC. For each Fourier mode, PFC constructs a state space model for the AO system and an atmosphere composed of an arbitrary number of wind-blown layers. The

layer parameters of wind velocity and turbulence strength (identified directly from system telemetry) are used in the model to solve the Algebraic Riccati Equation and determine the coefficients of that Fourier mode's Kalman filter. This predictive controller has an elegant structure: for each layer it predicts both the previous command and the just-measured residual, and then optimally weights each layer based on relative turbulence strengths and the overall noise level. Every 10 seconds, the system remeasures the atmosphere (in closed loop while prediction is occurring) and

adjusts the controllers if conditions have changed. Wind prediction further improves contrast (see Figure 2d), and might increase the operating range of GPI by a stellar magnitude. PFC uses the same fundamental framework as OFC and is computationally efficient enough to be used in GPI.

A key assumption of PFC is that the atmospheric phase aberration follows the frozen flow hypothesis. If it does not, a predictive control scheme that uses that model will not succeed. Using extensive observations from both the Keck AO system at Keck Observatory and the Altair AO system at Gemini North, we have detected frozen flow with high likelihood 94% of the time at Mauna Kea. From telemetry, we detect the peaks in the temporal PSDs (see Figure 3b). By analyzing the layers detected in each Fourier mode, we can estimate
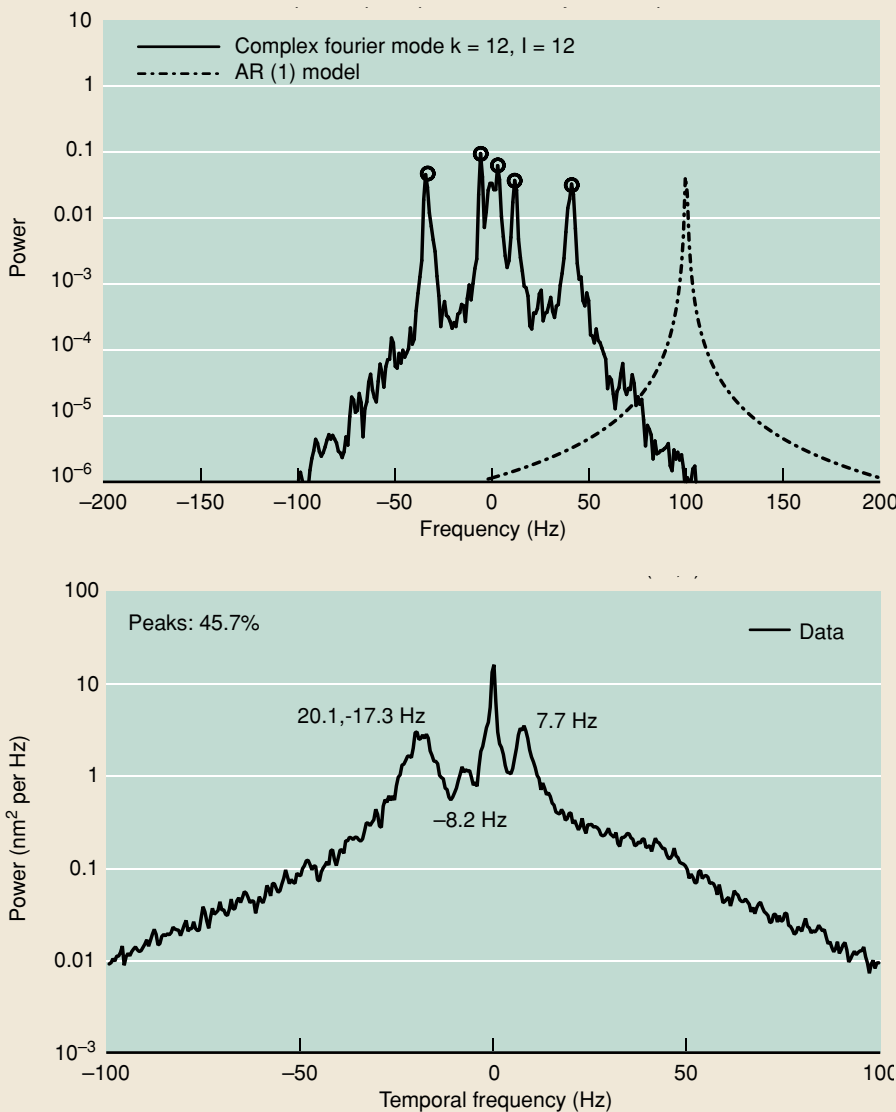




Figure 3. Each layer of frozen flow produces a distinctive peak in the temporal PSD of a Fourier mode as seen by the AO system. (top) A GPI simulation with a pure flow model of five layers. (bottom) Actual observation from the Altair AO system.
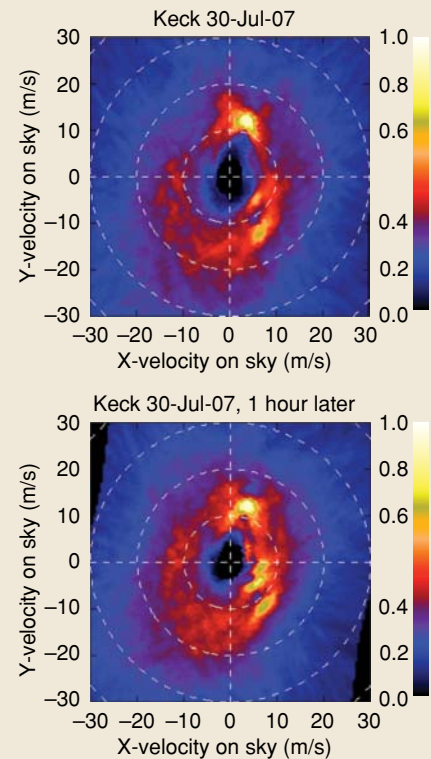




Figure 4. "Windmaps" showing the likelihood of a layer of frozen flow at a given velocity vector, based on analysis of Keck AO system telemetry during regular closed-loop observations. (top) First observation on July 30, 2007. Four layers are easily identifiable. (bottom) One hour later the wind velocities are very similar, and three layers are evident.

the overall atmospheric wind structure (see Figure 4). The frozen flow of the turbulence contributes a substantial amount of power to the phase error, implying that predictive control to specifically correct it would result in a noticeable performance improvement. Furthermore, our study showed that the temporal variation in wind velocity of the layers was small enough that an identify-and-adapt scheme that updated the controller every 10 seconds would be sufficient to keep up with the changing atmosphere.

## The Potential of AO for Exoplanet Discovery

The Fourier reconstructor, the spatially filtered wavefront sensor, and the optimized controller were all validated together in 2011 during the build-and-integration and test phases of GPI's AO system (see Figure 5). Developed after GPI was designed, our predictive controller could be implemented in a system software upgrade after instrument commissioning. We are currently exploring opportunities and collaborations to implement and test the PFC algorithm in the laboratory or on-sky in another astronomical AO system.

GPI will be the world's most powerful astronomical AO system. Recently allocated 890 hours of Gemini observing time over three years, the GPI Exoplanet Survey program will study 600 nearby stars, potentially imaging up to a hundred new extrasolar planets. Through a large-scale survey, the underlying properties of Jovian planets can be characterized and used to understand the mechanisms of planet formation and migration.
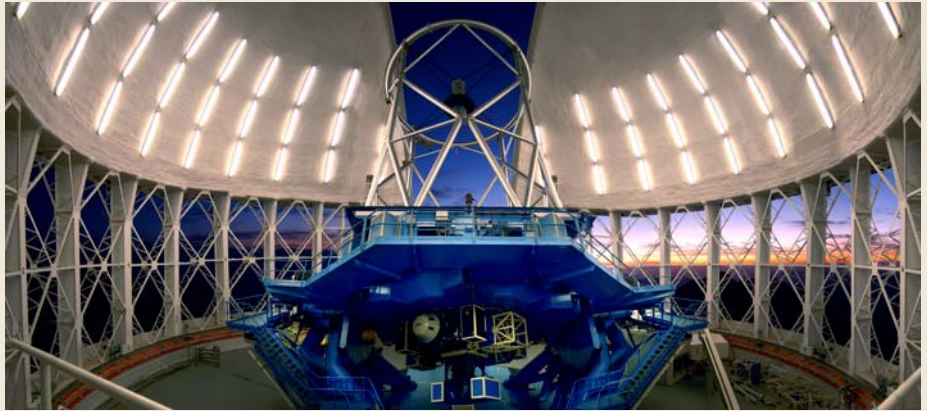


**Figure 5. Interior of the Gemini South Observatory in Cerro Pachón, Chile. (Image credit: Gemini Observatory.)**



**Figure 6. The GPI Instrument in the integration clean room at UC Santa Cruz, July 2011.**

# Fast, Flexible, Automated Sample Preparation to Meet National Biosecurity Challenges

**Maxim Shusteff**
925-423-0733
shusteff1@llnl.gov
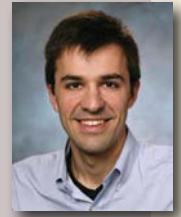
**B**IOSECURITY is increasingly viewed as critical to overall national security. Concerns about biosecurity include not only preparedness for deliberate bioterrorism, such as the anthrax mail attacks of 2001, but also combating natural threats. Indeed, preparedness and response to the spread of infectious diseases may prove to be the defining security and public health challenge of the coming decades. Yet in spite of increased attention at the highest levels of national leadership, key policy and scientific leaders agree that significant improvement is still needed in the areas of pathogen detection and disease diagnosis.

Today's state-of-the-art methods for detection and diagnosis are collectively termed "bioassays," and they aim to identify and quantify pathogen molecular signatures (nucleic acids or proteins). Tremendous progress in this area has been made in recent decades, but the samples collected for analysis often must be extensively preprocessed for an assay to succeed. Current standards for such sample preparation still involve many manual steps, requiring significant effort from skilled laboratory technicians or bioscientists.

Automating and speeding up the required preprocessing is the aim of a team of LLNL engineers and biologists developing technologies for microfluidic sample preparation. This team has built and tested a group of microfluidic "virtual filters" designed to extract broad classes of biological particles from a mixed sample (see Figure 1). The goal is to replace and augment the function of standard laboratory equipment, such as centrifuges, membrane-based filters, and bead-based capture technologies. LLNL's devices separate bioparticles based on intrinsic physical properties, eliminating the need to attach affinity-based labels to the targets. Importantly, no membranes or surface-binding agents are used to accomplish filtration, minimizing sample loss, and allowing both separated fractions to be analyzed downstream when necessary. Finally, the devices are modular, so they can be assembled in any order necessary and quickly reconfigured for a different application. These design principles will make the system compatible with a variety of input samples, such as blood, swabbed material, and environmental aerosols, and many downstream assays, such as polymerase chain reaction (PCR), DNA sequencing, or microarrays. The objective is to create a universal, flexible, nonspecific sample preparation platform (see Figure 2).

**Figure 1. A summary of the common features of LLNL's microfluidic separation devices. A mixed input sample is introduced and flows side-by-side with a clean buffer (the streams do not mix), into which a set of particles is shifted by an applied field. The rest of the sample passes through. Channel dimensions are 10s to 100s of micrometers in width and depth and a few centimeters in length.**
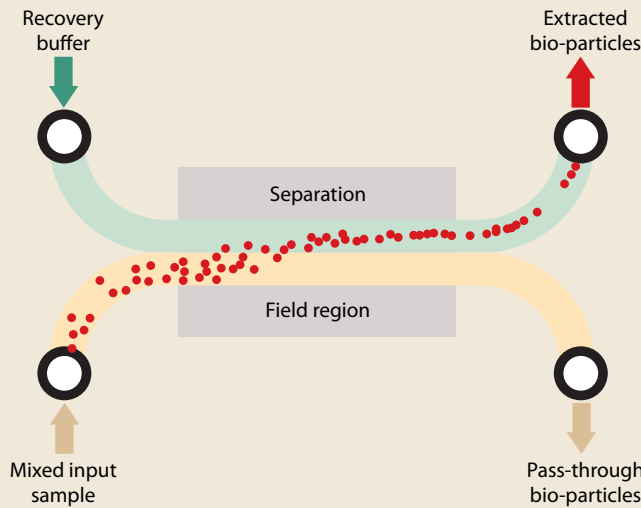


**Figure 2. Possible approaches within the "paradigm space" of sample preparation. LLNL's aim is to design the most universal, widely applicable, and sample agnostic platform.**
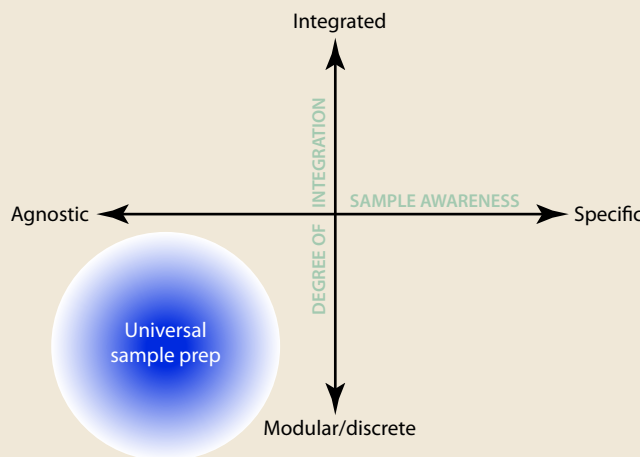


## Advancing the State of the Art for Sample Preparation

Each microfluidic device has at its heart a microfluidic chip approximately 1 cm × 7 cm × 1 mm in size, and uses a different physical mechanism to separate

sample components. Figure 3 shows the approximate sizes of typical bioparticles and the size ranges at which the LLNL devices are effective. Some of these technologies were first demonstrated decades ago, but LLNL engineers have advanced each one into a performance realm relevant to processing samples for biosecurity needs.

A natural approach to sample processing is to work from the largest particles down to smaller ones. Therefore, LLNL's acoustic focusing module is used for extracting particles larger than 2–5 µm in diameter: large (nonbacterial) cells, debris, and pollens. In this device, MHz-frequency ultrasound waves are generated using a piezoelectric crystal. The ultrasound is tuned to resonate as a standing wave in the microfluidic channel, and particles focus into a tight stream at the location of minimal sound pressure amplitude. The strength of the acoustic forces most strongly depends on particle size, giving this filter an effective size cutoff of a few microns. The larger particles flow out a separate chip outlet, while smaller particles pass through unaffected for analysis or further separation downstream.

LLNL's innovation in acoustic focusing is to use a microchannel subdivided by a thin wall, allowing the stream of focused particles to be placed almost anywhere in the separation channel (see Figure 4). Coupled with the use of higher-harmonic

standing waves, this allows for significantly higher separation efficiency and device throughput. This device has been used to separate a large range of sample types, including human epithelial and blood cells, yeast, and viruses, in each case extracting 95% or more of the larger particles, and rejecting 70–90% of the smaller ones.

The next stage in LLNL's sample processing sequence is a dielectrophoretic (DEP) bacterial filter. DEP forces arise from gradients in nonuniform high-frequency electric fields, such as those found at the edges of electrodes with an AC waveform applied. The strength and direction of DEP forces depends on particle size and dielectric
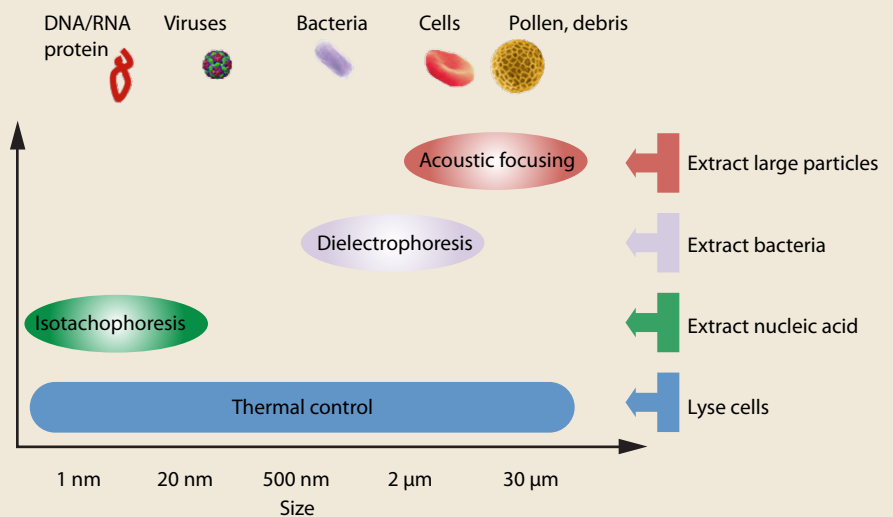


Figure 3. Size is one of the key physical properties by which LLNL's devices separate samples. This figure shows typical particles that can be manipulated by each of LLNL's four modules.
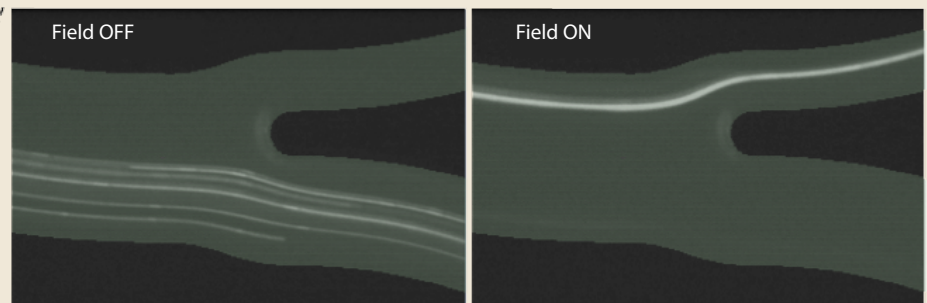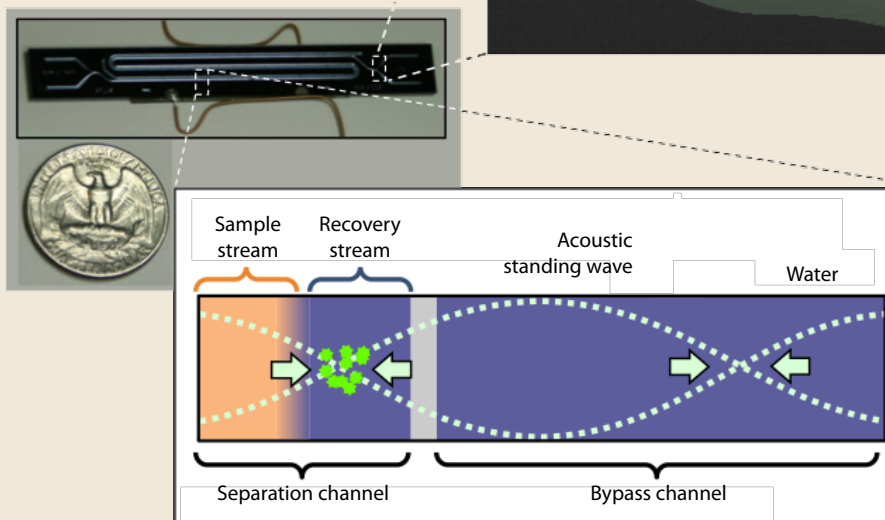


Figure 4. The photo of LLNL's acoustic chip shows its size compared with a quarter. The bottom inset is a cross-sectional sketch of the microchannel: particle focusing and separation takes place to the left of the wall, and the fluid to the right of the wall simply provides a larger resonant cavity for the ultrasound. The fluorescence microscopy images of the chip outlet at right show clean transfer of cell-size particles from one outlet into the other.

properties, as well as applied signal frequency and the conductivity of the fluid. This multidimensional parameter space means that DEP devices can achieve a rich variety of effects, but also makes them challenging to design.

To successfully build a DEP bacterial extraction device, LLNL microfluidics engineers aimed to overcome three major limitations that typically constrain the utility of other DEP devices: particle size, fluid throughput, and solution conductivity. Reports in the published literature typically manipulate large particles (cell-scale of 5–15 μm) at very low flow rates (1–5 μL/hr) in nearly de-ionized conditions (0.01–0.1 mS/cm). In contrast, LLNL has recently demonstrated filtration of *E. coli* bacteria (rod-shaped, 0.5 × 2 μm) at a 50-μL/min flow rate, in nearly physiological conductivity (2 mS/cm). Figure 5 summarizes these results.

The innovation that enables this was conceived and developed by LLNL postdoctoral researcher Dietrich Dehlinger. The key is a pair of electrodes on the top and bottom of the microchannel, placed at a constriction (mesa) within the channel (see Figure 6), which creates a very narrow gap (approximately 5–10 μm) between the electrode edges. The narrow gap forces the particles to pass near the electrode edges, where DEP forces are strongest. In addition, the mesa is positioned at an angle to the fluid flow. These design features are the key to the optimal force balance, which enables the device's superior performance. In essence, a force field is created that prevents bacteria from passing through the mesa constriction, shifting them into the adjacent buffer stream, while smaller particles (*e.g.*, cell-free viruses, dissolved biomolecules) continue unimpeded.

The third separation device in the Laboratory's microfluidic toolkit performs nucleic acid extraction using a DNA focusing method called isotachophoresis (ITP). This approach promises a number of advantages over standard solid-phase extraction (SPE) methods for DNA, such as improved recovery of low-abundance samples and increased automation. ITP focuses the analyte of interest between two ionic buffers, one moving faster, and one slower under applied electric fields. As these ions migrate due to the applied field, the analyte becomes spatially confined between the faster and slower ions. Unlike in a gel, where mobility is size-dependent, nucleic acids in solution all have approximately equal mobilities, so buffers can be chosen to focus all the DNA and RNA to one location.

Conventional ITP is performed in capillary tubes, so volumes above a few microliters cannot be processed. LLNL engineers have teamed with staff from Prof. Juan Santiago's laboratory at Stanford, experts in standard capillary ITP, to design a device in which the electric field is applied transversely to the
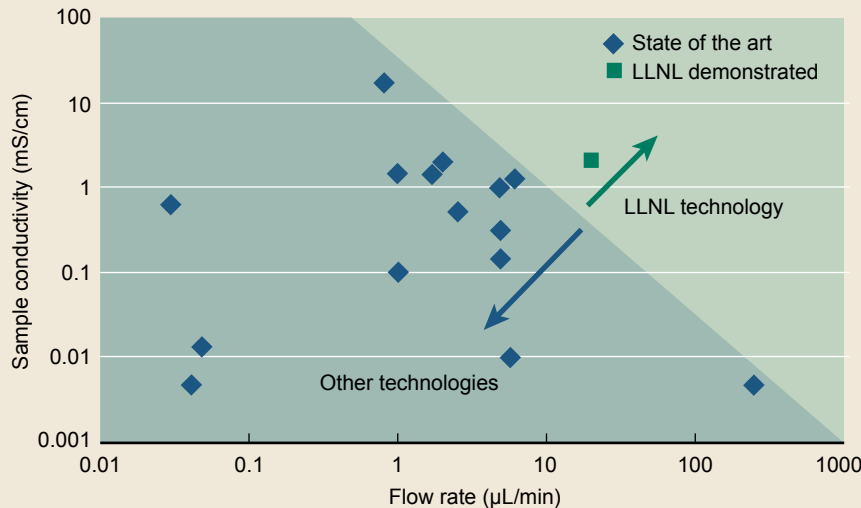


**Figure 5. This plot highlights the advantage of LLNL's DEP device over alternative technologies.**
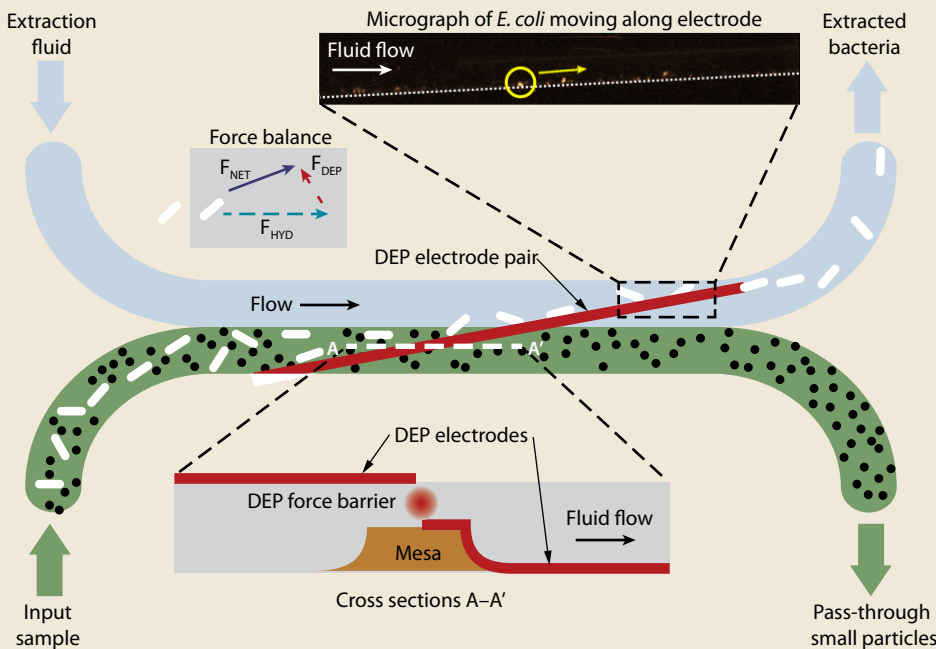


**Figure 6. A schematic of LLNL's DEP device shows the angled placement and geometry of the constriction (mesa) in the fluid channel. This enables the critical balance between DEP and hydrodynamic forces that allows bacteria-size particles to be filtered out at high flow rates.**

continuously flowing sample (see Figure 7). This design allows the processing of much larger (mL-scale) sample volumes, with the nucleic acids focused into a tight band steered into its own separate outlet, away from contaminating species. Preliminary measurements indicate 60–90% DNA recovery from the device. The LLNL team is currently further quantifying DNA throughput and contaminant removal and optimizing performance.

The final device in LLNL's microfluidic toolkit performs thermal lysis of cells. Using an attached resistive heater, the chip is heated to 90–95 °C, which is sufficient to lyse (break open) most cells. The advantages of this approach are its simplicity compared with chemical or mechanical lysis methods, and its fast, efficient heat transfer compared with bulk-volume benchtop techniques. Some cell components (*e.g.*, small molecules like ATP) come out of cells after only 10 seconds of heating. To recover significant quantities of cellular DNA, cells must be heated for at least a minute, but even at slower flow rates, 1 mL samples can be processed in about 10 minutes.

## New Sample Processing Paradigm Enables New Capabilities

One key advantage of LLNL's modular, reconfigurable, end-to-end system architecture is that samples can be processed through the modules in any order, enabling a great variety of applications. For instance, extracellular viruses from a nasal rinse sample can be purified by first using the acoustic device to filter out cells, then filtering out bacteria with the DEP chip, and finally removing extracellular DNA using the ITP device. This is the only effective approach when trying to sequence the genomes of unknown viruses, as their tiny genomes are otherwise drowned out by the much-larger host or bacterial genomes. An entirely different application of LLNL technologies is speeding up and improving DNA profiling for human identification in bioforensics. Human genomic DNA can be extracted from a

blood sample by first collecting the human cells with the acoustic filter, then lysing them, and using the ITP device to purify and collect the released genomic DNA. The LLNL team is currently testing the performance of its system with a range of forensic samples, including bloodstains, fingerprints, and cheek cells.

The Laboratory's vision for sample preparation is to develop a system that enables us to ask and answer new kinds of questions. Until now, biodetection technologies could only ask, "Is a

particular agent (such as anthrax) present?" With LLNL's modular toolbox (see Figure 8), we can move toward being able to answer the question "What is present in this sample?" As such, this architecture enables new capabilities such as metagenomic analysis, in which we may need to track the entire bacterial or viral population in a given sample and monitor its evolution over time. Looking toward a system integration effort, we anticipate that a truly universal sample preparation platform is within reach.
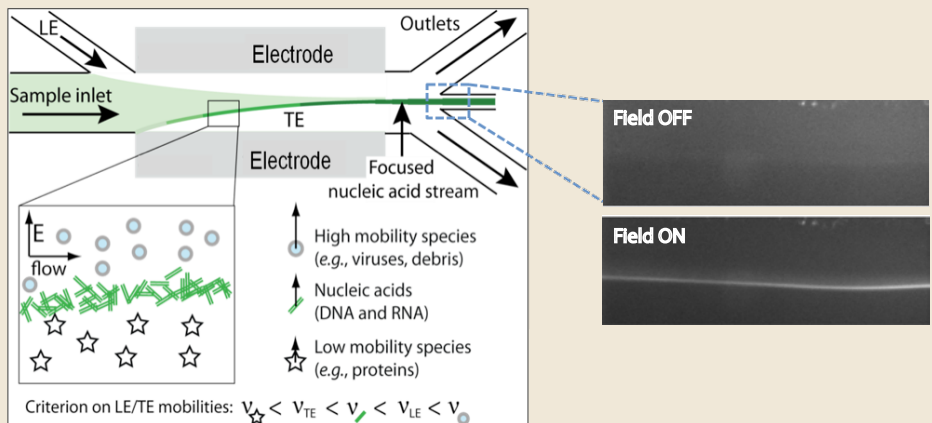


**Figure 7. A sketch of the physical mechanism that enables DNA focusing by transverse free-flow ITP. Migrating ions line up in order of their mobilities under the transversely-applied electric field, with nucleic acids focusing into a tight band. The images at right show focusing of fluorescently-stained DNA.**
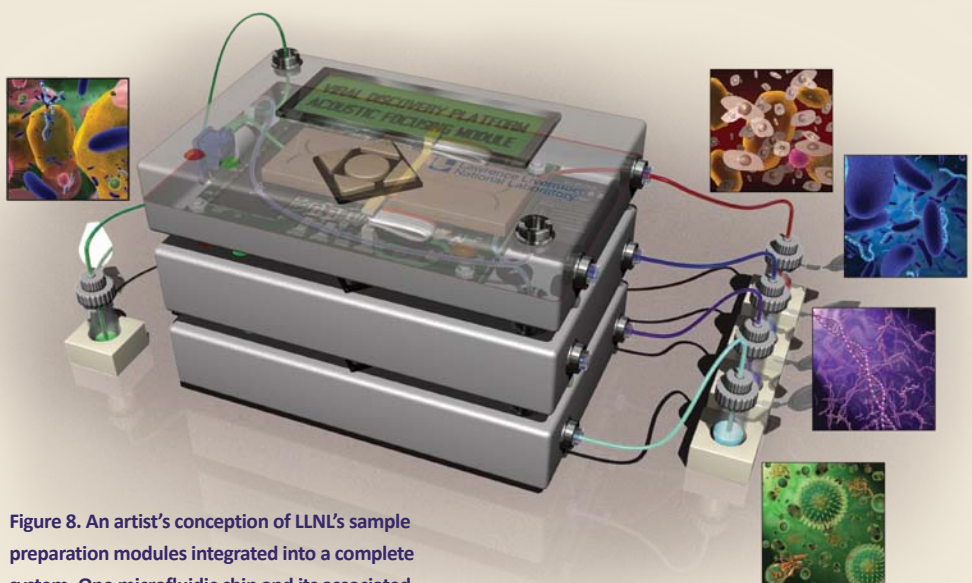


**Figure 8. An artist's conception of LLNL's sample preparation modules integrated into a complete system. One microfluidic chip and its associated pumps, valves, and electronics is at the heart of each textbook-sized device in the stack.**
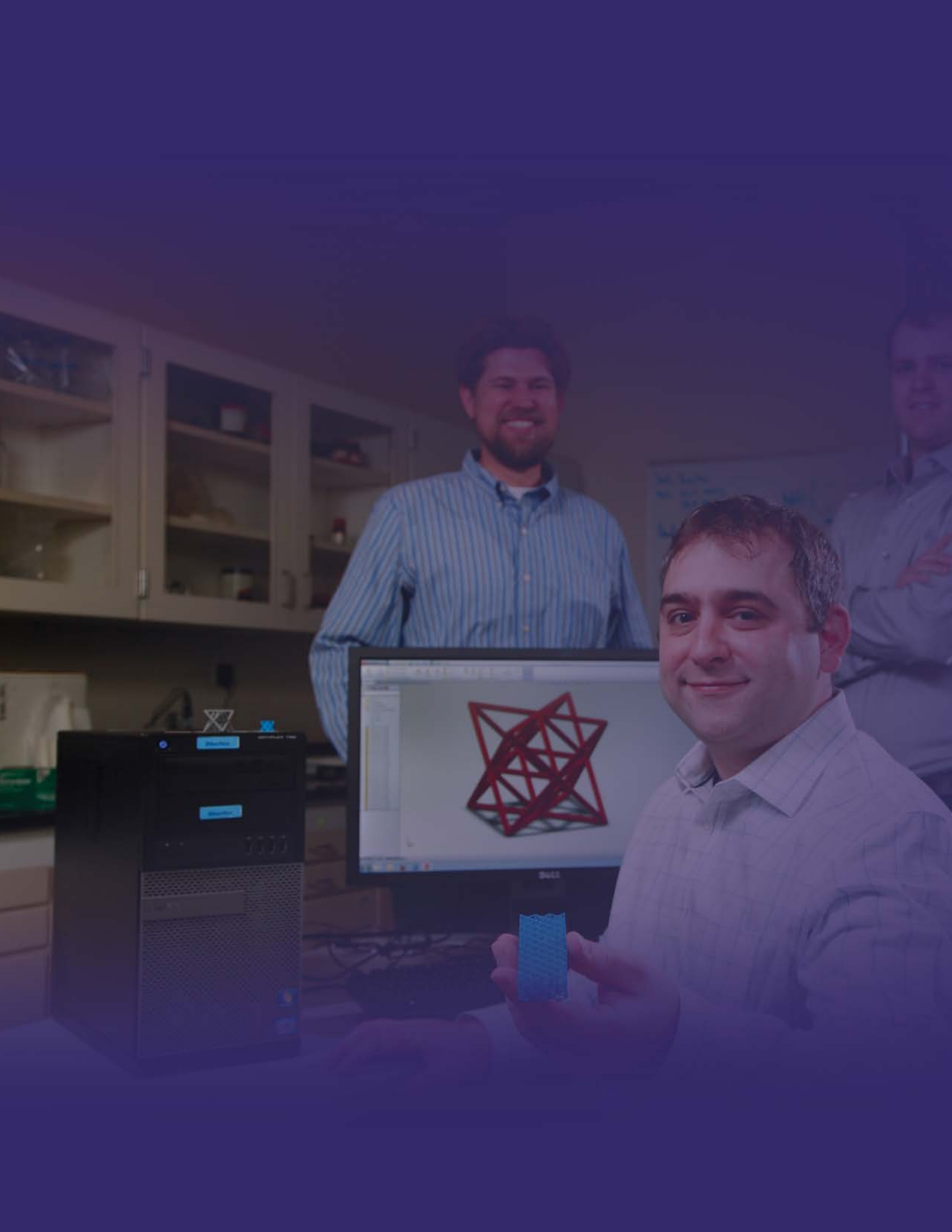
# Advanced
# Manufacturing

# Disruptive Fabrication Technologies Initiative

**Christopher M. Spadaccini**
925-423-3185
spadaccini2@llnl.gov

## Project Overview

This project aims to fundamentally understand and develop new additive micromanufacturing techniques that enable both designer materials and 3-D mesoscale structures. To achieve these goals the processes must: 1) be compatible with multiple materials such as polymers, metals, and ceramics, and be capable of creating heterogeneous structures; 2) be able to produce complex 3-D mesoscale geometries with micron scale precision; and 3) be scalable to eventually achieve high manufacturing volumes at low cost.

There are no current fabrication technologies that adequately address all of these needs. Projection Microstereo-lithography (PµSL), Direct Ink Write (DIW), and Electrophoretic Deposition (EPD) have the potential to impact these needs. We are developing this tool set. Figures 1, 2, and 3 are process schematics for these technologies.

Material properties are governed by the chemical composition and spatial arrangement of constituent elements at multiple-length scales. This fundamentally limits material properties with respect to each other, creating trade-offs when selecting materials for a specific application. For example, strength and density are inherently linked so that, in general, the more dense the material, the stronger it is in bulk form. Other coupled material properties include thermal expansion and thermal conductivity, hardness and fracture toughness, and strength and thermal expansion. The coupling between these properties creates significant unpopulated, yet potentially desirable design spaces that cannot be accessed using standard material synthesis methods such as alloying. Properties of materials may be decoupled via control of the micro- and nanostructure; however, the appropriate fabrication and manufacturing tools are not currently available to realize these goals.
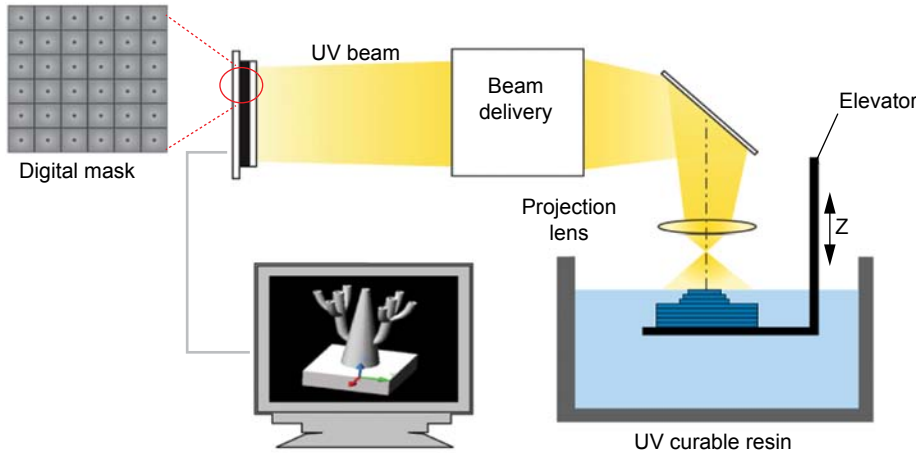


Figure 1. Process schematic of PµSL. A CAD model is sliced into a series of closely spaced horizontal planes. The slices are digitized as an image and transmitted to a spatial light modulator that projects the image through a reduction lens into a bath of photosensitive resin. The exposed material cures and the substrate on which it rests is lowered to repeat the process with the next image slice.
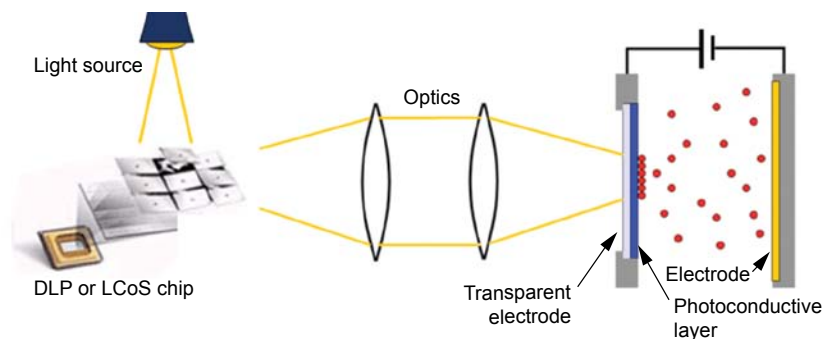


Figure 2. Process schematic of EPD. Electric fields are used to deposit charged nanoparticles from a solution onto a substrate. Once the particles are deposited, the green body can be post-processed to produce the final part.

## Project Goals

Our overall project goals are to:
1. Investigate and understand the physics associated with each process that we are developing via parametric experimentation and modeling;
2. Demonstrate the use of metals, ceramics, and polymers in each process by incorporating nanoparticles of these materials into a suspension or colloidal gel compatible with the specific process;

3. Demonstrate fabrication of arbitrary 3-D mesoscale structures with microscale features and precision; and

4. Design and fabricate a "new" material with specified properties (*e.g.*, stiffness vs. weight) outside the bounds of those attainable with bulk materials processed via traditional synthesis methods. The new material will demonstrate the properties that can be obtained by controlling the structure's architecture at the microscale.

The specific goals for FY2011 were to:

1. Fabricate 3-D, microscale structures with minimum features sizes (~ tens of μm);

2. Produce a microstructured material with high Young's modulus and low density;

3. Build and characterize a microstructured functional material with high propagation velocity and high energy density; and

4. Demonstrate integration of fabrication processes to create heterogeneous structures.

## Relevance to LLNL Mission

There are a host of LLNL programmatic applications for this work, including, but not limited to, high-energy-density targets and laser fusion targets that can be 3-D, mesoscale, and multi-material; stockpile stewardship; WCI's fabrication toolkit; and the energy and environment program.

## FY2011 Accomplishments and Results

Significant progress has been made during FY2011, including:

1. The fabrication of the smallest known embodiment of the "octet truss," a high-stiffness low-density structure (Figure 4);

2. The experimental validation of an EPD process model that correctly predicts the packing orientation of nanoparticles for varying electric field strengths;

3. A demonstration of improved energetic material performance by depositing thermite materials with EPD. At least a 2x power density over conventional



Pressure
Nozzle
Printed filament
Print speed ≈ flow rate ≈ Solidification rate
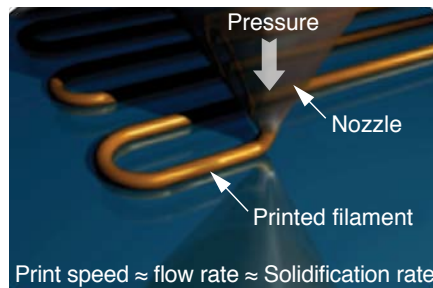
**Figure 3. Process schematic of DIW, a layer-by-layer printing approach in which concentrated inks are deposited in planar and 3-D layouts with lateral dimensions (minimum ~200 nm). Paramount to this approach is the creation of concentrated inks that can be extruded through a fine nozzle as filament that then undergoes rapid solidification to maintain its shape.**

deposition has been shown with further improvements expected; and

4. A demonstration of combining DIW with EPD to form the heterogeneous multi-material structure shown in Figure 5.

## FY2012 Proposed Work

In FY2012 we expect to accomplish the following:

1. Expand the usable material set for all of our fabrication technologies to include metallic, polymeric, and ceramic materials;

2. Generate heterogeneous multi-material microstructures with a single fabrication technology;

3. Improve the performance and control the energy release rates of thermite materials beyond the current demonstration by designing and fabricating the microstructure; and

4. Fabricate and test lattices of the high-stiffness low-density octet truss.

## Related References

1. Cox, A., C. Xia, and N. Fang, "Microstereo-lithography: A Review," **55**, *ICOMM*, 2006.

2. Sun, C., et al., "Projection Microstereolithography Using Digital Micro-Mirror Dynamic Mask," *Sensors and Actuators: A Physical*, **121**, pp. 113–120, 2005.

3. Lewis, J. A., "Direct-Write Assembly of Ceramics



SEM
100 μm
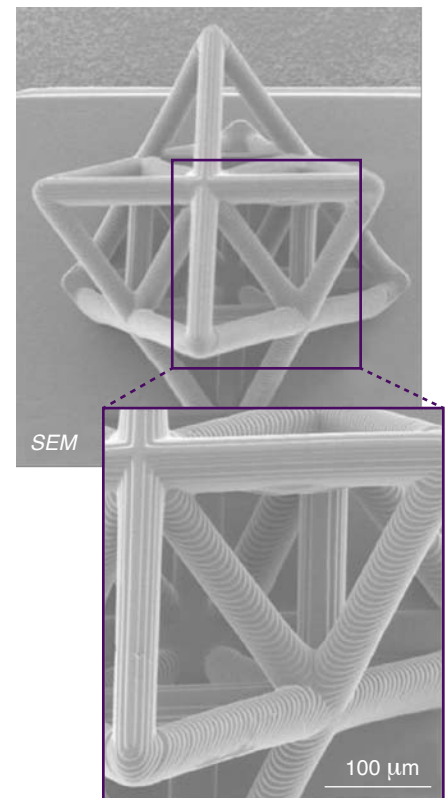
**Figure 4. The smallest known embodiment of the octet truss, fabricated with PμSL.**



DIW lattice
1.5 mm
EPD backfill with nanoparticles
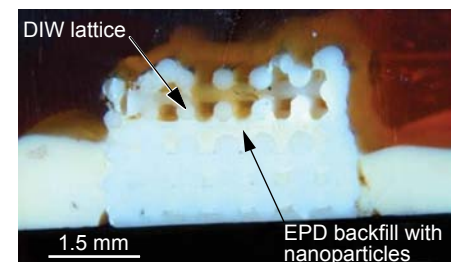
**Figure 5. EPD combined with DIW to backfill a lattice with nanoparticles to obtain unique combinations of materials in a single structure.**

from Colloidal Inks," *Curr. Opin. Solid State Mat. Sci.,* **6** (**3**), pp. 245-250, 2002.

4. Smay, J. E., J. Cesarano, and J. A. Lewis, "Colloidal Inks for Directed Assembly of 3-D Periodic Structures," *Langmuir*, **18** (**14**), pp. 5429–5437, 2002.

5. Besra, L., and M. Liu, "A Review on Fundamentals and Applications of Electrophoretic Deposition (EPD)," *Progress in Materials Science*, **52**, pp. 1–61, 2007.

# Massively Parallel Multi-Axis Micro-Reflector Array for High-Speed Directed Light-Field Projection

**Jonathan B. Hopkins**
925-423-5569
hopkins30@llnl.gov

## Project Overview

The purpose of this project is to fabricate and test a massive array of tightly-packed (95%) micro-mirrors (50-x-50 array, each 1 mm x 1 mm) that may be independently controlled in two axes (tip and tilt) at high speeds (> 5 kHz) over large ranges (±10 degrees). Some applications of this array include high-definition multi-threaded auto-stereoscopic displays, bullet defeat force fields, and high-speed, multi-material, nanomanufacturing 3-D printers. A CAD model of a 3-x-3 array of the mirror configuration is shown in Figure 1 along with the layer details of a single mirror.

## Project Goals

The project goals were to select an array configuration, and to learn how to and begin to fabricate a 3-x-3 array of mirrors, where each 4-mm-x-4-mm mirror's dimensions have been scaled up fourfold.

## Relevance to LLNL Mission

The realization of the proposed mirror array would enable a number of useful applications that would be directly applicable to the mission of LLNL. The most prevalent application for LLNL's LIFE project is beam steering for tracking and igniting the deuterium capsules fired into the fusion chamber. Another application important to the Laboratory's defense mission is that of shooting down close-range, high-speed bullets/projectiles with focused laser beams that are rapidly steered using the mirror array. The mirrors could also be used to simultaneously corral, place, and sinter millions of various nanoparticles as 3-D printed structures using the principle of optical tweezers. This application directly supports an ongoing LLNL project on disruptive fabrication initiative. Furthermore, the mirror array project will bring the Laboratory future sources of funding and opportunities for research collaborations with other institutions.



Figure 1. Micro-mirror array configuration.

## FY2011 Accomplishments and Results

We have successfully selected a micro-mirror array, shown in Figure 1. We conducted experiments for assessing the feasibility of the most challenging fabrication features. We conducted these experiments and were
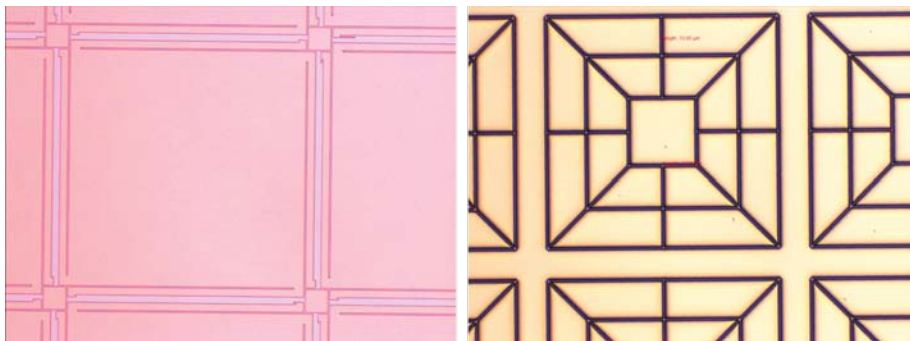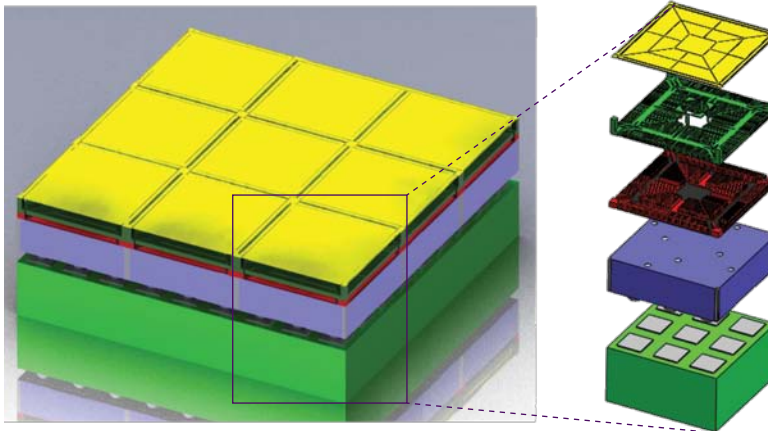


Figure 2. Mirrors in progress.

successful in implementing the final fabrication process for creating a 3-x-3 array of 4-mm-x-4-mm mirrors. We then fabricated the two most critical layers of the final mirror array, shown in yellow and green in Figure 1. We oversaw the fabrication of the bottom layers, shown in red and blue in Figure 1. Images of each layer for the complete device are shown in Figures 2 through 5.

## FY2012 Proposed Work

In FY2012, we intend to have the 3-x-3 array of 4-mm-x-4-mm mirrors assembled and tested. We plan to fabricate and test a 3-x-3 array of 1-mm-x-1-mm mirrors and to have an array that is capable of achieving our target range and speed. We also plan to test the software and electronics for independently controlling each mirror in a coordinated fashion, and to fabricate the final 50-x-50 mirror array. We will then be ready to use this final mirror array for the various applications described above.

## Related References

1. Bernstein, J., et al., "Two-Axis-of-Rotation Mirror Array Using Electromagnetic MEMS," *IEEE MEMS*, Kyoto, Japan, January 19–23, 2003.
2. Tsai, J., and M. C. Wu, "Gimbal-Less MEMS Two-Axis Optical Scanner Array with High Fill Factor," *Journal of Microelectromechanical Systems*, **14**(**6**), pp. 1323–1328, 2005.
3. Katoh, S., T. Nanjyo, and K. Ohtaka, "A Two-Dimensional MEMS Mirror Array Device Based on New Structure," *Ricoh Technical Report 33*, December 2007. *http://www.ricoh. com/about/company/technology/tech/021. html*.
4. "NAOS—Nasmyth Adaptive Optics Systems: Technical Features," *ONERA*, *http://www. onera.fr/conferences-en/naos/ caracteristiques-techniques-conica.php*, accessed January 22, 2011.
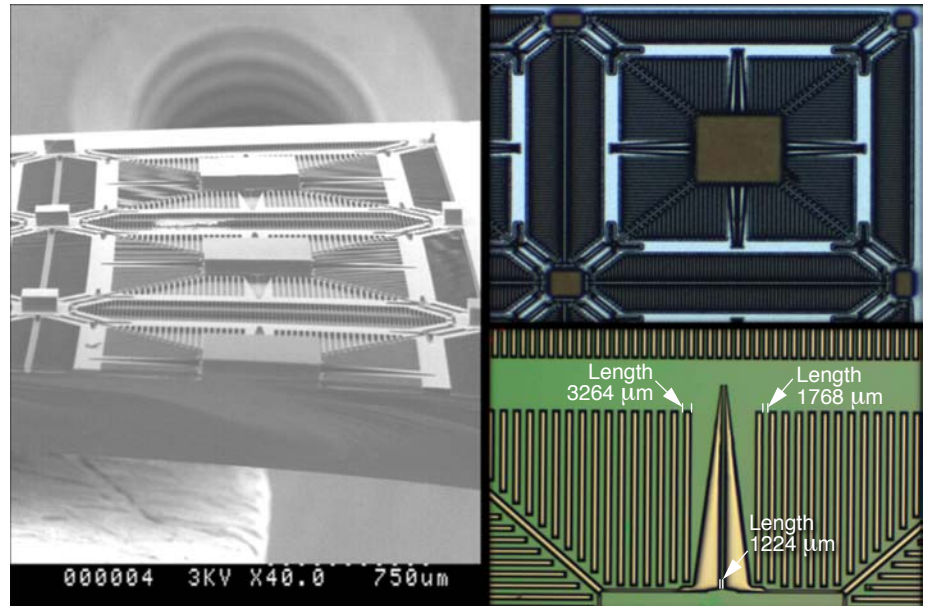
**Figure 3. Rotary comb shuttles.**
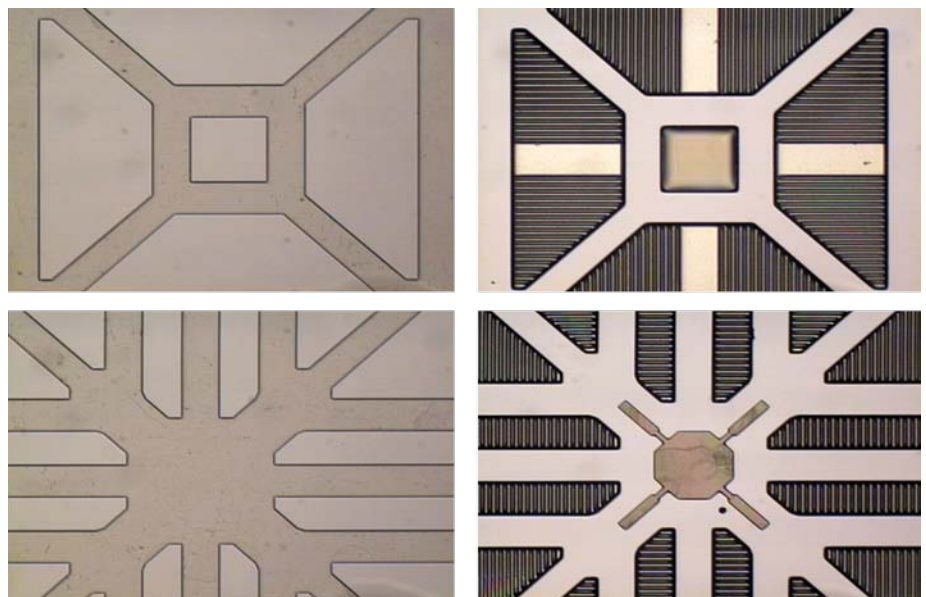


**Figure 4. Back plate comb pads.**
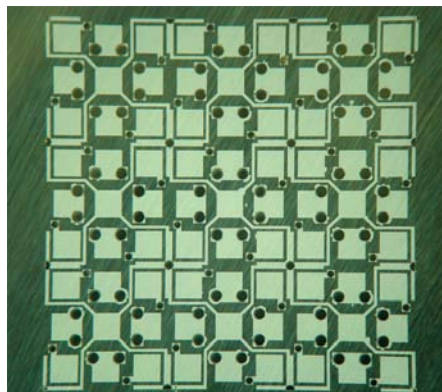


**Figure 5. Back plate traces and vias.**
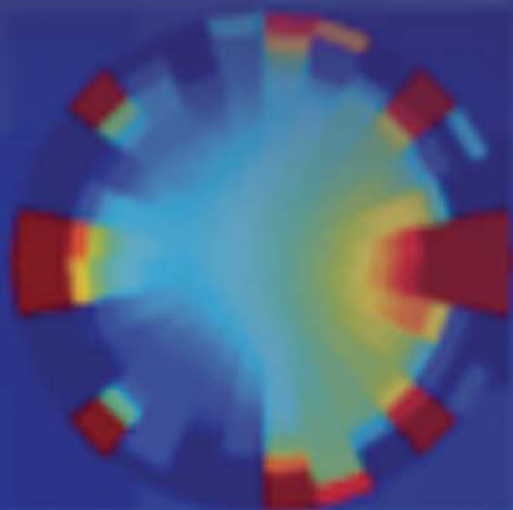
# Computational Engineering

# In Situ Observation and Characterization of Phase Transformations and Twinning

**Joel V. Bernier**
925-423-3708
bernier2@llnl.gov
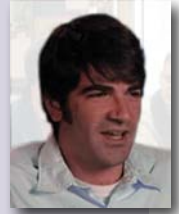
## Project Overview

Martensitic phase transformations (MPT) and mechanical twinning (MT) are complex phenomena observed in crystalline materials, including metals, ceramics, minerals, and high explosives. Both can have significant effects on critical material properties, such as equation of state, strength, conductivity, and magnetism. In situ observations at the nanometer scale are essential for discovering and characterizing the phenomenology required for formulating, validating, and verifying advanced constitutive models. The recent availability of large, fast flat-panel detectors at high-energy synchrotron x-ray sources, such as the Advanced Photon Source (APS) has enabled the development of novel experimental techniques that have the potential to address this deficiency.

**Measured intensities on the unit sphere (equal-area projection) for the indicated crystallographic planes of ε-iron immediately following the phase transition. The glyphs indicate the locations of diffracted intensity predicted by both models relative to the original crystal orientation. The "splitting" is an unambiguous signature of the Burgers mechanism.**



$\epsilon\{01\bar{1}0\}^-$

$\epsilon\{01\bar{1}0\}^+$

15.1GPa

$\epsilon\{01\bar{1}0\}^-$

$\epsilon\{01\bar{1}0\}^+$

□ Burgers A
○ Bain
◇ Burgers B
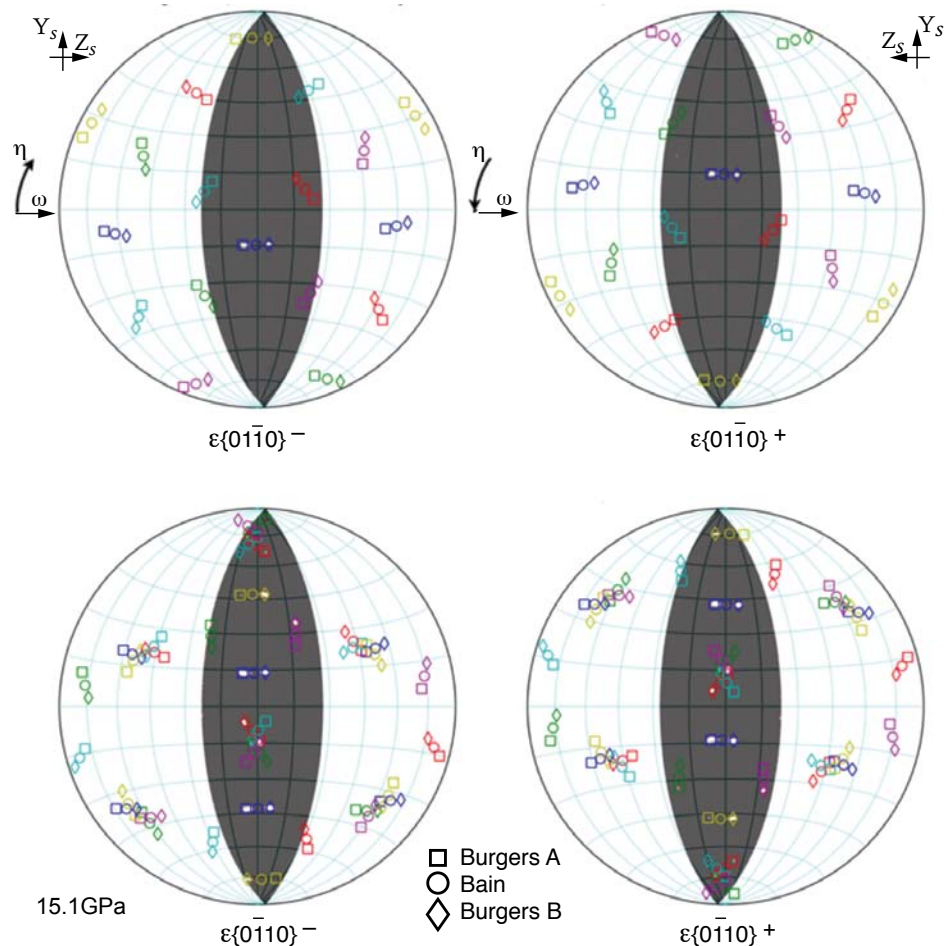
## Project Goals

Our goal is to develop a fully 3-D, in situ characterization technique capable of 1) identifying the orientations and centers of mass of individual parent/product domains (≤ 0.05° and ≤ 5 μm, respectively) in polycrystalline aggregates containing up to 1000 grains; 2) calculating average strain/stress tensors over each of these domains with strain resolution of at least 0.0001; and 3) accommodating quasistatic thermomechanical loading in situ up to 100 GPa and 1000 K using a diamond anvil cell (DAC).

The technique, referred to as High-Energy Diffraction Microscopy (HEDM), is essentially a high-energy (*i.e.*, ≤ 40 keV) analog of the classical rotation method. Our project is developing this capability, including hardware, methodologies, and analysis software, and applying them to material systems of interest to the missions of the Laboratory.

## Relevance to LLNL Mission

This work contributes directly to LLNL's technical proficiency outlined under the Science, Technology, and Engineering pillars, encompassing Materials on Demand and Measurement Science and Technology. High-fidelity materials models also comprise a critical piece of the multiphysics simulation codes used at LLNL in support of Stockpile Stewardship Science goals.

Other fields benefiting from an enhanced understanding of twinning and phase transformations include geophysics (*e.g.*, paleopiezometry and planetary interiors) and industrial deformation processing (*e.g.*, forming of low-symmetry metals like magnesium). Direct observations of these phenomena in situ at the crystal scale represent first-of-kind discovery-class science.

## FY2011 Accomplishments and Results

In addition to major developments in the analysis software, we obtained the first direct experimental evidence that the BCC→HCP phase transformation in iron follows a mechanism proposed by Burgers at quasistatic loading rates and ambient temperature. This result is significant because two distinct mechanisms, the "Bain" and the "Burgers" paths, have been proposed in the literature.

The Bain path has never been observed directly in experiments, but has been predicted by large-scale molecular dynamics simulations corresponding to very high deformation rates. No direct observation of the Burgers path had previously been made, although it has enjoyed more favor in the high-pressure community due to its similarity to other shear-driven martensitic transformations.

The correct mechanism has never been determined because the orientation difference between the HCP variants they produce is only ~ 5°, which is beyond the resolving power of traditional diffraction methods. The HEDM method provides the necessary resolution (see figure).

## FY2012 Proposed Work

The experimental program of FY2012 involves several new studies, including 1) high temperature and pressure study of the $\alpha \rightarrow \gamma$ and $\gamma \rightarrow \varepsilon$ phase transitions in iron with the goals of isolating the transformation mechanisms and obtaining a single crystal of $\varepsilon$-iron; 2) high pressure study of the $\alpha \rightarrow \omega$ phase transformation in zirconium; and 3) high pressure study of the $\alpha \rightarrow \gamma$ phase transformation in cerium. Zirconium is of interest due to its importance in the nuclear industry; cerium's bizarre behavior has been previously studied at LLNL.

Deformation in the high-pressure phase fields will also provide data that informs mechanism-specific strengths, which are critical for modeling efforts.

Also in FY2012, our open-source analysis software package, HeXRD, will be released for public distribution to the greater synchrotron user community.

## Related References

1. Bernier, J. V., N. R. Barton, U. Lienert, and M. P. Miller, "Far-Field High-Energy Diffraction Microscopy: A Tool for Intergranular Orientation and Strain Analysis," *J. Strain Anal. Eng.*, **46** (**7**), pp. 527–547, October 2011.
2. Edmiston, J. K., N. R. Barton, J. V. Bernier, G. C. Johnson, and D. J. Steigmann, "Precision of Lattice Strain and Orientation Measurements Using High-Energy Monochromatic X-Ray Diffraction," *J. Appl. Cryst.*, **44**, pp. 299–312, 2011.

# Computational Studies of Blast-Induced Traumatic Brain Injury Using High-Fidelity Models

**Michael J. King**
925-422-0627
king74@llnl.gov

## Project Overview

Traumatic brain injury (TBI) has become the signature injury of modern warfare. However, the specific biomechanical pathways by which the brain can be injured are not well understood. Significant traumas like impacts, abrupt head rotations, or blast waves are known to damage the brain and cause symptoms of TBI. The specific pathways by which these traumas load and damage the brain tissue are still unknown, although many hypotheses have been proposed.

Our work seeks to use high performance computation in partnership with experimental studies conducted by collaborators to improve the understanding of brain injury event and correlate mechanical loads in the brain tissue with the observed damage, in order to elucidate the biomechanical pathways by which the brain is damaged. Once validated against animal models, we plan to apply the same techniques to study the damage mechanisms in humans.

## Project Goals

Our goals are to use high fidelity computation to study how various traumas create localized mechanical loads of various kinds in the brain, and to correlate which of these loads, if any, correspond to observed injuries. Once we have determined what kinds of localized mechanical loads lead to brain damage, we can apply the same techniques to computer models of human brains in both impact and blast injury events, with the intent of developing better protective strategies, diagnoses, or treatments.

## Relevance to LLNL Mission

Over the last several decades, LLNL has developed massively parallel computational capabilities and corresponding simulation capabilities for modeling blast and impact insults on structures. We are applying this technology to a different kind of structure—the human brain—leveraging LLNL's scientific investment to tackle a problem vital to the national interest.

## FY2011 Accomplishments and Results

Figures 1, 2, and 3 represent our results. In the first year of this effort, we developed the computational machinery for transforming 3-D medical images (MRI or CT) into high fidelity finite element meshes of the head and
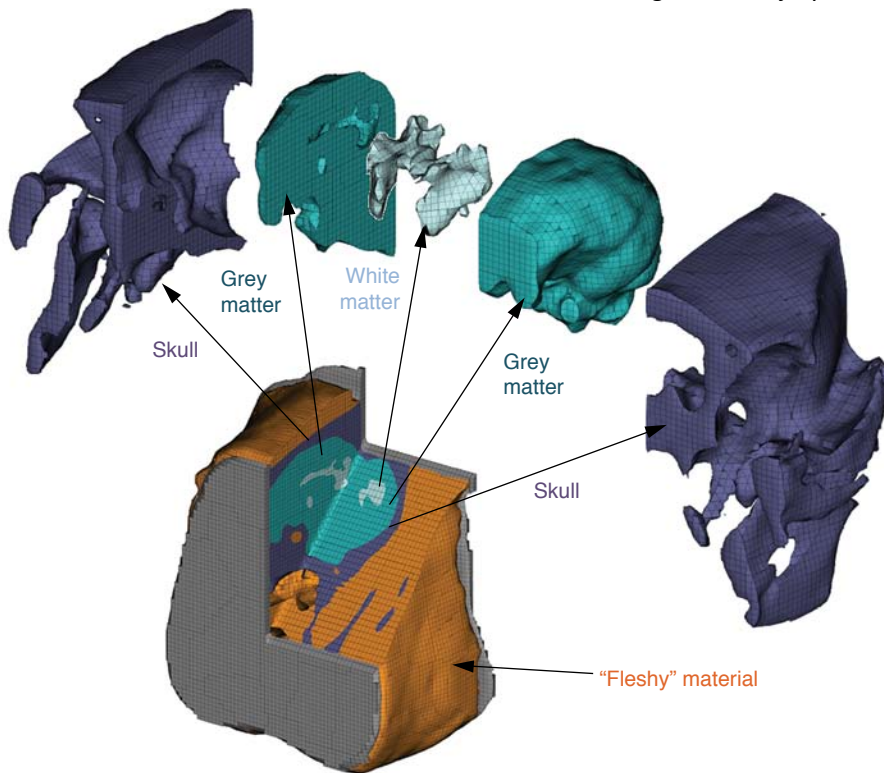


Figure 1. Regions of one pig head model, showing a moderately high fidelity brain and skull.

Grey matter
White matter
Skull
Grey matter
Skull
"Fleshy" material

brain. We have used these techniques to create accurate models of the heads of the pigs used in the UPenn CBIR experiments. We then populated these models with the most up to date material properties reported in the literature, and simulated the injury experiments conducted at the CBIR. We have explored how experimental variations in the loading function could affect the character of the forces, and hence the injury, in the brain tissue. Specifically, for rotationally-induced injury, we have studied the effects of varying both the peak rate of rotation, and the rate of change of the rotational velocity. We have begun to perform initial correlations between experimentally observed damage and localized mechanical loads in our brain models.

We have also created a high fidelity model of a human head using publically available 3-D MRI and CT images. We are working to integrate this model into realistic impact and blast simulations.

## FY2012 Proposed Work

We are currently working to expand our simulation capabilities to capture effects of anisotropy in the white matter in the brain, and investigate the effects of loads that align with the axonal tracts compared to loads that act in other directions. This is a vital step toward completing the correlation between simulation-predicted mechanical loads and experimentally observed damage pathways. We are also working with the CBIR to conduct further experiments with more detailed scans, allowing us to conduct higher fidelity simulations. The key milestone of this work will be identification of any quantifiable mechanical loads in the simulation that correlate to observed damage.

We then will conduct impact and blast simulations on a human head model, and determine if and how these events cause localized mechanical loads that have been correlated with injury.
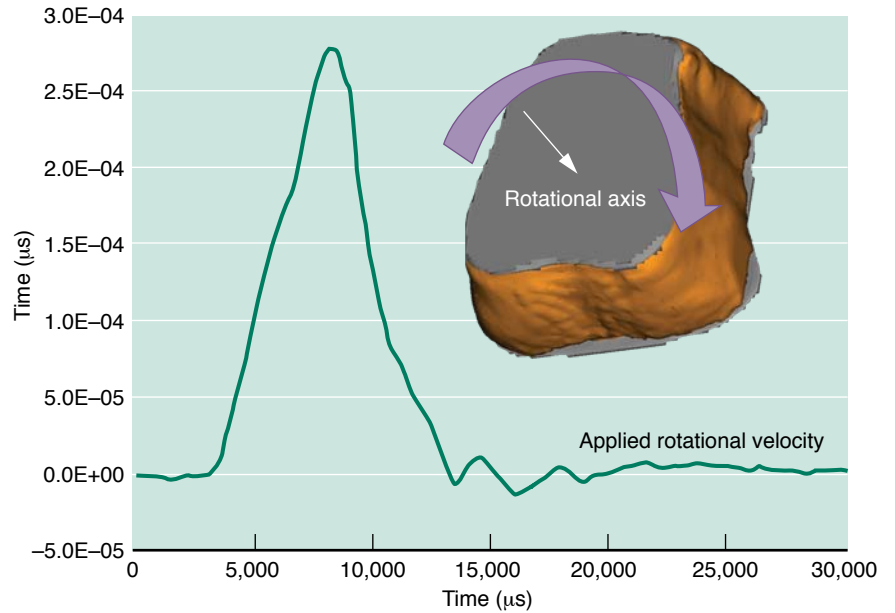


**Figure 2. Typical rotational load applied to animal head.**



Simulation predictions of peak pressure distributions in pig brain
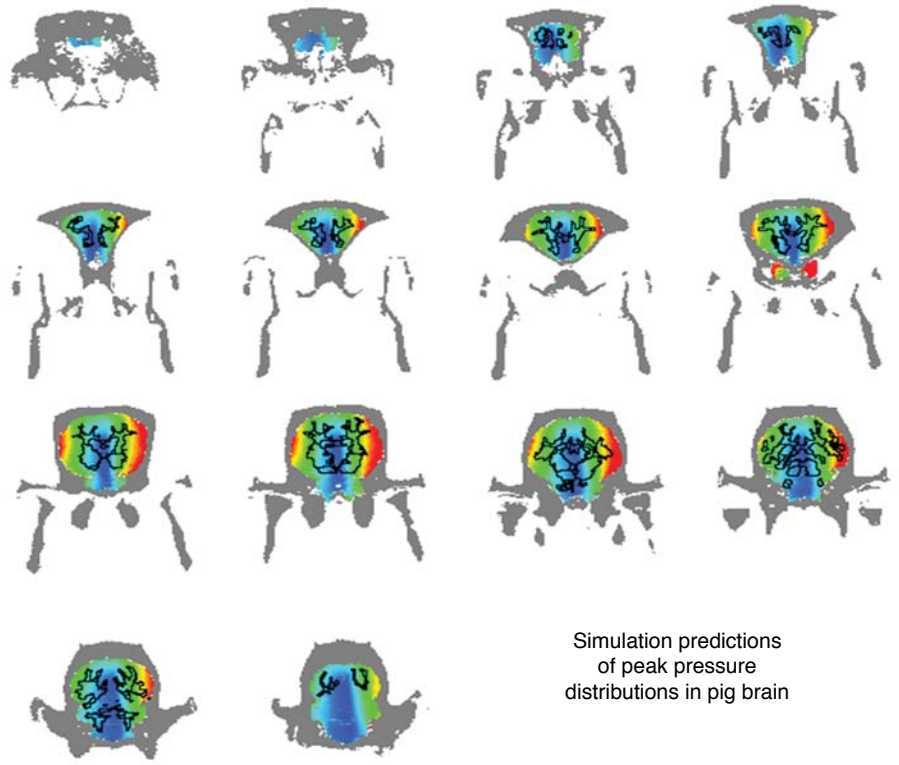
**Figure 3. Typical peak pressure contours on vertical cross sections through the animal brain occurring at any time over the load history. Grey regions represent the skull. Black outlines show white matter—grey matter interface.**

# Lagrange Multiplier Embedded Mesh Method

**Michael A. Puso**
925-422-8198
puso1@llnl.gov

## Project Overview

We are developing a new technique for using superposed meshes within a common simulation. Such an embedded mesh method can model fluid structure interaction without a conforming body-fitted mesh (Figure 1a) by simply superimposing the solid mesh on the fluid grid or mesh (Figure 1b). The method can drastically simplify the meshing process and avoid mesh-tangling problems, which can occur where large mesh motion is required to conform to a Lagrange body.

Past approaches have not become popular due to a variety of side effects, such as reliance on penalties and poor convergence behavior. Close attention to the accuracy and efficiency of our approach makes the method practical. Research issues such as mesh locking are addressed. The new methods have been implemented in the newly developed FEusion software library. The software is modular in form and is the basis for a new DoD-funded project.

## Project Goals

Our goal is to develop a software tool to interface embedded mesh models. The formulation as implemented should be able to accommodate the speed expected from an explicitly time-integrated program. It should also be extendable to handle different physics and finite element discretization. Example problems are Lagrange solid and shell meshes



(a)

(b)
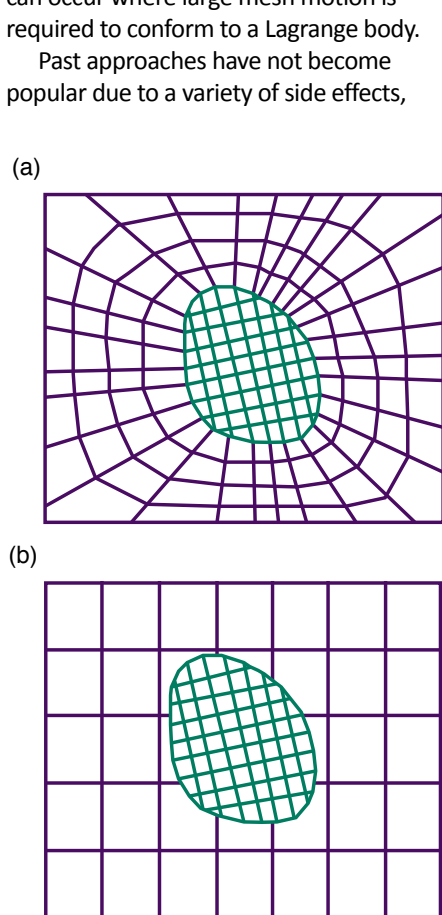
Figure 1. Fluid mesh in blue with solid mesh in brown. (a) Typical body fitted conforming mesh approach; (b) embedded grid approach. In the latter, the numerical algorithm reconciles the coupling between fluid and moving solid automatically.



(a) $E = 50$   $E = 5,000$   $E = 50,000$   $E = 50,000$   $P = 1$

(b)

(c)

(d)

(e)

Slope = 1.15

Slope = 1.97

Error

- ● Background displacement
- ■ Background energy
- ● Foreground displacement
- ■ Foreground energy

Mesh size: 0.2675   0.675   0.9125
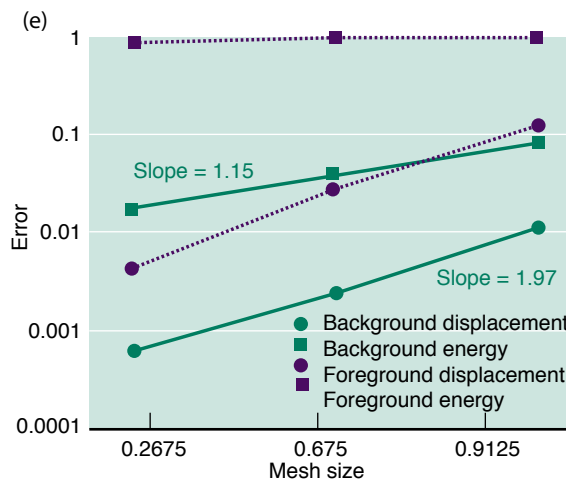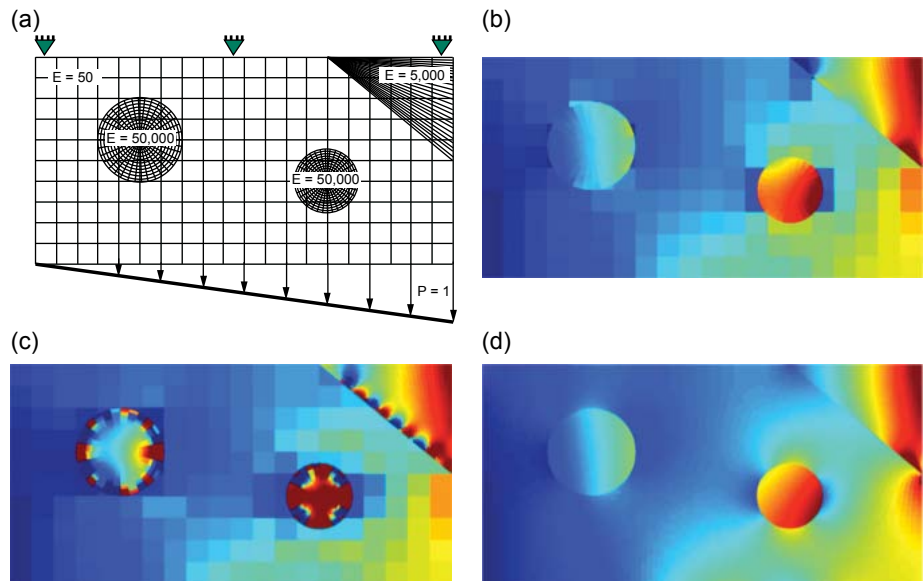
Figure 2. (a) Background matrix material with modulus E = 50 and stiff foreground inclusions E >> 50. Pressure fields are shown from (b) conforming mesh, (c) foreground multiplier, and (d) new background multiplier results. (e) Convergence plot demonstrating rate of convergence in displacement and energy norms for foreground and background approaches.

subjected to blast on an ALE or Eulerian mesh. Verification will be provided by comparing embedded grid results to the standard conforming mesh analysis in a mesh refinement study.

## Relevance to LLNL Mission

The tools developed in this project support LLNL's national security and defense mission. Most notably, the effects of explosives and blast can be more easily analyzed with the new capability, which strengthens a core competency for the Laboratory's Engineering programs. In addition, evaluation of the effects of improvised explosive devices on armored vehicles is a high priority for the DoD.

## FY2011 Accomplishments and Results

This project focused on developing new methods for analyzing models that use overlapping meshes.

There are two basic ways to couple overlapping meshes. The "foreground approach" effectively constrains the solid surface nodes to move at the velocity of the background fluid. This approach is simple but can be over-constrained in some instances, causing pressure oscillations on the meshes. The "background approach" constrains an appropriate set of background fluid nodes to move with the foreground solid mesh. This approach applies the appropriate amount of constraints and eliminates spurious pressure oscillations.

Our original FY2010 implementation used the foreground approach and was found deficient in some cases. That approach is most similar to typical commercial implementations. The FY2011 work identified a new background multiplier approach. Figure 2 demonstrates the improved results when stiff materials represented by a fine mesh are embedded in a softer, coarser mesh. Background multipliers converge optimally, while the foreground multiplier results show little to no convergence in energy norm.

The FY2010 approach used an approximate diagonalization of the mass matrix. In FY2011 work, we moved to an iterative calculation of the Lagrange multipliers enforcing the constraint that proved to be more robust.

The ALE3D implementation is verified in the following example: A 5-cm-thick steel plate is exposed to an explosive blast, and an analysis is made using the new method. The results are shown in Figure 3. The resulting velocities at the plate center and corner are plotted in Figure 4, and compare well to the conforming ALE meshes. The new approach was also demonstrated using structural shell elements.

During this project, four research papers were prepared, with three accepted to refereed journals and the other in submittal. The project has provided the technology basis for funding from the Army Research Laboratory to couple the ParaDyn and ALE3D codes. The coupled codes will be used to model the effects of improvised explosives on armored vehicles and their occupants.

## Related References

1. Laursen, T. A., M. A. Puso, and J. Sanders, "Mortar Contact Formulations for Deformable–Deformable Contact: Past Contributions and New Extensions for Enriched and Embedded Interface Formulations," *Computational Methods in Applied Mechanics and Engineering* (in press).

2. Sanders, J., and M. A. Puso, "An Embedded Mesh Method for Treating Overlapping Finite Element Meshes," *Int. J. Numer. Meth. Eng.* (accepted).

3. Sanders, J., M. A. Puso, and T. A. Laursen, "A Nitsche Embedded Mesh Method," *Computational Mechanics* (in press).

Var: material
- 1 ai_1 (red)
- 2 air _2 (green)
- 3 hardporous _3 (blue)
- 4 tnt _4 (cyan)



Mesh
Var: mesh_3d

**Figure 3. Buried explosive charge under plate. The aluminum plate (red) is Lagrange and is superimposed on a background mesh composed of air (green), soil (dark blue) and TNT (light blue).**



**Figure 4. Velocity response of embedded grid model at center and corner of plate exposed to blast. Results compare well to conforming ALE model of the same plate.**

# Multiscale Polymer Flows and Drag Reduction

**Todd H. Weisgraber**
925-423-6349
weisgraber2@llnl.gov

## Project Overview

Suspensions and polymer solutions exhibit a variety of complex physical phenomena and have applications across multiple disciplines, including blood flow and materials processing. In particular, drag reduction in bounded turbulent flows by the addition of long-chain polymers is a well-established phenomenon. However, despite decades of research, there is still a lack of understanding of the fundamental mechanisms. We believe that a complete description must incorporate wall roughness, a coarse-grained molecular representation of the polymer, and hydrodynamic fluctuations at the polymer length scale.

We are developing new algorithms, including an unconditionally stable, fluctuating lattice-Boltzmann (LB) solver coupled with molecular dynamics (MD), to enable fully turbulent, multiscale simulations of drag reduction.

## Project Goals

Our ultimate goal is to perform a series of large-scale simulations of dilute polymer solutions in turbulent flows with a detailed model of the polymer chains and the hydrodynamic interactions. To resolve the relevant scales we are incorporating the following improvements to our existing LB polymer code: 1) enhanced numerical stability; 2) accurate hydrodynamic fluctuations; and 3) integration of the solver with an adaptive mesh refinement (AMR) framework.

## Relevance to LLNL Mission

Our research aligns with LLNL's focus on high-performance computing and simulation. Specifically we seek to address fundamental scientific questions in hydrodynamics. The interaction between flow and suspended macromolecules is also relevant to the development of the next generation of emerging pathogen detection and analysis systems, an important component of the Laboratory's biosecurity strategic mission thrust.

## FY2011 Accomplishments and Results

Our second year emphasized finishing the AMR code development for the LB method using the Chombo library developed at LBNL. We have designed fully conservative interpolation and streaming algorithms to advance the solution at coarse–fine grid interfaces.

Our approach considers the fact that some of discrete lattice velocities are not aligned with the Cartesian axes and require both a spatial and temporal component to interpolation, unlike the spatial-only approach used in finite difference solvers. This innovation produced lower errors than in previous LB mesh refinement efforts.
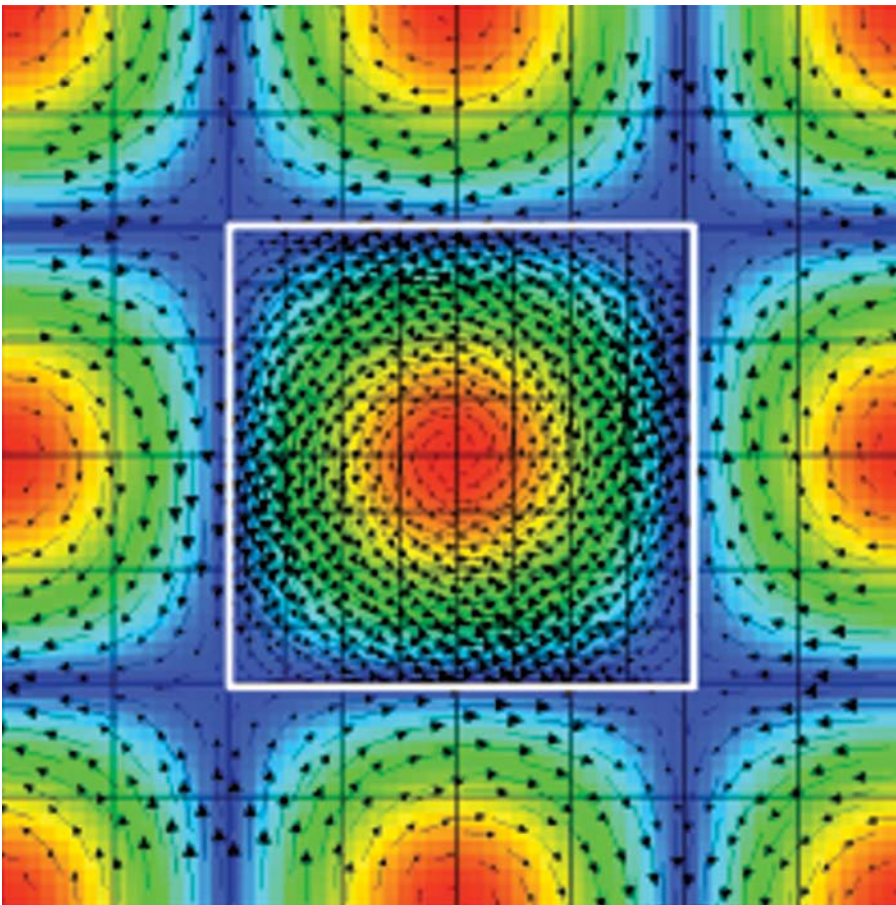


**Figure 1. Taylor-Green array of 2-D counter-rotating vortices. The colors denote vorticity magnitude; the arrows depict the flow field. A finer mesh covers the central vortex within the white box.**

Figure 1 shows the flow field for the Taylor-Green vortex benchmark, which has an analytical solution to the Navier-Stokes equations. A comparison of the velocity error between our method and the published state of the art AMR shows 3 to 10 times improvement, depending on resolution. With additional optimization, we have increased the performance of the coarse–fine interpolation by twenty times, while maintaining the improved accuracy.

Other benchmarks included a fully resolved direct simulation of turbulent channel flow between parallel plates at a Reynolds number of 5,500 with three levels of grid resolution. This simulation will serve as a baseline for comparison with the drag reduction simulations once we introduce the polymer molecules into the flow. Figure 2 contains different visualizations of this turbulent flow, including contours of flow structures and stream tubes.

To demonstrate that our method is fully adaptive we also ran a simulation of two co-rotating vortices that revolve around a common axis and eventually merge via diffusion. Two levels of refined grids designed to adjust to the local vorticity move and grow with the vortex centers, as depicted in the snapshot in Figure 3.

One of the main drawbacks of the standard LB method is that it becomes unstable for high Reynolds number flows relevant to drag reduction. Fortunately, a new generation of methods, known as entropic, and positivity preserving LB has overcome this stability issue, and we are developing these methods for AMR that strike a balance between stability, accuracy, and cost.

## FY2012 Proposed Work

In FY2012 we plan to: 1) include a representation of the polymer molecule in the AMR methodology; 2) investigate the effect of roughness as a source of flow perturbations that lead to turbulence; and 3) begin the large-scale drag reduction simulations of turbulent channel flow.

## Related References

1. Zhang, Y., A. Donev, T. Weisgraber, B. J. Alder, M. D. Graham, and J. J. de Pablo, "Tethered DNA Dynamics in Shear Flow," *J. Chem. Phys.*, **130** (**23**), pp. 234902–234913, 2009.

2. Rohde, M., D. Kandhai, J. J. Derksen, and H. E. A. van den Akker, "A Generic, Mass Conservative Local Grid Refinement Technique for Lattice-Boltzmann Schemes," *Int. J. Numer. Methods Fluids*, **51** (**4**), pp. 439–468, 2006.
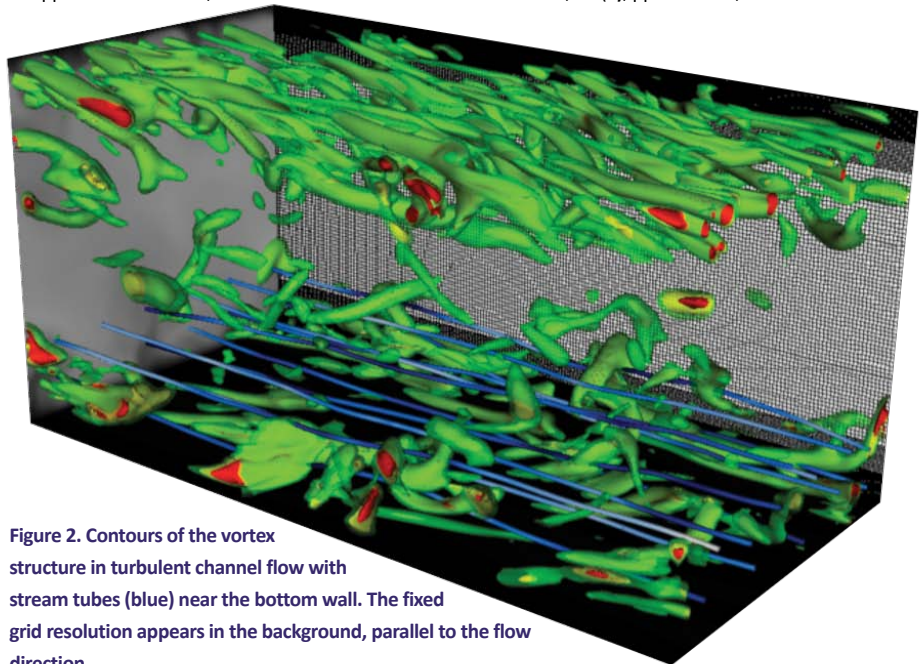
**Figure 2. Contours of the vortex structure in turbulent channel flow with stream tubes (blue) near the bottom wall. The fixed grid resolution appears in the background, parallel to the flow direction.**
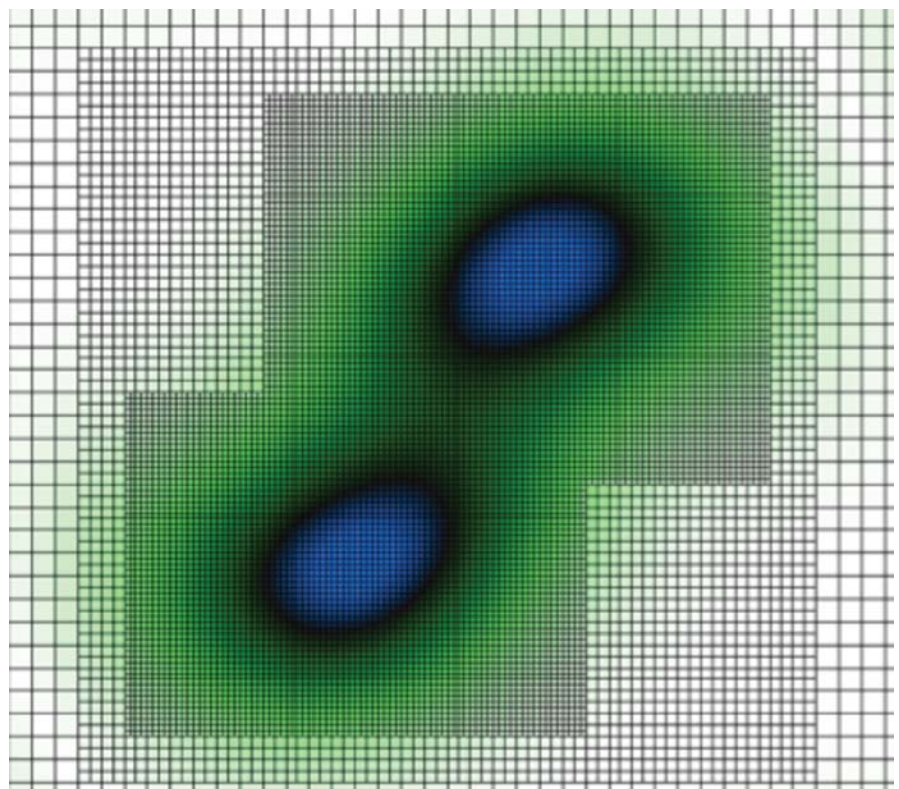


**Figure 3. A close-up of 2-D model of co-rotating vortices, highlighting the use of AMR to efficiently capture flow details.**
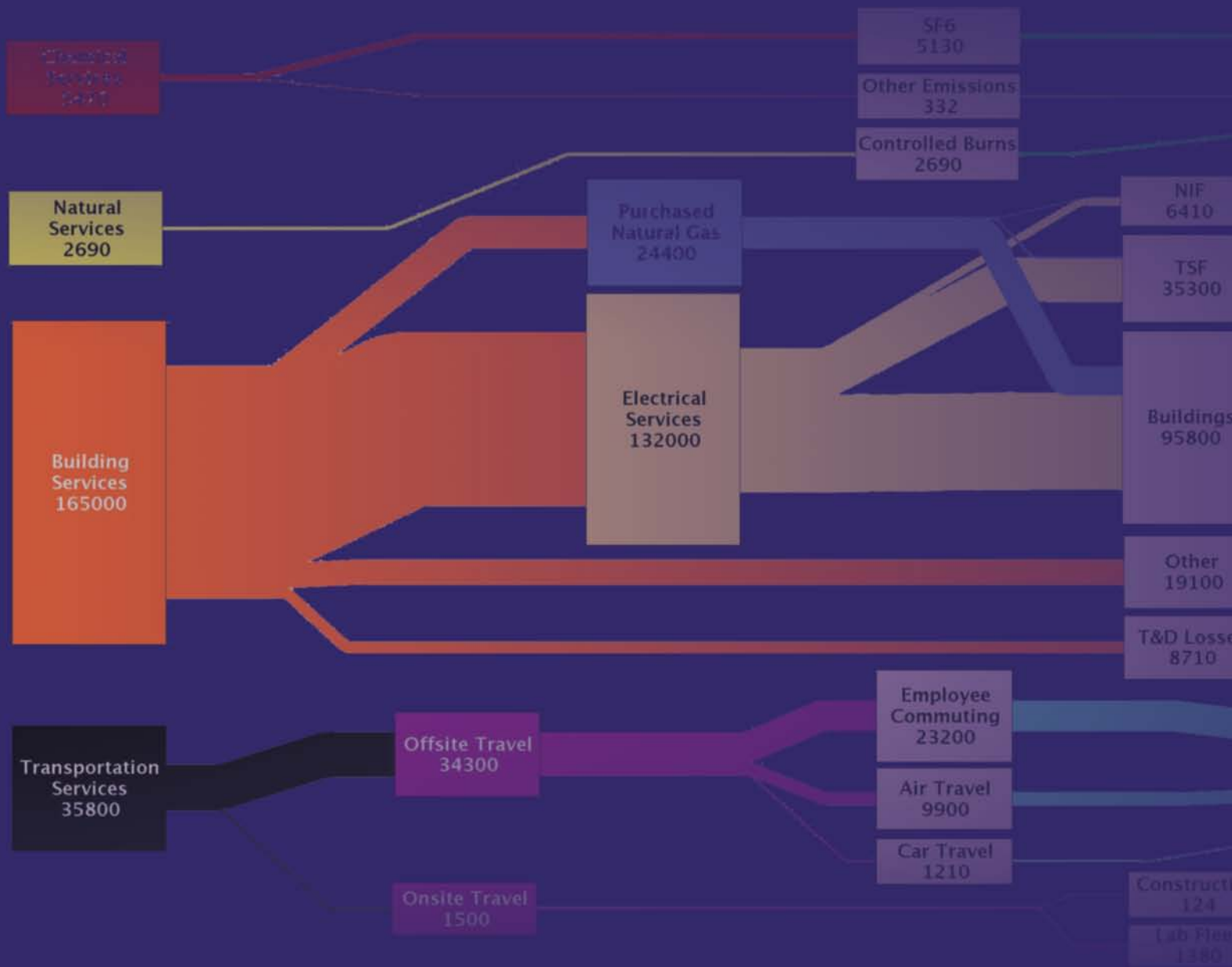
# Engineering
# Information
# Systems

# Establishing a Capability in Energy Systems Informatics

**Noah Goldstein**
925-423-0469
goldstein8@llnl.gov

## Project Overview

The U.S. energy system is in the midst of a significant transition; it is shifting from a top-down, easily predictable, homogeneous organization with few actors to a bottom-up, highly variable, heterogeneous mix of diverse actors. This large scale shift has its foundation in low-carbon policy, increased awareness of climatic shifts, and technological advancements. The new energy system will integrate renewable energy sources, at large and small scales, more closely monitored transmission, and "smart" meters and appliances. Ideally all of these new technologies will work with existing generation, transmission, and demand in a more efficient manner. Additional factors, such as snowpack estimates, local transformer weather estimates, and downscaled climate outputs will need to



**Figure 1. Increasing complexity of the electrical grid.**

be incorporated as well. The models and tools used to assess, forecast, and visualize the complexities of the new energy system will need to be highly resolved geographically and temporally in order to capture the nuances and outliers of a robust, yet fragile system.

Underlying the models and tools that explain and help manage the energy system is the diverse suite of data. Like the energy system writ large, those data are also transitioning into a different mode from the past, one that is less hierarchically structured, diverse in type and frequency of collection, and potentially quite voluminous. It is evident that the major stakeholders of the current energy system have not approached the current energy systems challenges of data management, analysis, and visualization in a cohesive manner, nor have they prepared for the upcoming challenges associated with more, diverse, and higher frequency data streams.

To address the data challenges of the greater energy system, as well as to assist current LLNL energy systems projects in grid forecasting, building energy management, and system-level visualization, LLNL is working on the Livermore Energy Systems Informatics Capability (LESIC). The LESIC will be used as the nexus of energy system data needs for LLNL projects, providing contributions in five key areas:
1) data models and standards;
2) data collection, including security and provenance;
3) data storage and dissemination;
4) data analysis; and
5) data visualization.

In addition the LESIC will reach out to energy systems stakeholders, standards bodies, and collaborators to advance the field of energy systems informatics.

## Project Goals

The primary goal of this project is to establish a foundation in energy systems informatics, as a resource for LLNL projects, as well as for the greater energy utility user base. With a common framework for the ingest, storage, analysis, visualization, and dissemination of energy systems data, energy systems stakeholder can begin to leverage the rich information that describes the energy system, improve models that describe the system, and visualize the variability and possibilities of the future.

## Relevance to LLNL Mission

This project is directly aligned with the strategic goals in LLNL's Energy and Climate focus area. The capabilities that are implemented in this work will benefit multiple programs, including Global Security's E Program (DOE, EERE), applied research in Global Security, Computation, and Engineering (LDRD and State of California smart grid and renewable energy programs), and O&B PAD programs (LLNL institutional energy, use and building energy efficiency, and sustainability).

## FY2011 Accomplishments and Results

In 2011, we created the concept of Energy Systems Informatics, and identified an implementation plan to leverage current LLNL capabilities in "Big Data" to external customers. Technical accomplishments include creating data models for the LLNL Energy Flow Charts, as well as rendering maps of interstate energy exports and imports. For the first time, the LLNL Energy Flow Charts were used to describe building-scale energy use, as well as the energy and carbon use of the LLNL site.

Estimate LLNL site energy use FY 2010
~1950 TJ

Estimate LLNL GHG emissions use in year: 2010
~209,450 mTCO2e
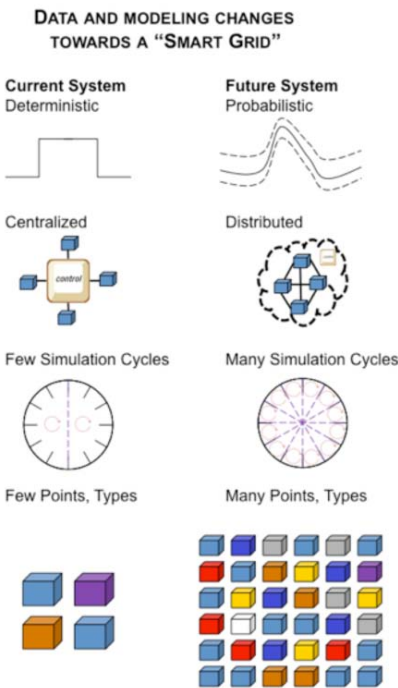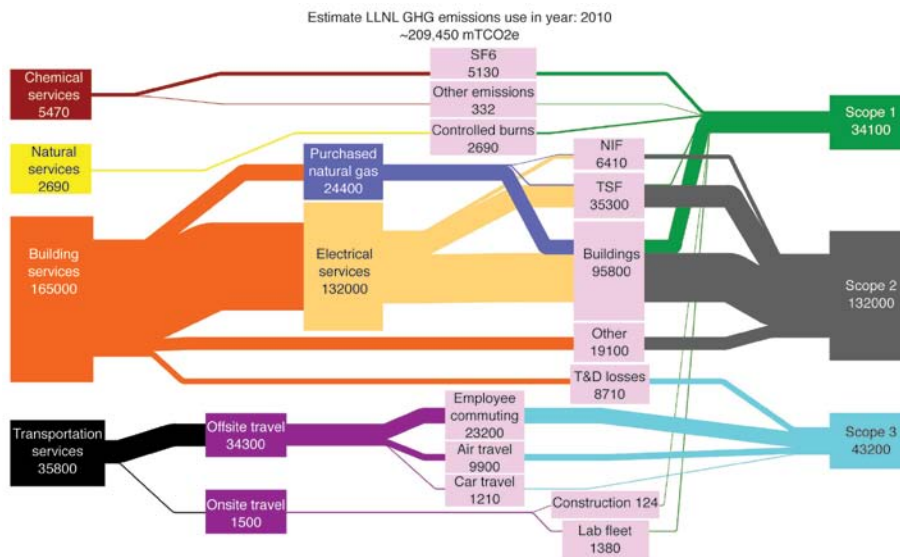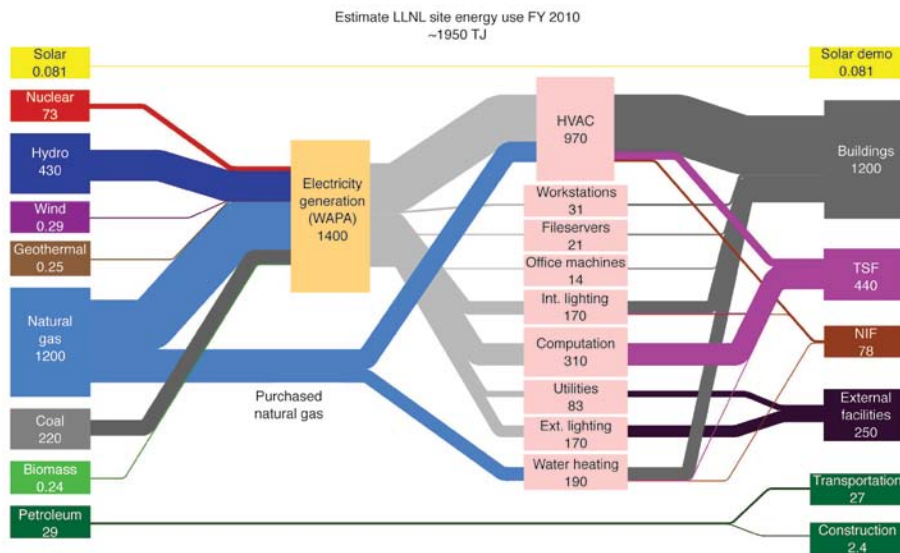
**Figure 2. Visualization of the LLNL site energy use, showing which locations and services demand electricity and natural gas, as well as the energy sources for LLNL.**



**Figure 3. Visualization of residential electrical demand in California.**



**Figure 4. Smart meter.**

This project excelled in its engagement with key California energy stakeholders including the California Independent System Operator (Cal-ISO), the California Energy Commission, the California Public Utilities Commission, and major California investor-owned utilities. Discussion of data and models led to multiple data sharing agreements and delivery of sensitive data to LLNL for preliminary analyses.

## FY2012 Proposed Work

In the upcoming year, we will extend LESIC in multiple ways. These include:

1) creating data models and metadata standards for energy systems data for LLNL projects in grid management, renewable energy forecasting, demand response, energy flows, and building energy use;
2) rendering and visualizing the LLNL electrical grid in DOE-developed grid simulation software;
3) creating an accessible smartphone "app" that presents the LLNL Energy Flowchart products;
4) continuing discussions with energy systems stakeholders, namely the California utilities, on their data, modeling, and security challenges; and

5) creating collaborations with key educational partners in energy systems informatics.

## Related References

1. Birman, K. P., L. Ganesh, and R. van Renesse, "Running Smart Grid Control Software on Cloud Computing Architectures," *http://www.cs.cornell.edu/projects/quicksilver/public_pdfs/SmartGrid-final.pdf*, 2011.
2. McDaniel, P., and S. McLaughlin, "Security and Privacy Challenges in the Smart Grid," *IEEE Security and Privacy*, **7** (**3**), pp. 75–77, May/June 2009.
3. McGranaghan, M. F., and S. Santoso, "Challenges and Trends in Analyses of Electric Power Quality Measurement Data," *EURASIP Journal on Advances in Signal Processing*, 2007.

# Adaptive Sampling Theory for Very-High-Throughput Data Streams

**Ana Paula De Oliveira Sales**
925-423-8358
apsales@llnl.gov

## Project Overview

Predictive modeling based on probabilistic models underlies all manner of modern data analysis tasks, including clustering, classification, regression, and anomaly detection. This project is motivated by the observation that the state of the art in predictive model design is far ahead of the state of the art in predictive model deployment. This is largely due to persistent advances in data collection capabilities. Modern data sources are high dimensional, high frequency, and essentially continuously observed. The reality of such data is that only sequentially computed, online statistical learning methods will be capable of providing real time situational awareness and decision support for many modern applications.

## Project Goals

The goal of this research is to create innovative computational learning algorithms that will enable the use of sophisticated predictive modeling techniques on modern streaming data sources. Over the course of this project, we will pursue an aggressive research agenda involving algorithmic innovation aiming to substantially boost the data ingestion rates of online learning systems. This includes developing alternative predictive models for accomplishing standard learning tasks at a fraction of the computational cost, and designing new self-adapting learning algorithms capable of automatically adjusting their computational characteristics in order to accommodate a target data throughput at minimal expense to prediction accuracy.

## Relevance to LLNL Mission

The goals of this project are particularly applicable to the Laboratory's Cyber, Space, and Intelligence (CSI) thrust area and the emerging Energy Systematics (CES21) programs. Both of these areas are characterized by large, distributed systems producing large, continuously available, distributed data sources (Figure 1), the fundamental security of which is a direct function of our ability to effectively anticipate, detect, and respond to significant deviations in those data feeds.

## FY2011 Accomplishments and Results

We have focused on the design of a highly customizable online learning system based on a new sequential Monte Carlo technique called particle learning (PL). At a high level, PL maintains a population of estimates of the underlying predictive model parameters, dynamically updating that population as new data arrives (Figure 2).

To ensure applicability to a wide variety of data sources, we designed the PL system around a novel class of composite mixture models that provide the ability to build generative models for nearly arbitrarily heterogeneous data types, while also facilitating classification and regression tasks. A key novelty of this system is the inclusion of sequential learning for probabilistic deterministic finite automata (PDFAs), a class of state space models with considerable
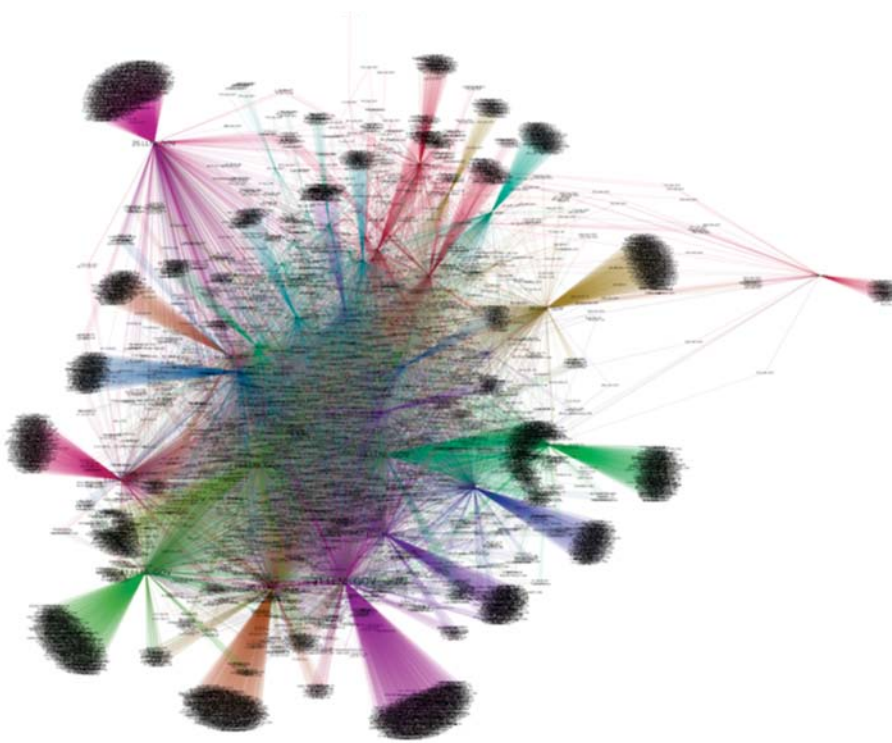


**Figure 1. Visualization of LLNL-based network connections collected by the Foraker distributed sensor network over a period of one month. Nodes represent unique IP addresses; edges are colored to highlight community structures within the graph.**

computational advantages over hidden Markov models (HMMs) (Figure 3).

The PL system will now serve as the basis for research on alternative computational strategies for particle-based learning. We are currently pursuing approaches for adaptively updating the size of the particle population so as to reduce computational complexity while ensuring the retention of "master particles" (Figure 4).

**Theory of computational pragmatism.**
Formal statistical learning methods enjoy a decision theoretic justification. However, that justification is rooted in the assumption of infinite computational power such that the appropriate statistic is always available at the precise time a decision is required. When this assumption of instantaneous inference fails, it is both appropriate and essential to incorporate the cost of computation into the decision theoretic justification of the method.

For example, suppose a decision can be calculated by either of two computational methods, one of which delivers answers with provably minimal error but requires substantially more computational resources than the other, which delivers a more error-prone answer instantly. If there is a per-time-unit cost associated with delaying the decision, the additional computational burden associated with the first method might be prohibitive, and acting on the result of the computationally inexpensive method would be preferable from a decision theoretic perspective.

We are studying this important direction for statistical research, and a novel perspective on data analysis: that in order to bring to bear modern predictive modeling techniques on modern streaming data sources, alternative approaches to inference that confer computational advantages, even at the expense of "theoretical" (*e.g.*, infinite computational) optimality are both essential and justifiable.

## FY2012 Proposed Work

In FY2012, we will continue research on a novel learning approach inspired by our theory of computational pragmatism.
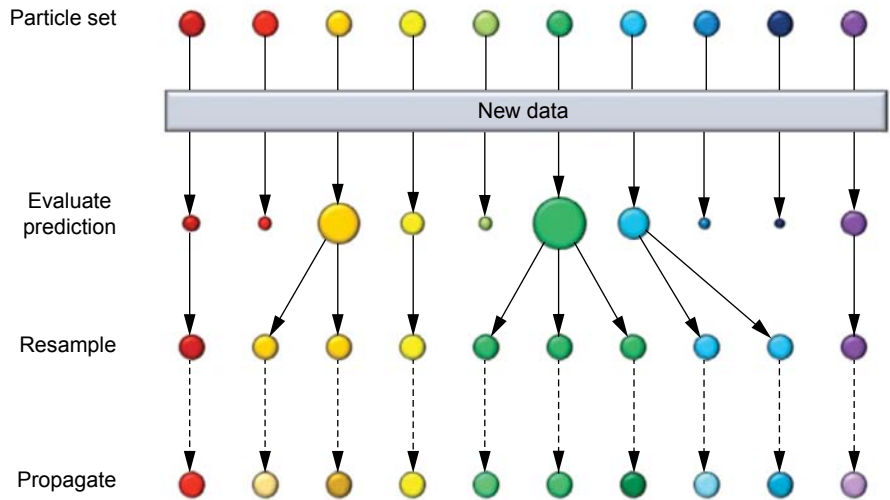


Figure 2. Schematic of the PL. PL provides full quantification of parameter uncertainty via a collection of particles that are dynamically propagated through time as data continues to arrive.
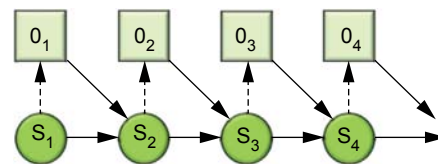


Figure 3. Graphical representation of a PDFA. PDFAs are characterized by an unknown hidden state sequence ($S_1$, $S_2$, ...) that evolves not according to a Markov chain like an HMM, but deterministically conditional on the previous state and the previous observable.
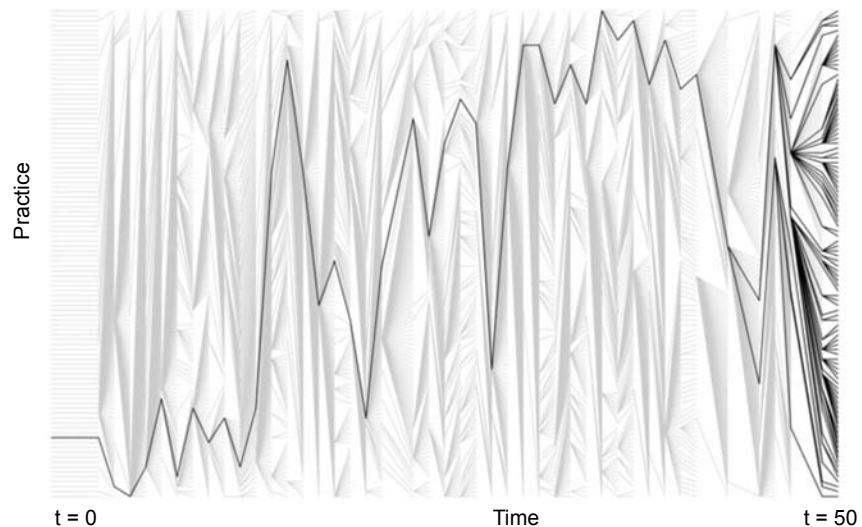


Figure 4. Genealogy of a PL. Dark lines trace the ancestry of each extant particle at time t = 50 back to a single master particle at time t = 0.
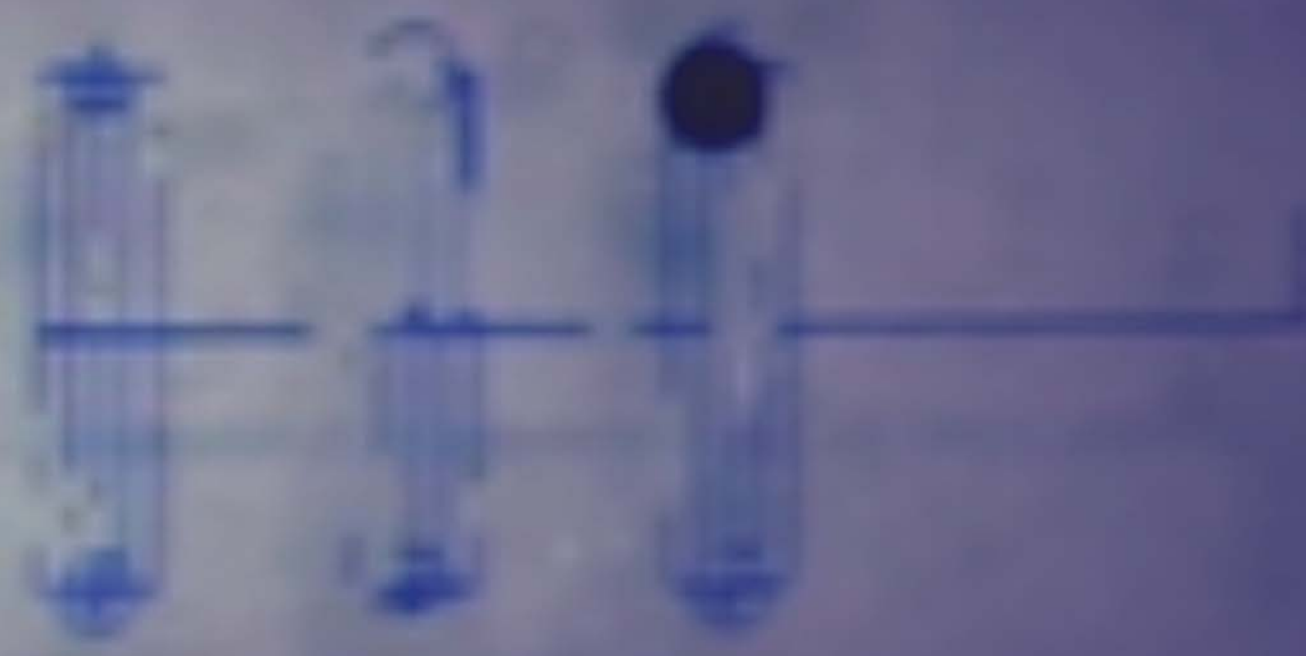
# Micro/Nano-Devices and Structures

# Integrated Microchannels and Membrane Filters for Viral Separation and Concentration

**Dietrich A. Dehlinger**
925-422-4030
dehlinger1@llnl.gov

## Project Overview

We are conducting viral evolution studies for multiple sponsors as part of implementing a capability to study and quantify emerging threats. This work involves repeated serial infection of mammalian cells by clinically relevant viruses, with genetic deep sequencing used to track the changes in the viral genome in response to selective pressures. Viruses produced from one group of infected cells are "passaged" to another group of cells with the sequencing being done on the viral population before and after each step of infection.

Ideally, this would be performed on microfluidic chips to better control cell growth conditions and the introduction of selective pressures in a highly controlled manner. For this to work, we need a system to store produced viruses locally on chip as they emerge from infected cells, as the viral infection can last as long as a week, and cells need a constant infusion of nutrients and removal of waste. To achieve this, we need a mechanism capable of filtering viruses on chip while removing accumulated waste products.

## Project Goals

We have extensive experience with microfluidic devices made from multilayer stacks of polydimethylsiloxane (PDMS) containing both fluidic and control microchannels. Each additional layer is stacked and bonded to previous layers. The adhesion of two layers must be able to withstand the presence of pressurized fluid for weeks to months. Our current devices are able to withstand operating conditions (aqueous, 30 psi) indefinitely.

In this project, we worked to integrate porous membrane filters into our existing
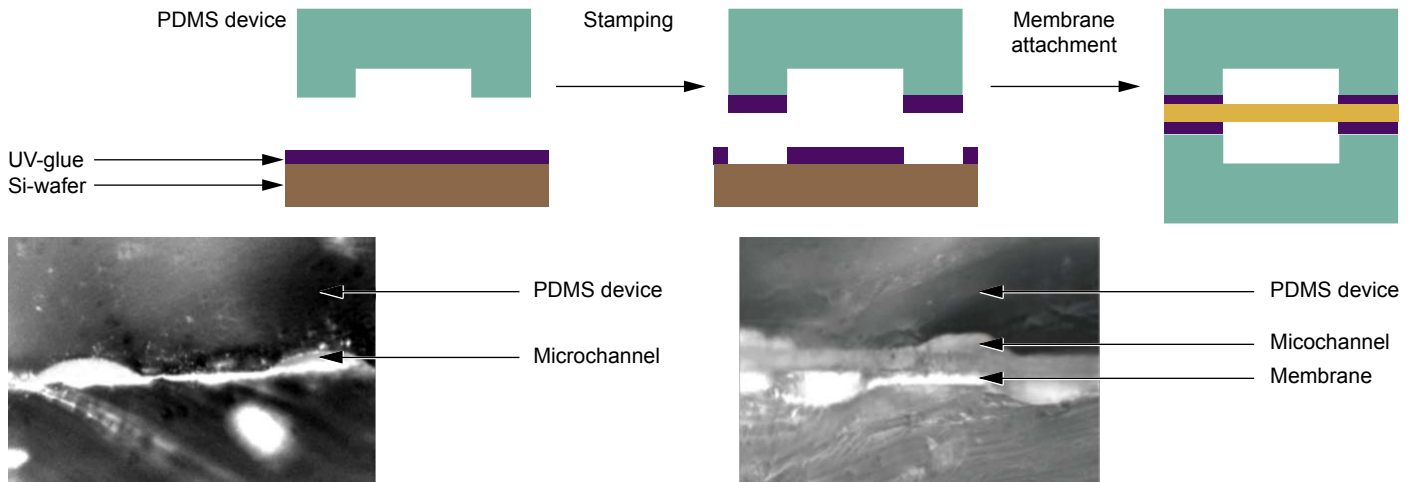


Figure 1. The bonding process.
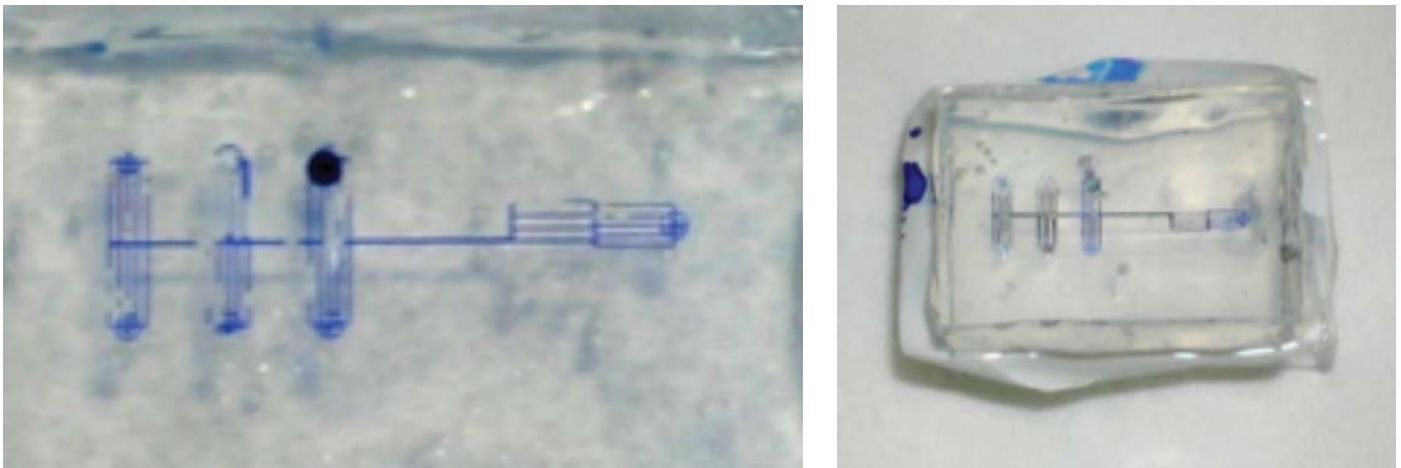
Figure 2. Two views of the dye-solution-filled microchannels, with no visible leaks at 15 psi. The sample is leak-free during the test at 7 psi for four days. All channels on both PDMS devices were filled with liquid.

process. Our current layers are made from PDMS, and adhesion between layers occurs when they are placed together in a partially cured state and then given a final bake. Because the membranes are made of different materials, we aimed for direct adhesion between the PDMS and membranes using a UV curable adhesive.

The goal of this work was to be able to bond our membranes between two PDMS layers, without delaminating, while being exposed to greater than expected fluidic pressures.

## Relevance to LLNL Mission

LLNL seeks to build a comprehensive model of viral evolution as part of a programmatic thrust to address emerging viral threats. We are leveraging a combination of our biology expertise, our computation/modeling, and our engineering facilities to meet this need. This work seeks to extend our microfluidic platforms to better deliver on this mission and to extend our future capabilities for viral and other host/pathogen studies.

## FY2011 Accomplishments and Results

The bonding process uses a UV curable adhesive as an intermediate adhesive layer to bond a PC membrane to PDMS device. The UV adhesive was spun to obtain a thin layer on a transfer Si wafer. Then, the adhesive was transferred to the PDMS device by stamping and the membrane was attached to the PDMS device. The adhesive was cured by UV exposure

A plasma activated PC membrane was immersed in the mixture of 5 vol% aminopropyltriethoxysilane (APTES) in water. After 20 min reaction at 80 °C, the reacted APTES-PC membrane was dried in air. Then, the APTES-PC and plasma activated PDMS were immediately brought into contact to form an irreversible bond. Figures 1 and 2 are representations of the process.

## FY2012 Proposed work

In FY2012 we plan on building a complete cell culture system using the techniques we have implemented here. Currently our systems are built to study bacterial growth, we will need to modify the fabrication processes to make channels optimized for mammalian cell dimensions (making them taller and wider). Now that we have bonded membranes to the PDMS surfaces, we will have to implement surface treatments for the membrane that prevent viruses from adhering to the membrane, while simultaneously modifying the membrane pore structure to allow a sufficient fluidic flow rate. This will be accomplished by controlling pore size and pore density. Once we have finalized all these processes, we will need to demonstrate both cell growth and repeated viral passage over several viral generations.

## Related References

1. Satyanarayana, S., R. N. Karnik, and A. Majumdar, "Stamp-and-Stick Room-Temperature Bonding Technique for Microdevices," *Journal of Microelectromechanical Systems*, **14**, pp. 392–399, 2005.
2. Aran, K., L. A. Sasso, N. Kamdar, and J. D. Zahn, "Irreversible, Direct Bonding of Nanoporous Polymer Membranes to PDMS or Glass Microdevices," *RSC Lab on a Chip*, **10**, pp. 548–552, 2010.
3. Niklaus, F., G. Stemme, J. Q. Lu, and R. J. Gutmann, "Adhesive Wafer Bonding," *Journal of Applied Physics*, **99**, 2006.
4. Chueh, B., D. Huh, C. R. Kyrtsos, T. Houssin, N. Futai, and S. Takayama, "Leakage-Free Bonding of Porous Membranes into Layered Microfluidic Array Systems," *Anal. Chem.*, **79**, pp. 3504–3508, 2007.

# Embedded Sensors for Gas Monitoring in Complex Systems

**Jack Kotovsky**
925-424-3298
kotovsky1@llnl.gov

## Project Overview

As the nation's nuclear stockpile is reduced in size, stockpile surveillance approaches must change to increase safety, security, and cost effectiveness. This project will explore broad-spectrum sensing technologies for this purpose. Broad-spectrum embedded sensors most efficiently address surveillance challenges and deliver the greatest overall impact. For this reason, this effort pursues broad-specie gas sensing to monitor the evolution of chemical species throughout a weapons system. Specifically, techniques for assessing non-noble species will be considered.

## Project Goals

This project seeks to develop two new, complementary sensing capabilities. Specifically, optic-fiber-based surface-enhanced Raman scattering and photo-acoustic spectroscopy are in development for detection of unknown gas mixtures.

Novel materials, fabrication processes, and designs will be explored for their applicability to the difficult constraints of in situ state-of-health stockpile monitoring.

## Relevance to LLNL Mission

This project will lay the groundwork for a game-changing, comprehensive sensor suite. Sensors will dramatically enhance stockpile surveillance and advance the entire nuclear weapons complex, supporting the Laboratory's national security and Stockpile Stewardship missions.

## FY2011 Accomplishments and Results

**PhotoAcoustic Spectrometer (PAS).** Three spectrometer designs were tested with the laser system designed in FY2010. A glovebox test environment with $CO_2$ monitoring has been set up to quantify the performance of PAS designs. Based on

this work, extensive modeling with COMSOL was used to further improve these designs and modifications are currently in fabrication (Figure 1).

Sensitivities of the system to acoustic resonator shape and size, laser stimulus, and detector geometries were explored in the models. The resulting designs anticipate enhanced detection sensitivity and include several features to speed the experimental development of the system.

Finally, a laser vibrometer system with a custom fiber assembly was acquired to continue the miniaturization of the overall detection system. FY2011 showed stellar progress in creating the building blocks for a successful LLNL PAS system.

**Surface Enhanced Raman Spectroscopy (SERS).** In FY2011 we have continued our experiments using the 532-nm fiber-based system under the fume hood, assembled in FY2010. We have focused on studying the behavior of toluene vapor as a representative of volatile organic compounds and a typical reference for SERS. The setup is sketched and pictured in Figure 2.

Time- and temperature-dependent studies of the toluene vapor SERS signal have been very successful and provided new insights into its adsorption kinetics. The time evolution of the SERS signal is shown in Figure 3a. The peak intensity of three main modes saturates with time (Figure 3b) as typical of SERS behavior, and fits well with a Langmuir trend (indicative of adsorption). We performed similar tests for several temperatures. For T <= 10 °C we observe an offset from the Langmuir surface effects explained by condensation, as the initial monolayer islands create energetically favorable spots for incoming molecules.

We have also progressed on the fiber implementation, and exploited photonic
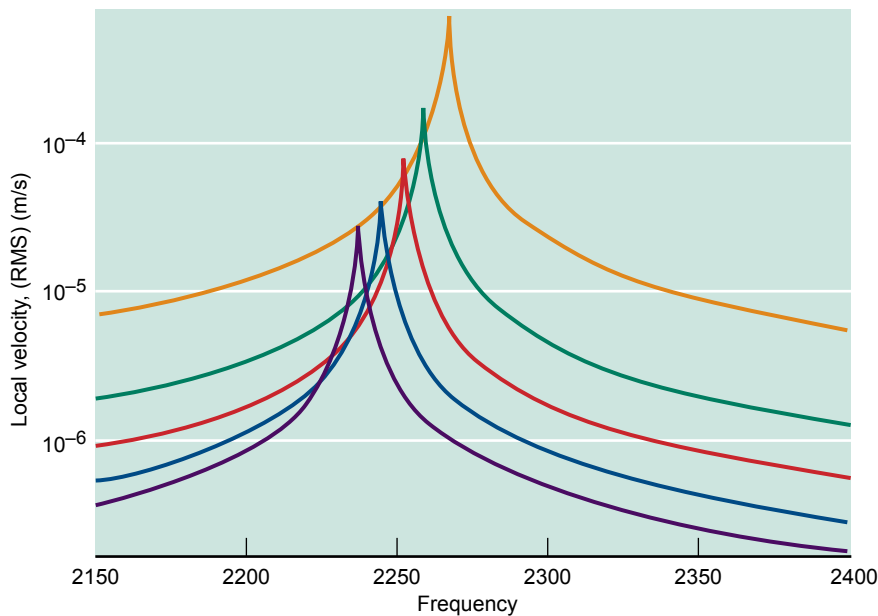


**Figure 1. Comparison of output velocities (measurement signal) of tubes of different diameters.**

(a)



(b)



**Figure 2. (a) Bubbler setup for vapor phase delivery; (b) photograph of hood setup.**
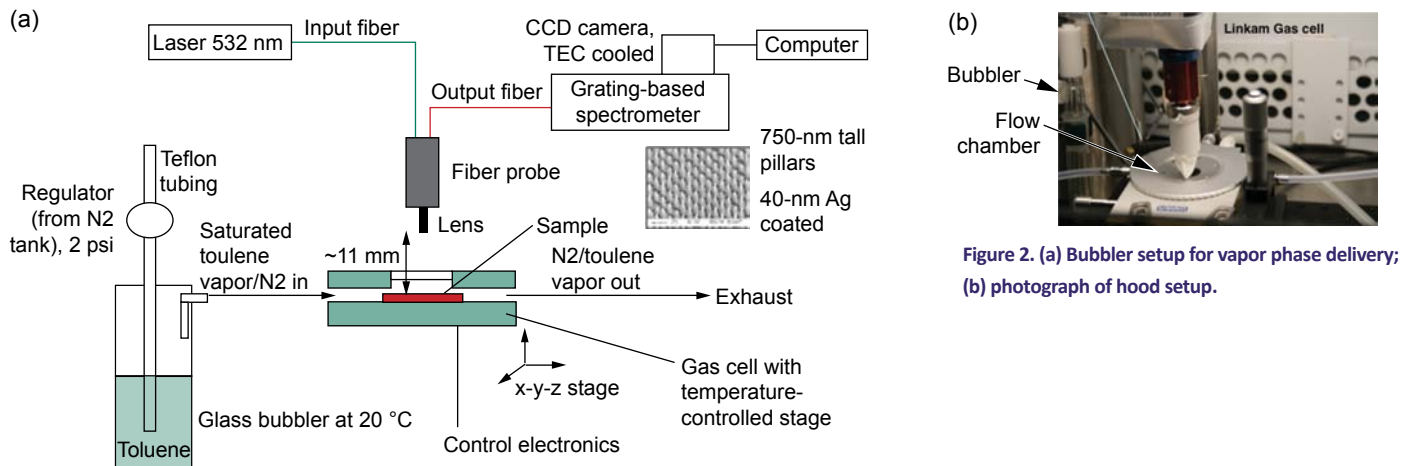
crystal fibers embedded with metal nanoparticles by high-performance liquid chromatography (HPLC). The first SERS results are very promising and we can control dilution of NPS very selectively.

## FY2012 Proposed Work

In FY2012, the PAS project will continually refine the acoustic resonator and optical detector designs to improve limits of detection (LOD). The laser noise-cancellation scheme will be developed on the new resonator and detector designs to further improve LOD. The PAS system will also be tested for drift and sensitivity to environmental disturbances. Finally, plans for complex mixture characterization will be pursued.

In FY2012, the SERS project will complete the concentration studies by exploiting an in-house gas-mixer and delivery system to reach concentrations <= 100 ppm. We will determine the LOD, accompanied by a quantum-based kinetics model. We will also pursue the dynamic study of inorganics such as NO and CO. Modified fiber configurations and tests will be examined in detail as well.

## Related References

1. Chang, A. S. P., et al., "Nanopillars Array for Surface Enhanced Raman Scattering," *SPIE Nanotechnologies for Defense Proceed.*, 2011.
2. Bond, T., et al., "Nanostructures for Surface Enhanced Spectroscopy," *CMOSET Workshop*, June 2011.
3. Bond, T., et al., "Broadly Tunable Plasmonic Nanogap Resonators or Black Plasmons," *Optical Micro-System Meeting*, September 2011.
4. Chang, A. S. P., et al., "Detection of Volatile Organic Vapors by Surface-Enhanced Raman Scattering," *FACSS*, 2011.

(a)



(b)



**Figure 3. (a) Plot of SERS Peak-to-Background vs. (b) Substrate Exposure Time to Toluene Vapor. Langmuir kinetics behavior is as expected with mean time constant of 12 min.**
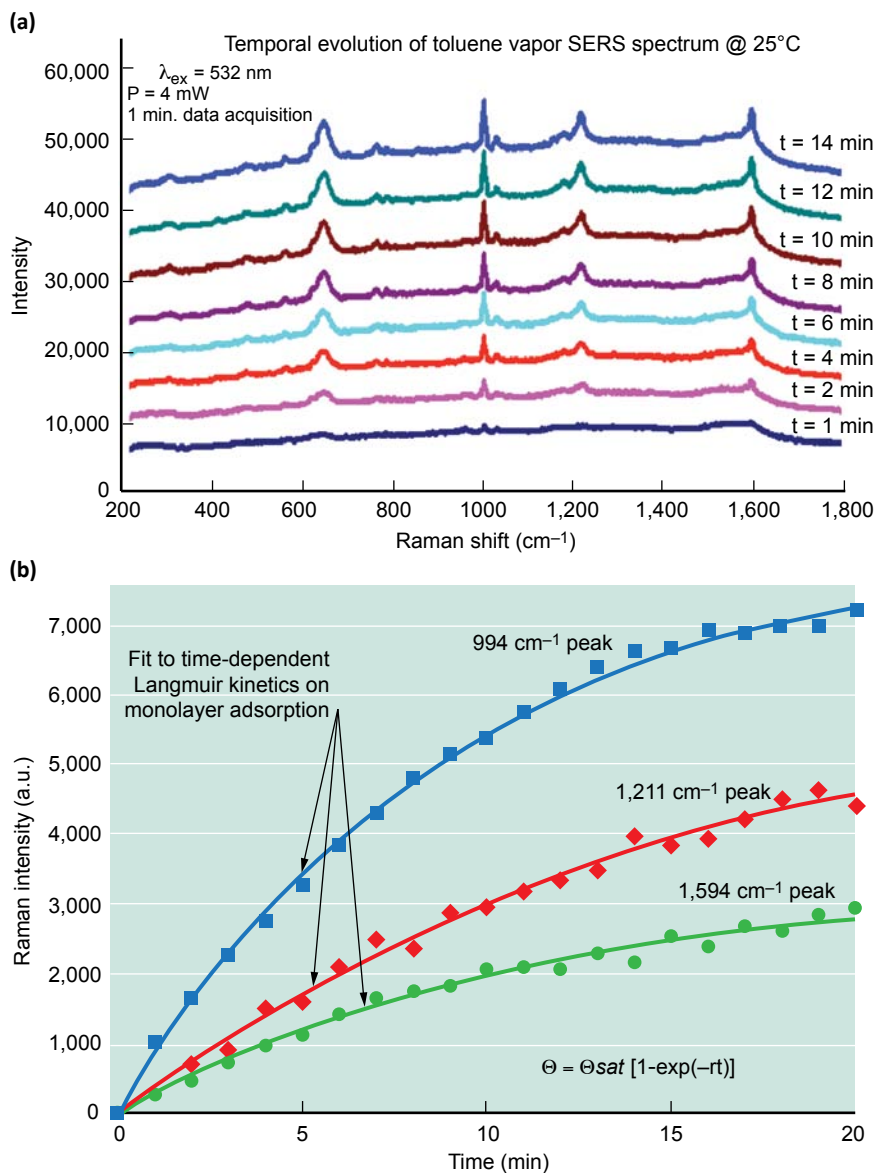
# Enabling Transparent Ceramics Optics with Nanostructured Materials Tailored in Three Dimensions

**Joshua D. Kuntz**
925-423-9593
kuntz2@llnl.gov

## Project Overview

We are developing a novel nanomanufacturing technique, based on the electrophoretic deposition (EPD) process, to create transparent ceramic optics with unique properties based on tailored nanostructures. The EPD process uses electric fields to deposit charged nanoparticles from a solution onto a substrate. We have expanded current EPD capabilities to enable controlled deposition in three dimensions by automating the injection of nanoparticle suspensions into the deposition chamber and dynamically modifying the electrode pattern on the deposition substrate. We can also use the electric field to control the orientation of non-spherical particles during deposition to orient grain structures prior to sintering. To enable this new functionality, we are synthesizing ceramic nanoparticles as our precursor material, implementing new instrumentation for the bench-top deposition experiments, and developing modeling capabilities to predict deposition kinetics and deposited structures based on the particle, solution, and system properties.

To guide our research and development efforts, we have identified transparent ceramic optics as a major area in which nanostructured functionally graded materials can have a significant impact. Laser physicists and optical system engineers are currently hindered by the small subset of materials available for their designs. The only crystalline materials open to them are those that can be grown as single crystals and isotropic cubic materials that can be formed into transparent ceramics. By depositing nanorods of a noncubic material in the same orientation, the resulting green-body can be sintered to a transparent ceramic. Additionally, current optics designs are material- and process-limited to uniform composition profiles across optical components and laser gain media. To date, only coarse step function composition changes have been produced in the most advanced transparent ceramic optics. Our EPD platform enables us to create new transparent ceramic optics with doping profiles tailored in 3D.

## Project Goals

The goals of this project are to demonstrate 1) the fabrication of functionally graded materials with composition profiles tailored in 3-D while maintaining desired bulk properties; 2) the use of the EPD deposition field to simultaneously align nanorod particles of precursor material as they are deposited; and 3) the fabrication of composite structures with controlled material composition and create smooth or sharp material transitions along the z-axis of a composite structure.

(a)



7.2 µm    7.4 µm

EPD film lifted off from electrode via resorcinol-formaldehyde gel

(b)



E = 10 V/cm



E = 60 V/cm
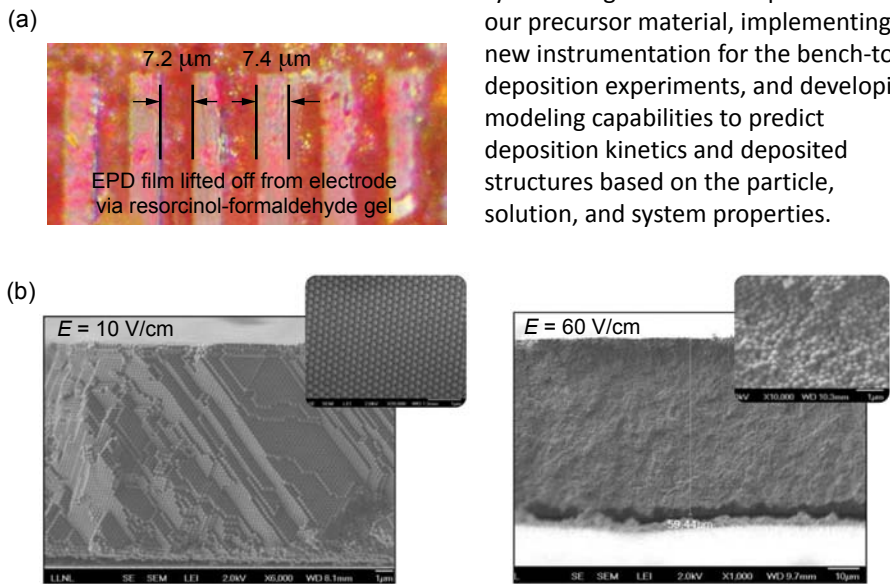
**Figure 1. Examples of 2-D extruded pattern with 7.5-µm resolution. The material is deposited onto a photolithographically patterned metal electrode. Note the sharp edges of the deposit.**

## Relevance to LLNL Mission

The project is intended to establish LLNL's leadership in bottom-up nanofabrication of functionally graded materials. Our dynamic EPD system will position us to deliver the next generation of nanomanufacturing capabilities for projects throughout the Laboratory. Using these capabilities, we are working to produce a number of novel materials and structures. These structures will both illustrate the capabilities of the new process and demonstrate materials and structures of relevance to LLNL missions and programs. The main demonstrations for this project align with current and future needs in NIF as well as in the LIFE and ALOSA thrust areas. These are 1) to create transparent ceramic optics with doping profiles tailored in 3-D to enable new high-powered laser designs (NIF/LIFE); and 2) to deposit aligned nanoparticles of noncubic ceramics to create a new family of transparent ceramics (NIF/LIFE/ALOSA).

## FY2011 Accomplishments and Results

Accomplishments and results in our second year include the following:

1. Successfully deposited a 2-D extruded pattern with 7.5-µm resolution (Figure 1). The material is deposited onto a photolithographically patterned metal electrode.
2. Developed and implemented a Brownian dynamics model for EPD. The model was validated through correlation of the model and experimental results at the ordered-to-disordered transition of monodisperse spheres (Figure 2).
3. Developed multiple synthesis routes to near-monodisperse fluorapatite nanorods (Figure 3) and demonstrated alignment of the rods in a 300-V/cm electric field.
4. Demonstrated FGM transparent ceramic structures fabricated using the EPD process with dopant concentration varied as a function of z-height.



Sections of deposit



Numbers nearest neighbors
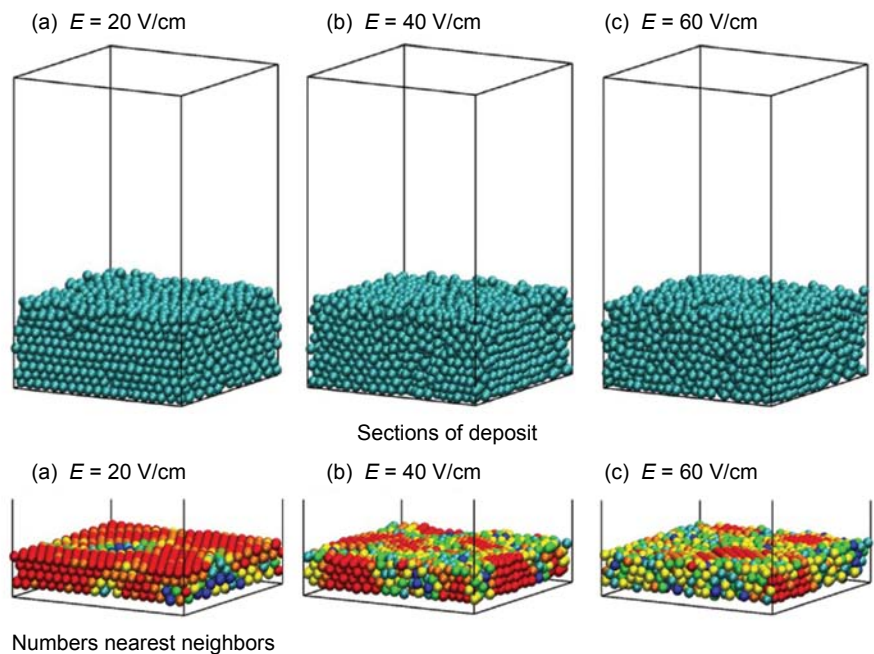
**Figure 2. Demonstration of ordered-to-disordered transition for both experiments and modeled depositions. Higher electric field strength results in disordered deposits.**
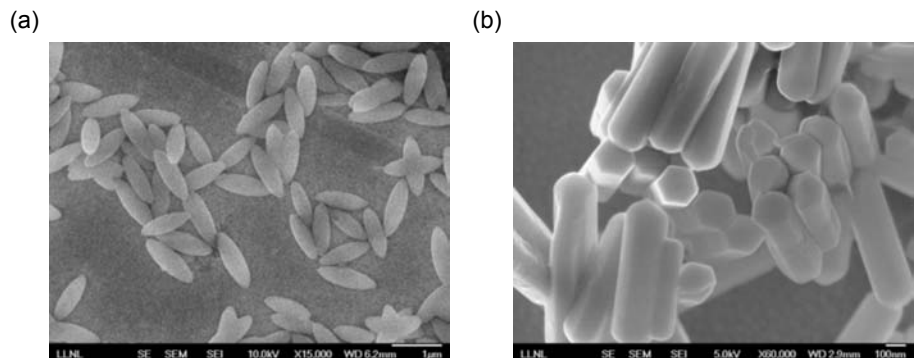


**Figure 3. Representative fluorapatite nanorods with morphology managed through control of the degree of supersaturation during synthesis and growth.**

# Deposition of a-Se on CZT

**Lars Voss**
925-423-0069
voss5@llnl.gov

## Project Overview

High performance gamma detectors are needed for unambiguous spectroscopic detection of special nuclear materials (SNM). The state of the art for high performance gamma detection is a cryogenically cooled high purity germanium detector. A room temperature alternative is preferred for ease of use and to decrease power requirements.

The current leader in performance for room temperature gamma detection is cadmium zinc telluride (CZT). However, existing crystal growth techniques are not sufficient to enable the performance required with sufficient crystal size to make the detectors economical. One pathway to bridging the remaining gap between theoretical and actual performance is electrically blocking contacts, to reduce system noise

through the use of amorphous layers with appropriate bandgaps and band offsets. We expect that this will enable an order of magnitude reduction in leakage current on CZT crystals, allowing for better signal identification of specific nuclear materials (SNM).

We have previously demonstrated the viability of this approach using amorphous selenium (a-Se) deposited by collaborators at TASC in Trieste, Italy and
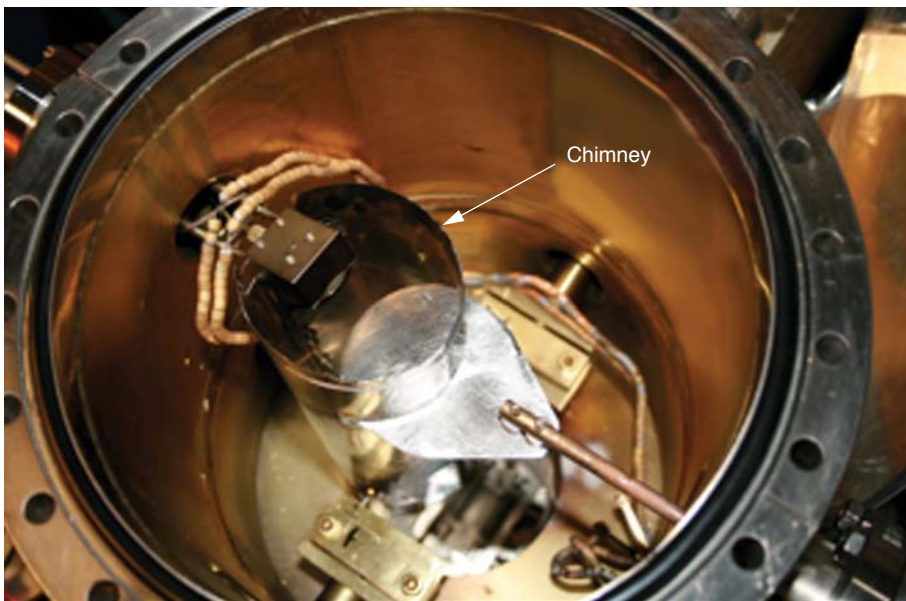


**Figure 1. Safety features of a-Se thermal evaporation system.**
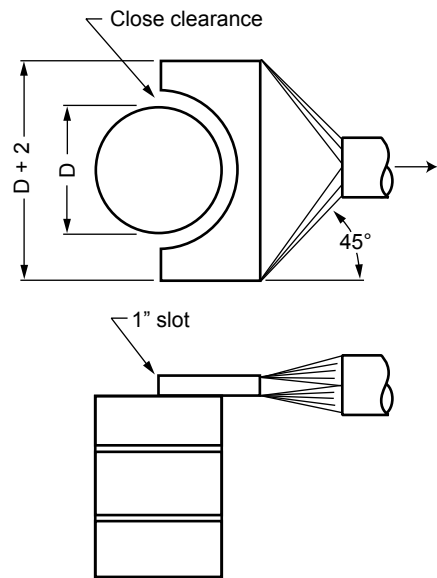
**Figure 2. Deposited films that are
(a) uncrystallized and amorphous and
(b) crystallized.**
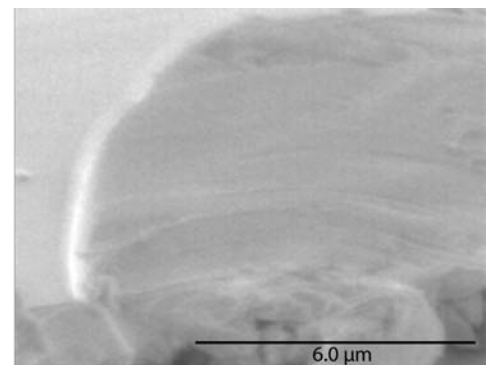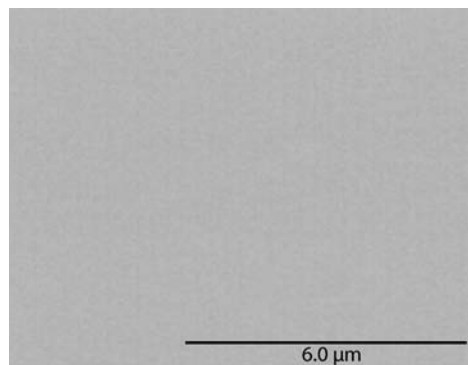
amorphous silicon (a-Si) deposited at LLNL to drastically improve CZT detector performance.

## Project Goals

This project was focused on reducing to practice the deposition of a-Se layers on CZT crystals. Deposition of a-Se requires strict engineering controls to minimize the possibility of exposure to toxic Se dust, as well as to carefully monitor the deposition conditions in order to eliminate the possibility of crystallization. The latter is critical to the performance of the films, and it is well known that a-Se can crystallize upon moderate heating at > 60 °C.

## Relevance to LLNL Mission

Radiation detection is part of LLNL's mission. This capability will significantly enhance the ability of LLNL to produce high performance, room temperature gamma detectors.

## FY2011 Accomplishments and Results

During this project we have successfully brought online a thermal evaporator capable of depositing a-Se. Specialized safety features have enabled minimized deposition of a-Se on the vacuum chamber through the use of a removable vertical chimney, and the minimization of potential airborne exposure through the use of a vacuum attachment. Both are shown in Figure 1.

Crystallization has been eliminated through monitoring the deposition temperature, which is influenced by the deposition rate of the a-Se. Films (Figure 2) were characterized via spectroscopic ellipsometry in order to determine the band gap, shown in Figure 3, which was determined to be 2.017 eV, in close agreement with reported values of a-Se (~ 2 eV).

Finally, the resistivity of the films was demonstrated to be extremely high, with measurement possible only at elevated temperature. To determine the room temperature resistivity, data (Figure 4) was extrapolated and resistivity observed

to be $6.25 \times 10^{10}$ Ω-cm. This deposition capability will enable fabrication of high performance gamma detectors at LLNL.

## Related References

1. Voss, L. F., P. R. Beck, A. M. Conway, R. T. Graff, R. J. Nikolíc, A. J. Nelson, and S. A. Payne, "Surface Current Reduction in (211) Oriented CdZnTe Crystals by Ar Bombardment," *J. Appl. Phys.*, **108**, 014510, 2010.

2. Conway, A. M., A. J. Nelson, P. R. Beck, L. F. Voss, R. T. Graff, R. J. Nikolíc, S. A. Payne, M. Fanetti, and S. Rubini, "Amorphous Semiconductor Blocking Contacts on CdZnTe Gamma Detectors," *MRS Spring Meeting*, San Francisco CA, April 2011.

3. Voss, L. F., A. M. Conway, B. W. Sturm, R. T. Graff, R. J. Nikolíc, A. J. Nelson, and S. A. Payne, "Amorphous Semiconductor Blocking Contacts on CdTe Gamma Detectors," *IEEE Nuclear Science Symposium*, October 2009.

4. Nelson, A. J., A. M. Conway, C. E. Reinhardt, J. J. Ferreira, R. J. Nikolíc, and S. A. Payne, "X-Ray Photoemission Analysis of CdZnTe Surfaces for Improved Radiation Detectors," *Materials Lett.*, **63** (**180**), 2009.
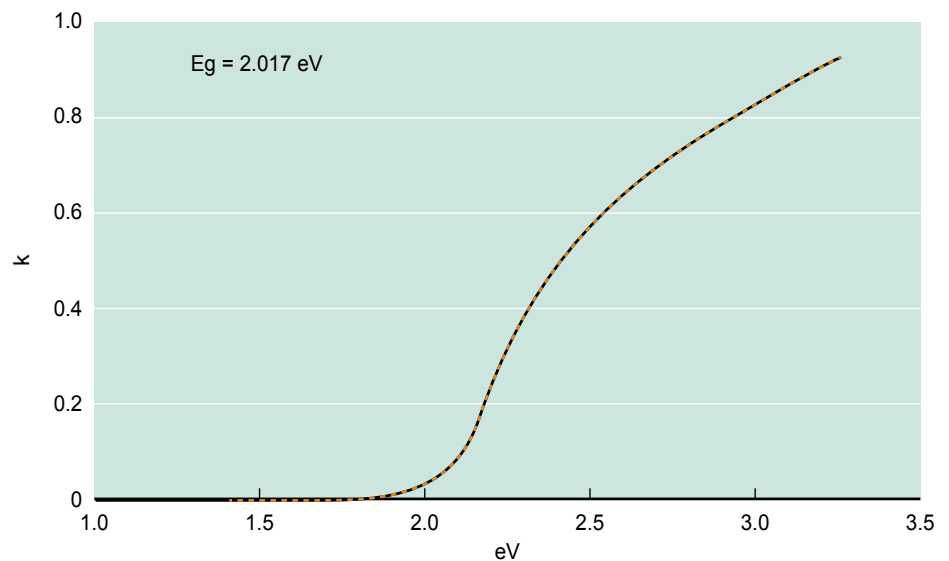
**Figure 3. Modeled ellipsometric value for the extinction coefficient and band gap using a Cody-Lorentz oscillator.**
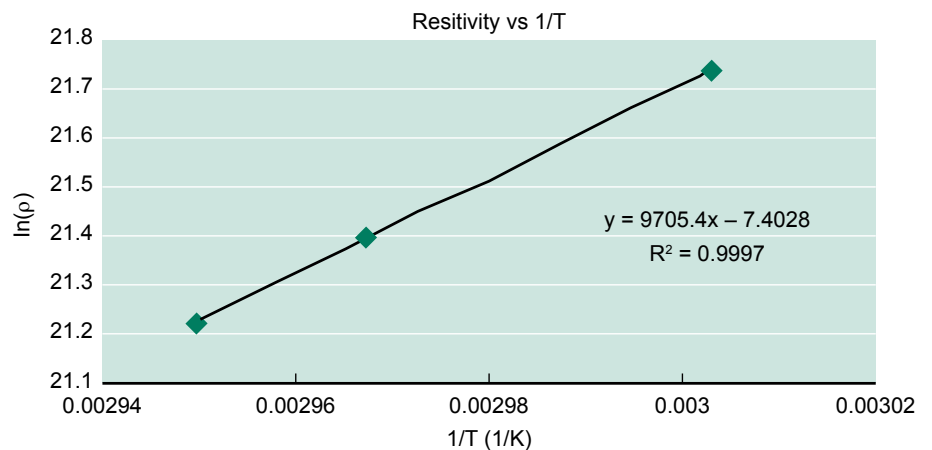


**Figure 4. Arrhenius plot of the resistivity for deposited a-Se films.**

# Hybridization and Selective Release of DNA Microarrays

**Elizabeth K. Wheeler**
925-423-6245
wheeler16@llnl.gov

## Project Overview

DNA microarrays contain sequence specific probes arrayed in distinct spots numbering from 10,000 to over 1,000,000, depending on the platform. This tremendous degree of multiplexing gives microarrays great potential for environmental background sampling, broad-spectrum clinical monitoring, and continuous biological threat detection. In practice, their use in these applications is not common due to limited information content, long processing times, and high cost. Our work seeks to characterize the phenomena of microarray hybridization, regeneration, and selective release that will allow these limitations to be addressed. This will revolutionize the ways that microarrays can be used for LLNL's Global Security missions.

## Project Goals

The goals of this project were two-fold: automated faster hybridizations and selective release of hybridized features. The first study area involves hybridization kinetics and mass-transfer effects. The standard hybridization protocol uses an overnight incubation to achieve the best possible signal for any sample type, as well as for convenience in manual processing. There is potential to significantly shorten this time based on better understanding and control of the rate-limiting processes and knowledge of the progress of the hybridization. In the hybridization work, a custom microarray flow cell was used to manipulate the chemical and thermal environment of the array and autonomously image the changes over time during hybridization.

The second study area is selective release. Microarrays easily generate hybridization patterns and signatures, but there is still an unmet need for methodologies enabling rapid and selective analysis of these patterns and signatures. Detailed analysis of individual spots by subsequent sequencing could potentially yield significant information for rapidly mutating and emerging (or deliberately engineered) pathogens. In the selective release work, optical energy deposition with coherent light quickly provides the thermal energy to single spots to release hybridized DNA.

## Relevance to LLNL Mission

This work leverages LLNL expertise in optics, microfluidics, and bioinformatics.
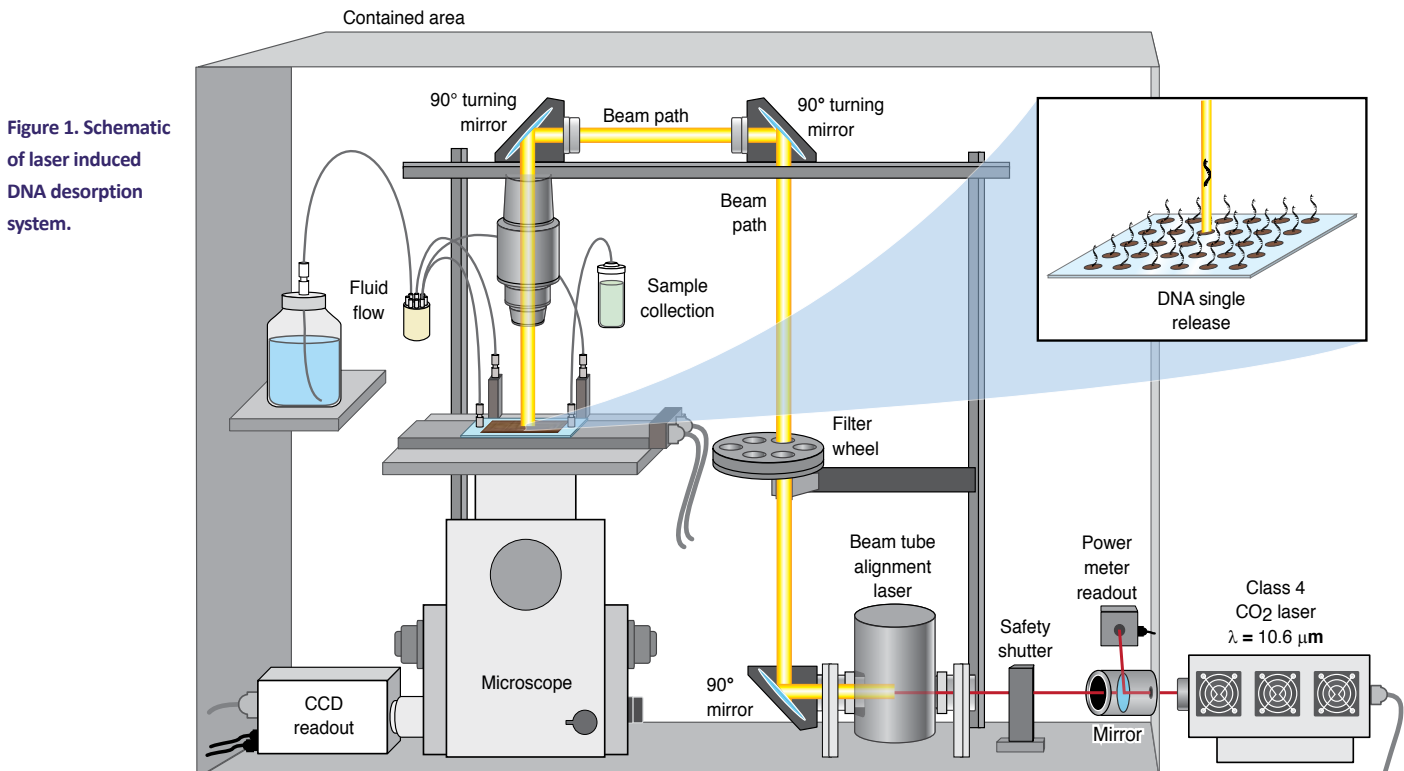


**Figure 1. Schematic of laser induced DNA desorption system.**

Scan of microarray

Pre-laser elution



Intensity along line of scanned image
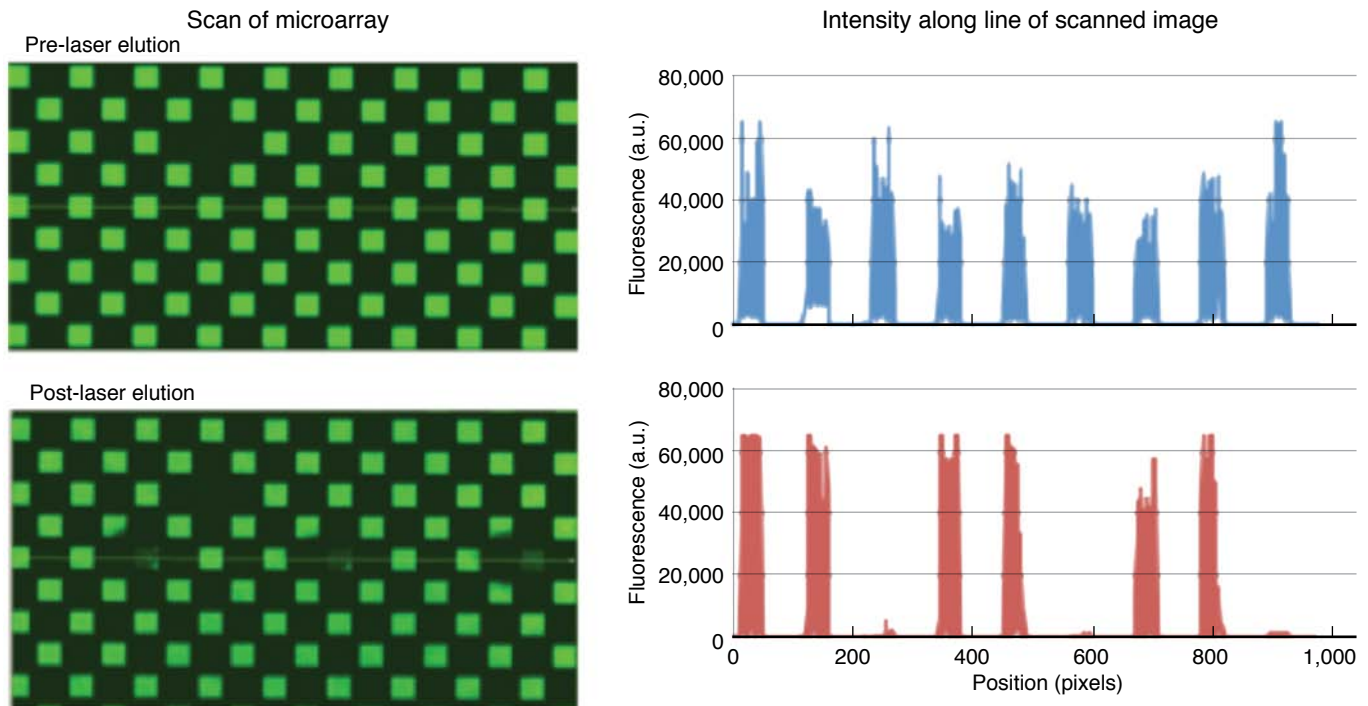


Post-laser elution





**Figure 2. Typical experimental results. Prior to elution (top images) all features are fluorescent. After laser elution (lower images) features targeted by the laser show a dramatic decrease in intensity (red plot).**

## FY2011 Accomplishments and Results

As described above, post-processing microarrays can yield important information about anomalous hybridization patterns. However, until recently, the state of the art for selective recovery of a feature of interest involved scraping the surface to recover the DNA. In our work, we recently demonstrated an automated method to selectively release DNA bound to the surface of a microarray and recover the DNA for downstream analysis.

Our approach for selective release uses laser heating to elute the DNA of interest, and then microfluidics to recover the eluted DNA for analysis. A schematic of our laser induced DNA desorption (LIDD) system is shown in Figure 1; results are shown in Figure 2.

To confirm that we are not simply damaging the fluorophore, we collected the eluted DNA and performed PCR assays. Results are shown in Figure 3.

Having demonstrated not only selective feature release but also DNA recovery, we are now well positioned to

enable even more widespread use of microarrays. Selectively releasing a feature for downstream sequencing or analysis will potentially enable microarray use in personalized medicine, cancer diagnostics, drug discovery, or biosurveillance.

## Related References

1. Jaing, C., S. Gardner, K. McLoughlin, N. Mulakken, M. Alegria-Hartman, P. Banda, P. Williams, P. Gu, M. Wagner, C. Manohar, and T. Slezak, "A Functional Gene Array for Detection of Bacterial Virulence Elements," *PLoS ONE*, **3** (**5**), e2163, 2008.

2. Wang, D., A. Urisman, Y. Liu, M. Springer, et al., "Viral Discovery and Sequence Recovery Using DNA Microarrays," *PLoS Bio.*, **1**, pp. 257–260, 2003.

3. Wang, Z., L. T. Daum, G. J. Vora, D. Metgar, E. A. Walter, L. C. Canas, A. P. Malanoski, B. Lin, and D. A. Stenger, "Identifying Influenza Viruses with Resequencing Microarrays," *Emerging Infectious Diseases*, **12** (**4**), pp. 638–646, 2008.

**Figure 3. Agarose gel image showing bands for SARS and Rhinovirus amplicons proving that the recovered DNA was undamaged and could be analyzed.**
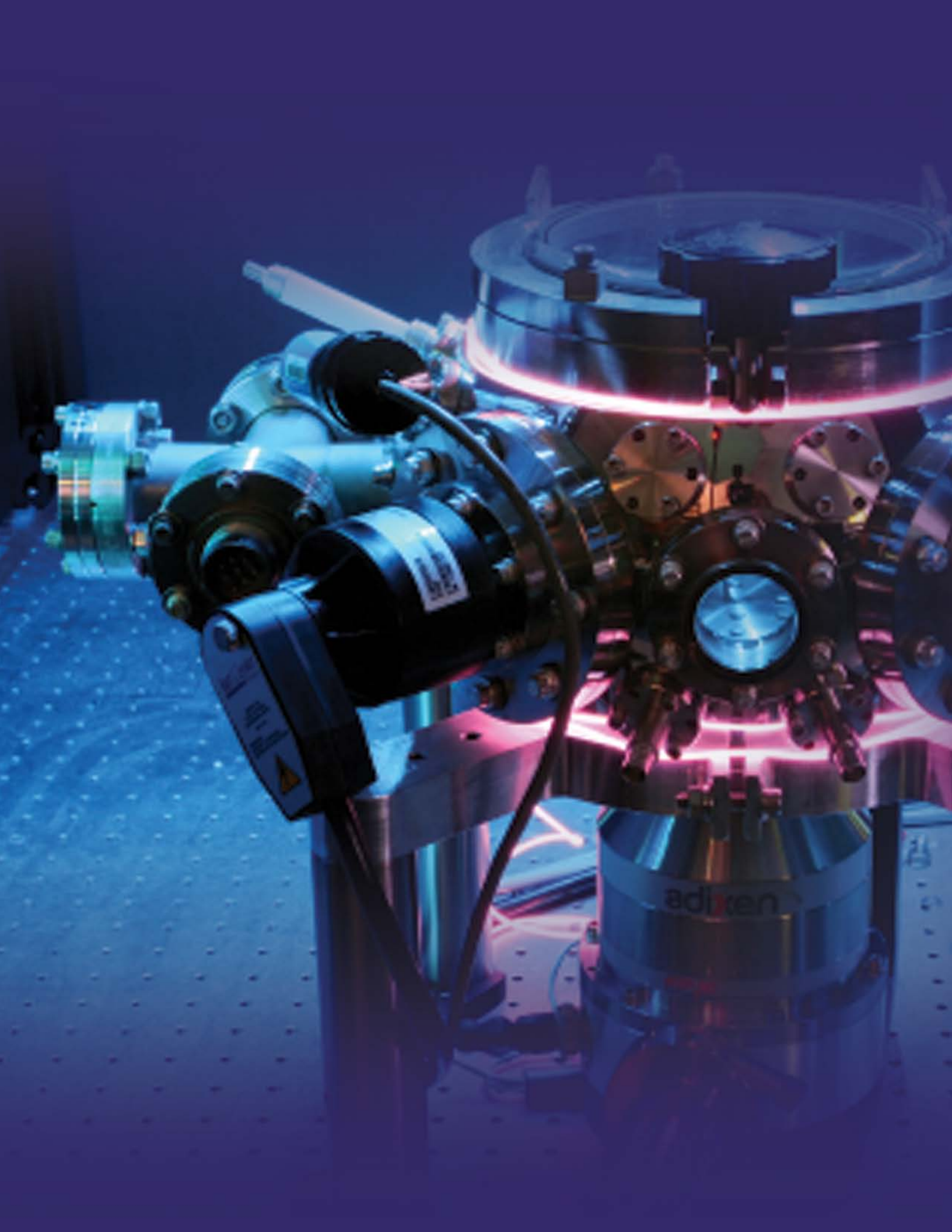
# Measurement Technologies

# Non-Acoustic Secure Speaker Verification in High Noise Environments

**John Chang**
925-424-4624
chang16@llnl.gov

## Project Overview

This two-year project was initiated to demonstrate experimentally noninvasive, real-time voice-authentication capability using non-acoustic electromagnetic voice sensing. We will first build a dual transducer sensor system using existing LLNL micropower ultrawideband impulse radar (MUIR) technology and a traditional microphone. Next we will evaluate the system on a statistically relevant sample of subjects. We will develop a new near field low profile antenna that provides efficient sensing of the vocal cord region of the speaker. We will build upon prior research of single parameter detection algorithm concepts to implement a computing architecture that will enable real-time implementation of multi-parameter detection algorithms for high confidence, real-time speaker validation, verification, and alteration.
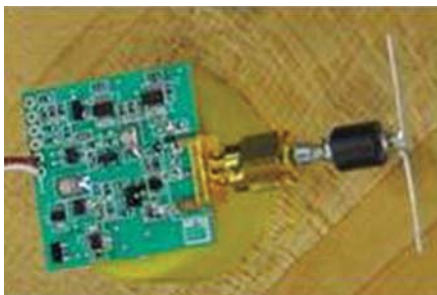


**Figure 1. Image of device. The image has been intentionally blurred to protect proprietary information such as circuit layout.**

By demonstrating noninvasive in situ sensing of the sound producing tissues of a speaker's voice box electromagnetically, new capabilities can be realized in areas of identification and biometrics, de-noising, and secured communication. Direct sensing of the voice box and vocal tract tissues will be used to authenticate the identity of an individual based on prior baseline information. It is also expected that this technology will be able to detect intrinsic levels of behavioral stress not detectable by traditional acoustic means. By integrating real-time processing and filtering, secured peer-to-peer communication, assisted by a new "cone of silence" algorithm, can also be realized. A realizable, miniaturizable radar device optimized for securing communications will have a tremendous impact on end users throughout the government and private sectors.

## Project Goals

Our goals included the design and assembly of a vocal tract sensor system and the experimental demonstration of a noninvasive, real-time voice-authentication capability using non-acoustic electromagnetic voice sensing.

## Relevance to LLNL Mission

This project directly impacts LLNL's Science and Technology Directorates and the Global Security Directorates by developing new technological capabilities as well as by addressing operational needs.

## FY2011 Accomplishments and Results

In FY2011, we were able to accomplish the following (Figures 1 and 2):

1. We designed and assembled a radar-augmented vocal tract sensor system. We have constructed two prototypes. One has been implemented for dedicated human subject studies. This system facilitates human-to-human variability and single subject sensitivity studies. The second system allows evaluation of new electronic and antennae configurations to enhance engineering performance such as dynamic range, coupling efficiency, and noise floor suppression.

2. We have examined, implemented, and documented new antenna coupling arrangements. We have performed numerical simulation of the model vocal tract. We have benchmarked the model fidelity and accuracy against experimental measurements, showing good performance to date. We will continue to refine the design to enhance the coupling efficiencies between the sensor and the human tissues/anatomy. We have observed that the current antenna, while effective, is more affected by surrounding cluttering movement than desired. It also exhibited limited standoff capability, which we aim to improve.

3. We have generated and documented human research subject data. We
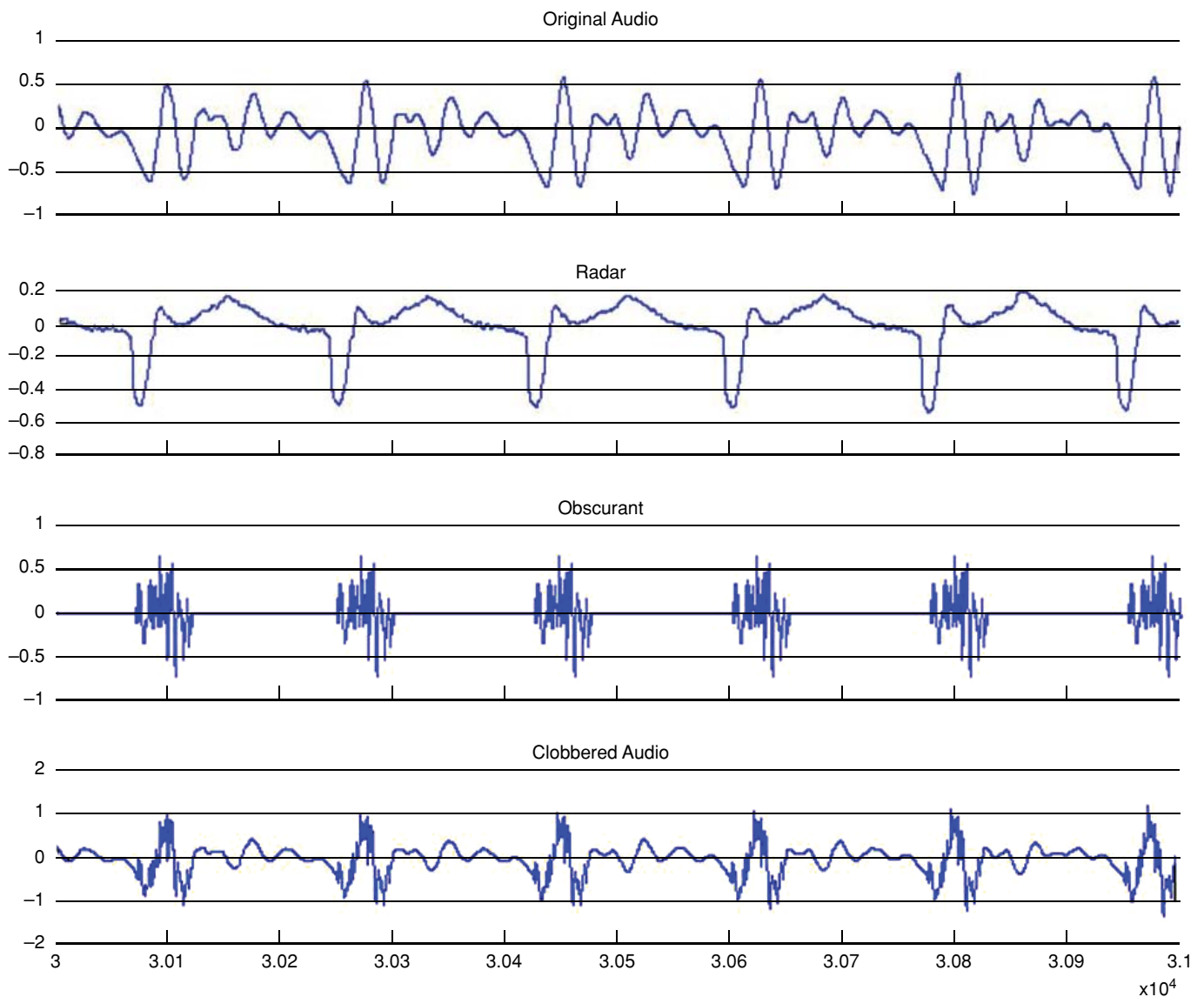
**Figure 2. Illustration of the effect of introducing correlated additive white Gaussian noise onto the radar-triggered voiced portion of the acoustic signal.**

have been able to collect data from four human subjects to date. The data has been undergoing analysis. The human subject protocol that was developed has proven to be very effective, efficient, and unencumbering to the volunteer subjects.

4. We have developed, implemented, and characterized a speaker validation algorithm. We have been pursuing signal analysis on the newly collected human subject data by benchmarking against historical data and acoustic signatures.

We have further initiated a dialogue with SRI to evaluate collaboration opportunities with their speech processing subject matter experts.

**FY2012 Proposed Work**

In FY2012 we will 1) continue with human subjects data acquisition, data analysis, and documentation; 2) demonstrate and document a background noise removal algorithm; 3) demonstrate and document a speech silencing algorithm; 4) demonstrate a real-time speaker voice signature alteration algorithm; and 5) disseminate results through conferences, publications, and ROIs.

# X-Ray Array Sources

**Sean K. Lehman**
925-423-3580
sklehman@llnl.gov

## Project Overview

This project studied the application of x-ray array sources. Arrays of acoustic and electromagnetic transducers have existed for decades but the technologies to manufacture and operate x-ray array sources have only recently become commercially feasible. In theory, x-ray array sources could reduce data collection times, enhance resolution, increase contrast, and reduce imaging artifacts.

## Project Goals

The goal of this project was to study the application of x-ray array sources to problems of importance to LLNL.

## Relevance to LLNL Mission

X-ray array sources have the potential to contribute to leading edge technology in areas such as nondestructive evaluation, where LLNL has a leadership role.
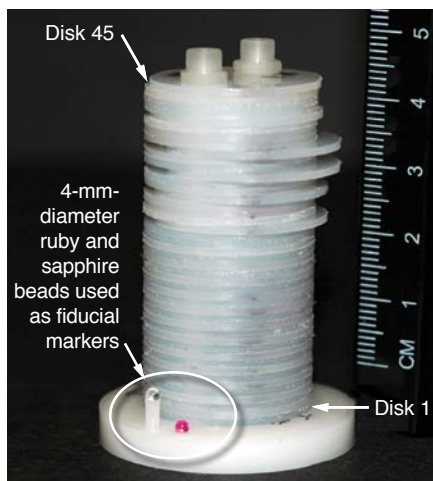


Figure 1. Contrast and Resolution Interleaved Stacked Plate (CRISP) phantom.

## FY2011 Accomplishments and Results

To demonstrate these imaging improvements, we designed the Contrast and Resolution Interleaved Stacked Plate (CRISP) phantom, a stacked disk assembly in which the materials differ in type and attenuation. They may also contain resolution patterns machined into the disks. The goal is to form a contrast, or contrast and resolution phantom. The materials used in the CRISP phantom are Kynar and low-density polyethylene (LDPE). Selected disks contain resolution patterns in the form of holes of varying sizes. Within the stack, selected disks are offset so as to model "As Built" versus "As Designed" issues as well. The assembled phantom is shown in Figure 1.

To achieve its goal, the project engaged Triple Ring Technologies, an x-ray array-source manufacturer, to collect data on the CRISP phantom. As a comparison, data were collected on a technologically mature single source cone-beam system at LLNL. Whereas single-source cone-beam reconstruction codes are mature, array-source reconstruction codes are nascent. LLNL implemented a variation on an expectation maximization (EM) algorithm to reconstruct these data.

EM is an iterative algorithm that computes maximum likelihood estimates for any statistical measurement scheme. In x-ray reconstructions, the statistical nature of the system arises from the stochastic nature of x-ray photon emission. EM also incorporates non-negativity constraints (physically, the number of photons never goes below zero) and measures of reconstructed image quality. Convergence toward a solution (an image) is achieved by iteratively going back and forth between an estimation step, and maximization step. Unknown parameters, such as number of photons emitted by the sources, are estimated in the expectation step and an image-likelihood is maximized in the maximization step.

Although reliable and robust, EM can be slow for large data sets. A speed-up was introduced where the expectation and maximization steps were performed after adding only a subset of the data at a time, instead of the full data set at each update. This new method, ordered subset expectation maximization (OSEM), is a standard tool for count-starved tomographic imaging modalities, such as the Triple Ring Technologies measurement system. In x-ray measurement systems, data are taken in a physically ordered fashion: a detector is swept around the object of interest, collecting data in neighboring angular swaths.

Using data ordered in this way creates artifacts (intensity anisotropies and feature blur). We developed a randomized subset expectation maximization (RSEM) implementation of the EM algorithm, which essentially eliminates these artifacts. The RSEM implementation can be run in a mode where subsets are constructed once of angularly randomized data and the same subsets are used in a round-robin manner to update the EM algorithm. The other method is to create subsets at each iteration (each time the entire data set is fully utilized) that are randomized.

Both methods have fewer artifacts due to event ordering and have been shown to be essentially interchangeable.

As a proof-of-principle that the RSEM algorithm offered an improvement over current reconstruction algorithms, a reconstruction was performed of a single-source fan-beam data set consisting
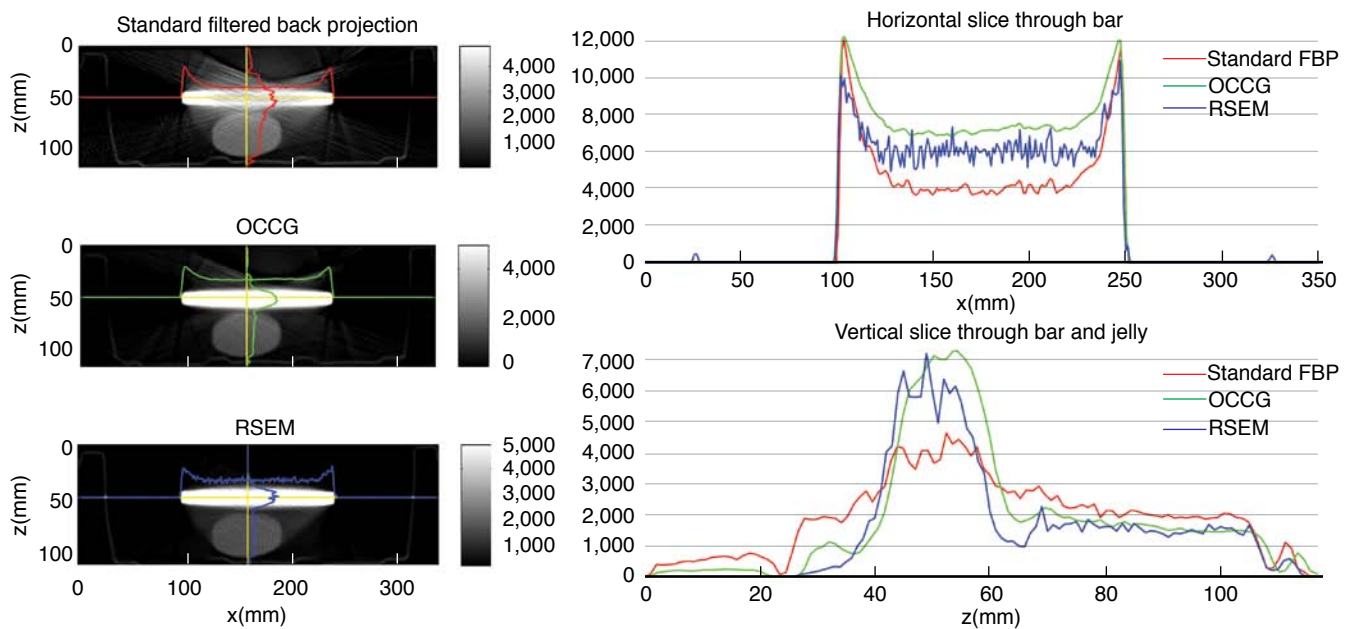
**Figure 2. Reconstruction comparisons of a data set consisting of a steel bar (white object) and a container of jelly (gray ellipsoid). Profiles through the reconstructions are shown for a standard CT algorithm, an OCCG algorithm, and the RSEM.**
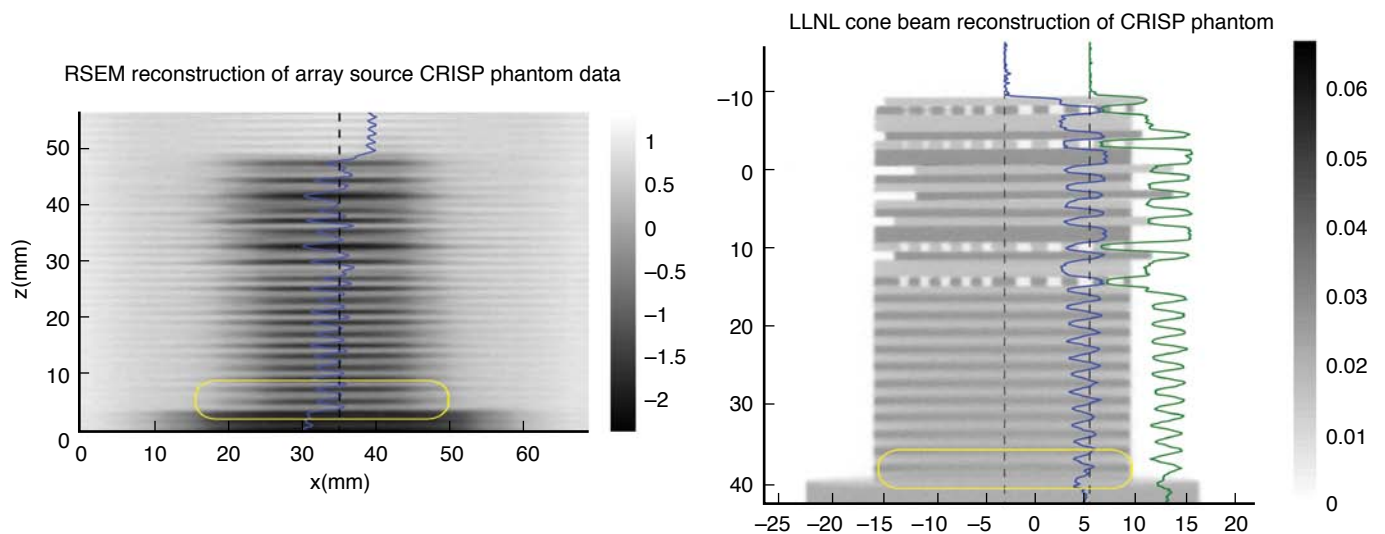


**Figure 3. Reconstruction comparison of vertical slices through the cone-beam array-source data (left) and a single-source cone-beam data (right). Superimposed on the images are line profiles through the data. Cone-beam artifacts are reduced in the array-source data, as indicated by the yellow boxes.**

of a steel bar and a container of jelly. The importance of these data lie in the large attenuation contrast between the two materials. Figure 2 presents a comparison of a standard (filtered back projection) computed tomography (CT) reconstruction algorithm with an occasionally constrained conjugate gradient (OCCG) algorithm and RSEM. The standard algorithm shows more artifacts and poorer contrast than the other two. The RSEM algorithm yields the fewest artifacts and best contrast and resolution.

With this single-source fan-beam success of the RSEM algorithm, it was used to reconstruct the Triple Ring Technologies array-source cone-beam CRISP phantom data. As a comparison, single-source cone-beam data were collected on the CRISP phantom and reconstructed. Slices through both reconstructions are presented in Figure 3.

Unfortunately, the array-source data proved to lack the photon count to achieve a fair reconstruction comparison with the single source data. However, off-angle blurring artifacts appear less in the array-source reconstruction. This provides hope that as photon counts and energy levels are increased in array sources, they will out-perform the current single source systems.

# Ultrafast, Sensitive Optical Radiation Gamma, Neutron, and Proton Detector Development

**Stephen Vernon**
925-423-7836
vernon1@llnl.gov

## Project Overview

The Ultrafast RadOptic Gamma, Neutron, and Proton Detector Development project seeks to build a novel class of radiation detectors that leverage recent advances in the development of high-bandwidth x-ray-to-optical converters and high-bandwidth optical recording technologies.

## Project Goals

The goal is to develop and field a new class of ~ps-response-time gamma ($\gamma$),neutron (n) and proton (p) detectors that provide enhanced sensitivity and temporal response for WCI and ICF experiments on NIF.

The detection approach involves conversion of the radiation signals to the optical domain, converting the radiation signature to an amplitude modulated optical beam. These detectors use unique radiation to secondary charged particle (electron (e)) converters, RadOptic sensors, and ultrafast optical recorders to efficiently convert the radiation signature to amplitude modulation of an optical probe beam.

The design and development of the converters is a major deliverable of the project. The n-e converters are relatively simple and rely on secondary electron generation in a CsI photocathode by interaction of a recoil p or deuteron (d) generated in an inelastic collision between the incident n and nuclei in a plastic foil.

The $\gamma$ detector is significantly more complicated in its design and uses a combination of pair production, Cherenkov radiation, secondary electron generation in CsI, charge concentration, and transport. Both detector implementations rely on electron impact ionization in the RadOptic sensor, in the final stage of the conversion processes.

In both cases the back-end recorder of the detection system will leverage recently developed and demonstrated high-bandwidth, RadOptic semiconductor sensors and ultrafast all-optical recorders. Initial testing of sensors will be accomplished using optical streak cameras and/or high bandwidth photodiode detectors and oscilloscopes as the data recording systems.

## Relevance to LLNL Mission

The project is well aligned with the institutional science and technology plan. The detection systems being developed address programmatic needs for 3-D, time-resolved validation of high-energy-density experimental results. The research is undertaken within the Measurement and Experimental Sciences Science and Technology Pillar supporting the Stockpile Stewardship Focus Area, and supports WCI and ICF experiments on NIF.

## FY2011 Accomplishments and Results

Major accomplishments for this year include the design and partial fabrication of prototype Fabry-Perot GaAs e sensors, MCNPX modeling of the $\gamma$ and n converters, initial modeling/design of a prototype electron optics system, and the build-out of a UHV electron optics testbed that incorporates an intense pulsed electron source driven by a frequency tripled short-pulse Ti:sapphire laser.
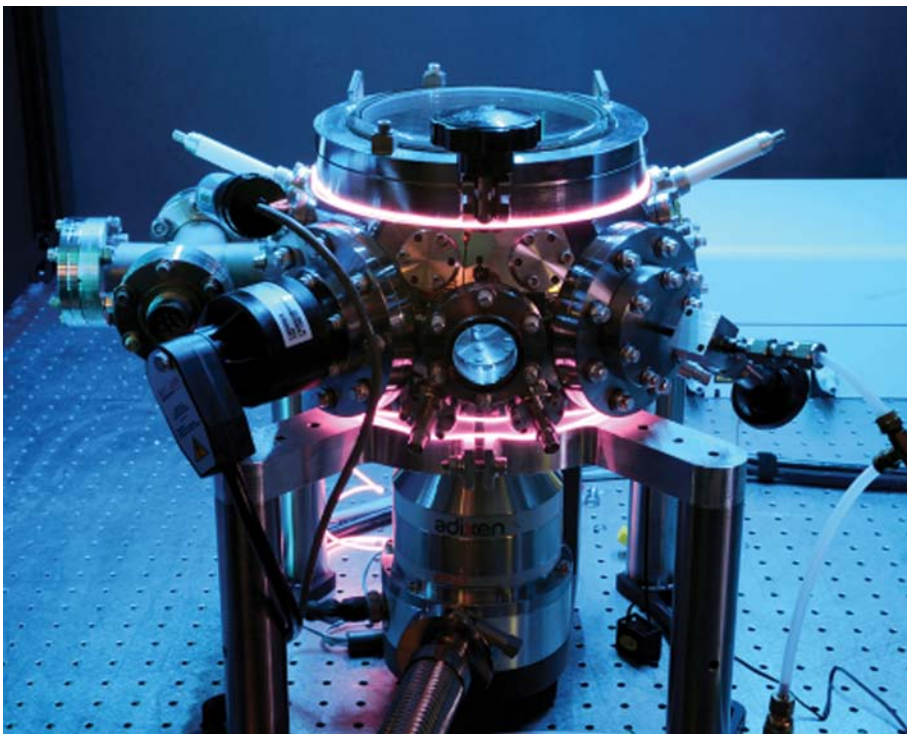


**Figure 1. UHV electron optics testbed.**

The Fabry-Perot sensors require a thin (preferably low Z) metal mirror in order to achieve high e transmission into the cavity and good detection sensitivity. Models indicate that Al mirrors are suitable for operating wavelengths near the GaAs band edge (970 nm). Two designs were partially fabricated in FY2011. Devices will be completed in early FY2012.

The initial MCNPX simulations are encouraging. The temporal response of the n and γ converters can be tuned by adjusting the angular acceptance of the knock-off p, d (for the n detector) or the relativistic e (for the γ converter). The simulations predict that both converters can achieve ~ps response. We are in the process of modeling the Cherenkov radiation produced by the relativistic e using the GEANT code.

The vacuum envelope of the UHV testbed is complete; the photocathode assembly has been designed; and we have developed a preliminary design of the electron optics system using the SIMION® code.

Figures 1 through 3 are photographs of our setup.

## FY2012 Proposed Work

In FY2012, we plan to complete the fabrication of the prototype e sensor, finalize the design of the e optics system, integrate the e optics with the prototype e sensor; and characterize the integrated system in the laboratory testbed. The Cherenkov modeling will be concluded. An end-end model of the γ converter temporal response will be constructed; optimized mode based designs will be developed for both γ and n converters; and prototype converters will be fabricated.

## Related References

1. Lowry, M. E., et al., "Radsensor: X-Ray Detection by Direct Modulation of an Optical Probe Beam," *Proc. SPIE*, **5194**, pp. 193–204, 2004.

2. Lowry, M. E., et. al., "X-Ray Detection by Direct Modulation of an Optical Probe Beam- Radsensor: Progress on Development for Imaging Applications," *Rev. Sci. Instrum.*, **75**, pp. 3995–3997, 2004.

3. Ziaja, B., R. London, and J. Hajdu, "Unified Model of Secondary Electron Cascades in Diamond," *J. Appl. Phys.*, **97**, 064905, 2005.

4. Lowry, M. E., et al., "RadOptic X-Ray Detection With Picosecond Resolution," *Ultra Fast Optics*, Monterey CA, September 2011.
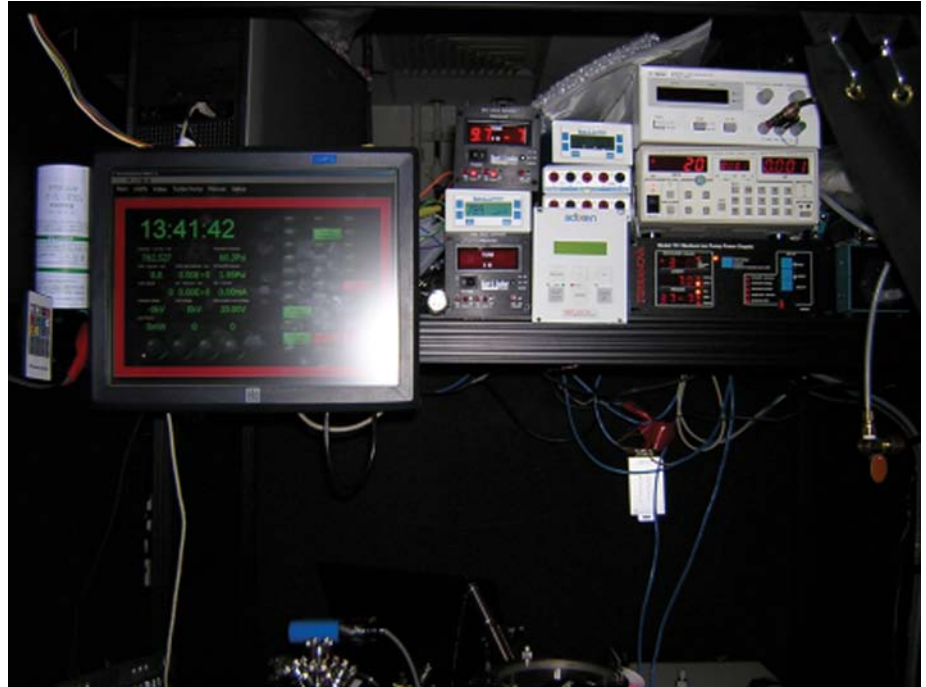
**Figure 2. Testbed for experimental control systems.**
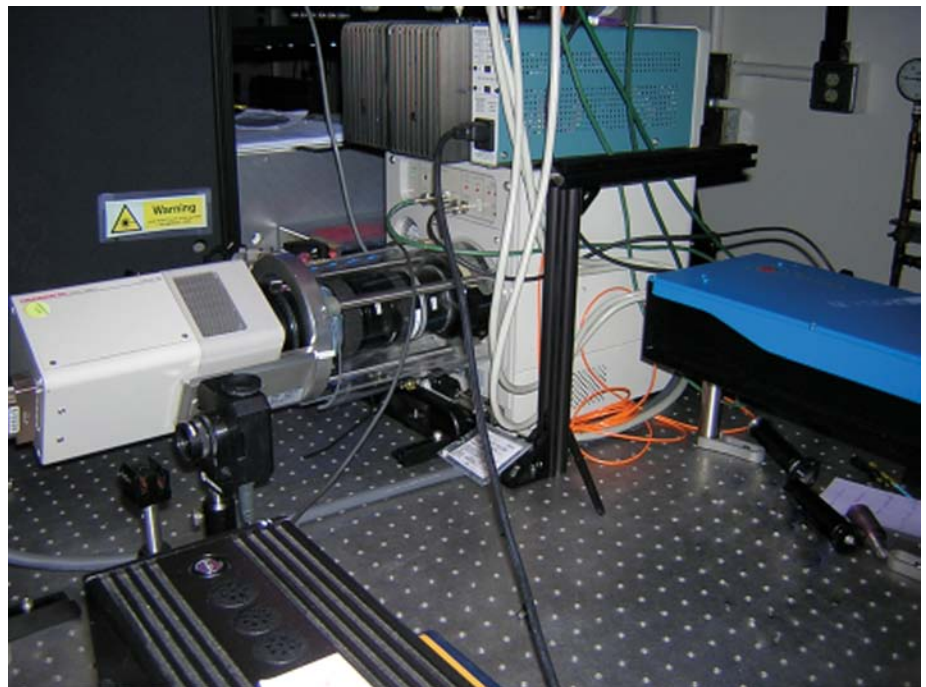


**Figure 3. Optical streak camera readout and electronics.**

# Investigation of Fast Z-Pinches for Scalable Large-Current High-Gradient Particle Accelerators

**Vincent Tang**
925-422-0126
tang23@llnl.gov

## Project Overview

Our objective is to obtain detailed understanding of extremely high (greater than 100 MV/m) acceleration gradients in fast Z-pinch plasmas for next-generation accelerator applications.

Z-pinch plasmas, such as those produced by technologically simple Dense Plasma Focus (DPF) devices, have emitted ion beams with up to ~10 MeV ions over ~cm scales. The mechanisms behind the large acceleration gradients responsible for these ion beams are still not well understood. In this project, we will perform unique, first-ever probe-beam experiments that will measure the gradients directly and develop state-of-the-art, fully kinetic plasma simulations to obtain greater understanding and predictive capability.

Our motivation is twofold. First, at the megavolt level, DPF Z-pinch devices optimized for beam production and acceleration could serve as the basis for compact, intense radiological sources, such as directional neutron sources, and also as unique high-current ion injectors. Second, if the acceleration gradients in fast Z-pinches can be scaled to higher levels, our research could lead to very-high-gradient plasma-driven accelerators notably simpler than current laser or electron-beam systems, thus revolutionizing accelerator technology and applications.

## Project Goals

We expect to produce a fundamental understanding of the acceleration gradients in DPF Z-pinch plasmas and use that knowledge to examine how these plasmas can be systematically exploited for accelerator applications. We will inject, for the first time, a 200-ps, 4-MeV ion probe beam into a DPF Z-pinch plasma and measure the acceleration of the probe beam to deduce the plasma's acceleration gradient, as shown schematically in Figure 1. We will refurbish a 4-MV RFQ for the probe beam and construct a table-top DPF for the plasma. The unique probe beam data will be compared with first-ever fully kinetic Particle-in-Cell (PIC) simulation of Z-pinch plasmas, to validate useful predictive simulations for applications.

## Relevance to LLNL Mission

The work supports LLNL's national security missions—specifically homeland security, nonproliferation, and accelerator science—by providing the technological and scientific basis for compact alternative radiological sources and next-generation accelerator



Figure 1. DPF and the proposed probe beam injection experiment. The Z-pinch plasma is formed at the end of a coaxial gun through multiple stages. The plasma sheath starts from flashover of the insulator (I), accelerates down the electrode along the coaxial gun (II, III), and collapses radially (IV) to form a dense, fast Z-pinch (inset).
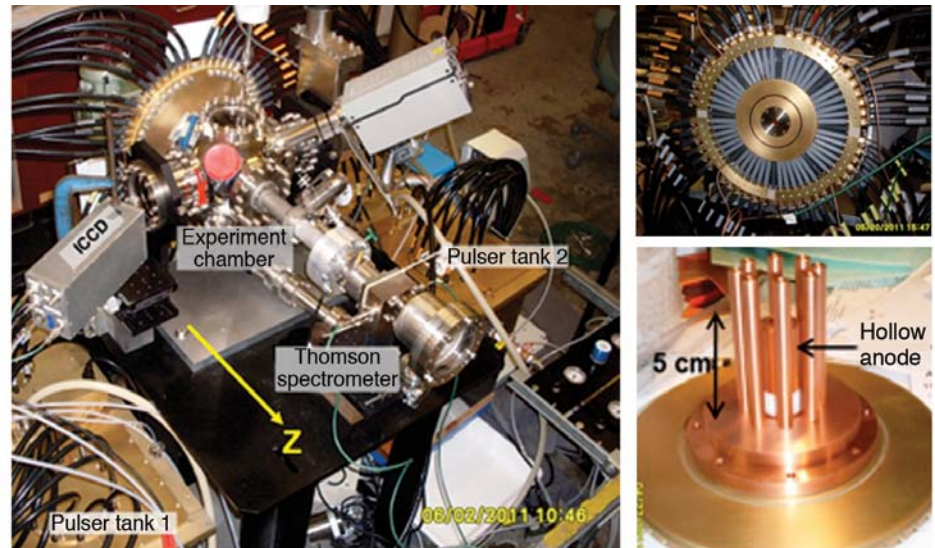


Figure 2: Photographs of 4-kJ DPF device: (left) overall experiment, including pulsed power tanks that drive the coaxial gun load at bottom right; and (top right) low-inductance cable feed system that transmits the power from the pulsers to the gun load.

(a) Current (kA) vs. time

V = 27 kV
V = 1.18 kJ
V = 4.1 TD$_2$
D = 91

148 kA at dip/pinch

(b)

20 ns exposures, images from same shot

Camera view

Central anode

Z

8x cathode rods
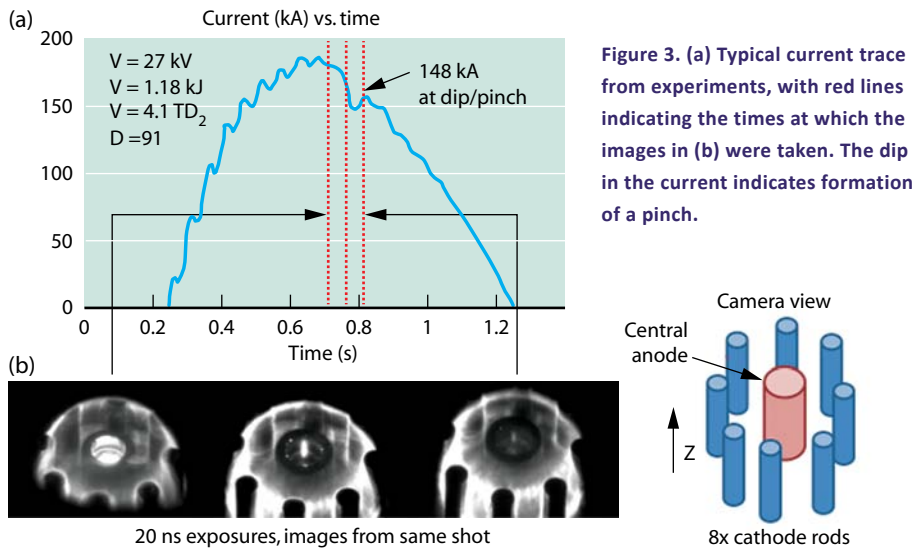
**Figure 3. (a) Typical current trace from experiments, with red lines indicating the times at which the images in (b) were taken. The dip in the current indicates formation of a pinch.**



Ion density (cm$^{-3}$)  x10$^{17}$   Fluid   Anode

Ion density (cm$^{-3}$)  x10$^{17}$   Hybrid   Anode

Ion density (cm$^{-3}$)  x10$^{17}$   Fully kinetic   Anode

r (cm)

Z (cm)
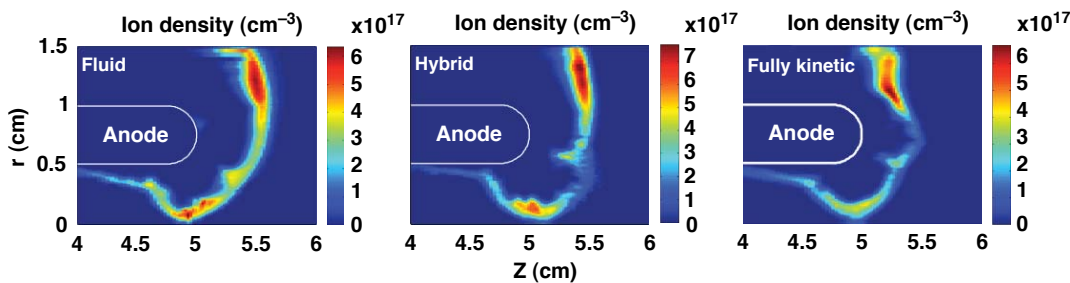
**Figure 4. Density profiles of DPF plasmas right at pinch formation from LSP fluid, hybrid and fully kinetic simulations of our DPF. Although the profiles look similar, the simulations predict different arrival times for the pinch (65, 60, and 39 ns from the start of the simulation). Possible tearing modes in the sheath are indicated in the hybrid and kinetic simulations.**

technology for active interrogation and radiography. Successful resolution of the physics behind the Z-pinch plasmas formed in a DPF device would resolve long-standing questions in plasma physics and in High Energy Density Laboratory Physics (HEDLP), both of which are core LLNL competencies.

## FY2011 Accomplishments and Results

In FY2011, we have 1) designed, fabricated, and assembled the 4-kJ DPF shown in Figure 2; 2) started initial DPF operations with successful formation and diagnosis of Z-pinch plasmas (Figure 3); 3) transferred and refurbished the 4-MeV RFQ accelerator for the probe beam that is key to our experiments; 4) completed simulations for our transport beamline and associated diagnostics; 5) hired a post-doc for modeling and analysis

efforts; and 6) completed first fully kinetic PIC simulations of the DPF using the LSP code, and performed comparison of these simulations with fluid and hybrid models (Figure 4) along with parameter scans.

## FY2012 Proposed Work

In FY2012 we will 1) complete characterization of the DPF Z-pinch plasma and beam output; 2) install and test the dual quadrupole beamline required for probe beam injection into the Z-pinch plasma; 3) begin and complete a first set of experiments using our 4-MV RFQ ion probe beam; 4) continue improving simulations of the DPF plasma and beam output using our PIC models; and 5) perform systematic comparison of new experimental data with the leading models via both direct and synthetic diagnostic approaches.

## Related References

1. Tang, V., M. L. Adams, and B. Rusnak, "Dense Plasma Focus Z-Pinches for High Gradient Particle Acceleration," *IEEE Transactions on Plasma Science*, **38** (**4**), pp. 719–727, 2010.

2. Mather, J. W., "Investigation of the High-Energy Acceleration Mode in the Coaxial Gun," *Phys. Fluids Suppl.*, **7** (**5**), 1964.

3. Mather, J. W., "Formation of a High-Density Deuterium Plasma Focus," *Phys. Fluids*, **8** (**2**), p. 366, 1965.

4. Decker, G., and R. Wienecke, "Plasma Focus Devices," *Physica*, **82C** (**155**), 1976.

5. Ryutov, D. D., M. S. Derzon, and M. K. Matzen, "The Physics of Fast Z-Pinches," *Rev. Modern Physics*, **72** (**1**), pp. 167–223, 2000.

# Author Index